Spatialized probabilistic flood risk assessment in urban areas protected by levees

by

Florence Marianne MAINGUENAUD

A dissertation submitted to the faculty of graduate studies and Ecole Doctorale 353
in partial fulfillment of the requirements for the degree of

DOCTOR OF PHILOSOPHY

Cotutelle with
Graduate Program in Civil Engineering -
York University, Canada
&
Ecole Doctorale 353: Sciences pour l'ingénieur, Génie Civil et Architecture -
Aix-Marseille University, France

Host laboratories	INRAE, UMR RECOVER, Aix-Marseille University Lassonde School of Engineering, York University

Abstract

Flood hazard assessment is a necessary input to a flood risk assessment. Integrated flood hazard assessment methods provide a good overview and distinguish three steps: assessment of the flooding event probability, reliability assessment of the flood defense system, flood propagation using numerical simulations. Flood hazard assessment results in one or several flood maps, each dependent on the intensity and duration of the modeled flooding event. A definition of flood risk assessment is the combination of hazard, exposure, and vulnerability. We identified several gaps in each step of the flood risk assessment process. Gaps found in flood hazard assessment include: the lack of decisive method to estimate a combined levee failure probability of various failure mechanisms and few probabilistic flood hazard assessments include levee failure scenarios. One of Integrated Flood Risk Management (IFRM) aims is to provide a standard for risk assessments to enable comparisons between different studies and better management on the long run.

To address those gaps, we propose a method, which estimate earthen levee failure probabilities for several return periods and failure mechanisms (backward erosion, slope stability, and overflow). We used limit equilibrium method and Monte-Carlo simulations to estimate sliding failure, compared seepage gradients to a critical gradient to estimate backward erosion failure, and used expert judgment to estimate overflowing failure probabilities. We aggregated failure mechanism probabilities into a global fragility curve using Monte-Carlo simulations, hence providing a comprehensive fragility curve for an earthen levee segment. We defined several scenario of flood and levee failure for backward erosion and overflowing mechanisms to compute a probabilistic flood hazard map. We modeled six flood events, each challenging the levee reliability, enabling the breaching of each levee segment. For each scenario, the resulting flood maps of water depth and velocity are associated with a flood occurrence probability and a levee failure probability. The maps are combined into a single probabilistic flood hazard map where for each pixel, a cumulative probability curve of depth and velocity is available.

Future works will propose a probabilistic flood risk map building on the probabilistic flood hazard method, and applying new vulnerability considerations.

Keywords: levee reliability, flood hazard, probabilistic flood, flood risk

Dedication

I would like to thank my co-workers at INRAE RECOVER for their guidance and discussions. Marielle Jappiot, the Feshco team who helped me understanding the hydrology aspects of my PhD, the G2DR team who gave me useful advice: Pierre Philippe, Rémy Tourment, Jérôme Duriez, Antoine Wautier, Julien Aubriet, and Stéphane Bonelli. Special thanks to Nathalie Heitzmann for her kindness and care. My fellow PhD and friends: Na Deng, Marie Miot, Adriane Clerc, Alexis Doghmane, Colin Lashermes, Luiza Sodera, Pénélope Brueder, Sacha Duverger, and Bastien Bourlier for the good laughs, questions, and making this PhD an enjoyable experience. My gratitude to my colleagues and friends at YorkU: Apostolos Vasileiou, Michael De Santi, Karen Dunbar, Rahma Shakir, Josephine Morgenroth, and Everett Snieder who helped me so much when I was struggling with my code, I am eternally grateful! And to many others for their kind words and encouragements.

Finally, to my family, to my french team: Lucie Le Scolan, Alice Delaunay, Aline Cissé, Camille Follet, Zayneb Lahlou, and Karina Tata, to my canadian team: Minami Sato, Deepali Saraf, Rachade Bireau, and Karuna, many thanks as always for the emotional support.

Acknowledgements

I would like to thank my principal supervisors Peyras Laurent and Usman T. Khan respectively from INRAE, France and Lassonde School of Engineering, Canada for their guidance, time, and kindness throughout those 3 years of PhD. I am grateful for the opportunity of being co-supervised by two experts in different specialities, which brought challenges but also various insights both on the core of the PhD and on the academic world.

I would like to also thank my co-supervisors Claudio Carvajal and Bruno Beullac for their support, guidance, technical knowledge, and advice when I was lost or unsure of my results. Professor Jitendra Sharma, as one of my co-supervisors provided precious feed back while I was writing my articles, which I am very thankfull for. Thank you to Théo Picton and Gautier Cocaign for their preliminary work on the Calgary levee system, providing insights on which direction to orientate this research.

This research would not have been possible without the support and funding of French National Research Institute for Agriculture, Food, and Environment (INRAE) and York University which welcomed me respectively in the RECOVER, G2DR team and as a graduate student at Lassonde School of Engineering. The City of Calgary provided geotechnical and hydraulic data of the Bow River, and the Toronto and Region Conservation Authority (TRCA) provided geotechnical and hydraulic data of the Etobicoke Creek.

Additional thanks to all jury members Sylvie Morin, Thierry Verdel, Peng Wu, Corinne Curt, Laurent Peyras, Jitendra Sharma for their time and accepting to partake in this jury.

Table of Contents

List of Tables

List of Figures

Chapter One: Introduction

Natural disasters like flooding occurs in most countries around the world, affecting social life and the economy. Every year, floods cause enormous damage all over the world. For instance, Hurricane Katrina in 2004 (ASCE, 2007), Storm Xynthia in 2010 (Kolen et al., 2013) or the floods in Southern Alberta in 2013 (Pomeroy et al., 2016) had terrible consequences for human life and assets. Flooding stems from various meteorological mechanisms, exacerbated by climate change in some areas. Due to sea level rise and more frequent heavy precipitations projected throughout the 21st century and beyond, International Panel on Climate Change (IPCC) has predicted that coastal and riverine systems will increasingly experience adverse impacts such as these major floods (Field et al., 2014).

Furthermore, Field et al., 2014 also state that if levee structures are to be a reliable mitigation approach to prevent flood events, this solution can only be effective if these structures are regularly operated and maintained. In fact, a breach in a levee system may cause more damage due to the flood wave than a gradual rise in water. In addition, this kind of failure is difficult to anticipate in terms of its location and characteristics of the resulting floods, and thus, the management of the resulting inundations is more difficult than for inundations which can be accurately forecasted, like those without levees or those with levees but without failure (Tourment et al., 2017).

To ensure a long-term performance of levee systems is necessary given the consequences of their potential failure, performance assessments and risk evaluations must be regularly carried out (Simm et al., 2012). To be effective and provide support to the development of optimal investment strategies, these actions must be integrated in a process of flood risk management, including flood risk analysis and flood risk assessment (European Environment Agency, 2007). Thus, the knowledge of the risk associated with the different parts of the levee system makes it possible to optimize its management to be able to propose measures to reduce the level of risk, or to maintain this level if it is acceptable (Tourment et al., 2014).

Based on the Source-Pathway-Receptor model, risk analysis of a levee systems estimates the overall level of risk associated with the system, according to a series of loading conditions, the performance of levees and the vulnerability to flooding of assets in the protected area (Samuels, Morris, et al., 2009). Requiring the identification and examination of all the components that determine the risk of flooding in the protected area, its process have been formalized in the International Levee Handbook (ILH) (CIRIA et al., 2013). Its main steps are: event probability estimation; inundation modeling; analysis of levee system failure; exposure and vulnerability estimation; estimation of level of risk; risk attribution; and assessment of remaining gaps in knowledge.

Event probability estimation aims to estimate the probability and the intensity along the levee system (flow discharge, water level) of a range of the different possible flood loading conditions. The goal of inundation modeling is to identify and characterize inundation routes and flood extents (including water depths, flow velocities, timing of inundation) in the protected area. These two steps of the risk analysis process, which are mainly related to hydrology, river morphology and hydraulic disciplines, are classic engineering and research topics with updated methodologies and modeling tools (Bedient et al., 2013; Knight et al., 2018). Modeling climate change scenarios consist in estimating the general variation of river flow in a given time-span. Many model and study the impact of climate change: Ward et al., 2014, Sayers et al., 2020, Romero, 2020, Mohammed et al., 2021, Russell et al., 2022.

Levee system failure, which is defined as the inability to achieve a defined performance threshold (Allsop et al., 2007), occurs when a levee segment is no longer able to achieve, at the defined or assigned loading water level, its function of flood protection within the levee system (Simm et al., 2012). Different deterioration mechanisms may have an impact on levee segments and lead to levee failure and possible breaching. These mechanisms have very different and complex forms and possible combinations, and a large variety of levee failure scenarios (sequence of deterioration mechanisms and associated damages on levee components) may be considered for a given levee segment (CIRIA et al., 2013). According to CIRIA et al., 2013, individual mechanisms of deterioration that affect levees, can be grouped into three generic types: (i) external erosion; (ii) internal erosions; and (iii) slope instability. The assessment of the performance of the levee system failure can be conducted through quantitative methods using expert judgment, index based methods, or mathematical models (based on physical or empirical equations). These consist of the estimation of failure scenarios probabilities for one or different loading events (van der Meij et al., 2012).

Consequences, which result when people or properties are exposed to a flood and suffer some harm, may be a direct result of flooding (e.g. damaged buildings and/or contents) or indirect (e.g. loss of business earnings due to recovery time) (Messner et al., 2006). The estimation of the consequences of inundation, which results from a combination of the results of hydraulic modeling of the inundation and the estimated vulnerability (a function characterizing damage according to hydraulic characteristics of inundation) of the different assets (exposure) located in the flood area (K. Smith et al., 1998; Parker et al., 1987). A natural flood area or a protected area may present different types of assets such as people, buildings, or network infrastructures. Their vulnerability can be approached in different ways, for example: social (casualties or life loss as in Jonkman, Kok, et al., 2008), economic, and environmental (Tapsell et al., 2008). Therefore, multi-criteria approaches prove to be very relevant for consequences analysis (Meyer et al., 2009).

There are many definition and formalization of flood risk as listed by Solin et al., 2013. In this dissertation, flood risk is considered as a combination of hazard, vulnerability, and exposure. First, flood hazard assessment provides a flood extent along with other flood parameters (e.g. depth, velocity). The area of affected by the flood provides a zone to identify and quantify existing assets (a.k.a. exposure). Then, for each asset, their resistance or capacity to recovery to floods (a.k.a. vulnerability) is estimated using various indicators (e.g. type of construction materials, family income levels, age of the population). Finally, the usual approach to combine hazard, exposure, and vulnerability consist in establishing a common level of risk scale before overlaying each element of flood risk. Therefore, in this dissertation, flood risk will refer to the overlay of flood hazard and exposed vulnerability layers.

Finally, risk attribution is based on the results of risk estimation, whose goal is to combine probabilities and potential consequences of the levee system failure (Samuels, Gouldby, et al., 2009). Using those results, flood risk is attributed to levee segments. It enables prioritization of intervention measures, hence reducing flood risk. Since it is not possible to protect against all flood events, all levee systems have a residual risk of flooding. Risk is attributed to every levee segment for each flooding scenarios, leading to their relative classification according to the risk attributable to each. The UK model (Gouldby et al., 2008; Flikweert et al., 2015) and the Netherlands model (Van Alphen, 2015) estimate flooding risk of levee protected areas including breaching scenarios. In the UK model, flood risk is attributed to levee segments by tracking from which levee segment came the flood water volume. To simulate multiple levee failures and flooding scenarios, a Monte-Carlo sampling procedure is used. In France, Pheulpin et al., 2019 achieved a sensitivity analysis to better understand the impact of breach parameters, used in a 1D hydraulic model, on the generated overflows. A model with storage areas of the Garonne River, preliminary built and validated with the HEC-RAS code was used. The methodology relies on an uncertainty propagation of the breach parameters, done through the coupling of two software (HEC-RAS and Promethee). The breach parameters are evenly distributed and randomly selected in order to generate a large number of breach scenarios. The Monte-Carlo and Fourier Analysis Sensitivity Test (FAST) analyses show the strong influence of the overflow parameter on the filling of storage areas, and the influence of the parameters linked to the breach geometry.

Due to the high complexity of levee systems and protected area, the incompleteness of the data, and the limitations of the methods used to treat them, the different steps of risk analysis imply many uncertainties, which affect the results of the whole process. Assessing remaining gaps in knowledge to better understand the impact of uncertainties within the process and results of risk analysis, give the opportunity to progressively refine the risk estimation and improve the levee system management. Recent research works (Vuillet et al., 2016; Peyras et al., 2015; van Gelder et al., 2008) propose a way to consider data uncertainties in the structural performance of levees. Input data uncertainties are modeled through subjective probabilities and propagated for each levee failure scenarios using Monte-Carlo simulation.

This PhD dissertation focus on urban fluvial floods and levee structures. We aim to develop and optimize a fully probabilistic method assessing flood risk at any location of the area protected by levees. Though guided by flood risk as a final objective, the main focus of this dissertation is flood hazard, one of its essential component. We will take advantage of the operational methods carried out in United Kingdom (UK) and the Netherlands, to build an operational method. Our approach is guided by a rigorous risk analysis academic framework. We will take particular care in modeling levee failures, which is done with excessive simplification in existing methods. We also introduce expert assessment uncertainties to reinforce the robustness of probabilistic risk assessment. Finally, the purpose of this research is to propose a probabilistic flood hazard representation considering flood events of different intensity and probability of occurrence along with consideration of levee breaching events.

To accomplish this, we have organized this research in three parts. First to which propose methods assessing the levee failure probabilities along with a combination method to represent a unique levee failure probability given a levee segment for various flood events. The second part consist of a method to assess probabilistic flood hazard considering potential levee failures. An integrated software able to model flood propagation and levee breaching is used to simulate flooding scenarios. The flood event probability is combined with levee failure probabilities to provide an exceedance probability for every simulation. The resulting flood depth and velocity are plotted against the exceedance probability. This study enables the identification of the levee most vulnerable locations. The third and last part of this research consist in presenting vulnerability assessment methods along with an application of a flood risk assessment of a levee protected area. This part opens on future works possibilities such as an improved probabilistic flood risk estimation using the probabilistic flood hazard presented in this dissertation and propositions of additional components to the vulnerability assessment.

This PhD dissertation is article based, some chapter of this dissertation are constituted by a journal or conference article, adapted to the format of a PhD dissertation manuscript.

- Chapter is a literature review presenting every aspects of a flood risk assessment and provides context along with the main concepts encompassed in this PhD dissertation.

- Chapter present the case studies in Canada used for our PhD: the first is located in Calgary, Canada were the Bow an Elbow Rivers flow through the city, the second is located in the Greater Toronto Area (GTA), focusing on a local levee which protects a residential area.

- Chapter presents a probabilistic method to estimate levee failure for several failure mechanisms and aggregate those into a fragility curve representing failure occurrence probability and associated to a levee segment. Literature review of failure mechanism and an introduction to estimation of the failure probabilities of the instability, backward erosion, and overflowing failure mechanism is provided. The method is applied to a case study located in Calgary, Canada. This chapter is based on the article published in Journal of Flood Risk Management (JFRM).

Mainguenaud, F., Peyras, L., Khan, U. T., Carvajal, C., Sharma, J., & Beullac, B. (2023). A probabilistic approach to levee reliability based on sliding, backward erosion and overflowing mechanisms: Application to an inspired canadian case study. *Journal of Flood Risk Management*, e12921. https://doi.org/10.1111/jfr3.12921

- Chapter presents a probabilistic flood hazard assessment method taking into consideration levee failure on different location for backward erosion and overflowing failure mechanisms. Literature review of flood assessments is provided with a focus on assumptions of hydraulic models. The method is applied to a local case study in the GTA, Canada. This chapter is based on the article submitted in JFRM.

  Mainguenaud, F., Khan, U. T., Peyras, L., Carvajal, C., Beullac, B., & Sharma, J. (2024). Probabilistic assessment of flood hazard of a levee protected area considering different breaching scenarios. application to a levee on etobicoke creek river. *Journal of Flood Risk Management*

- Chapter 0.0.0.1 presents anew the steps of a flood risk assessment. We present vulnerability assessment methods and an application of a flood risk assessment: building from previous chapters, the flood hazard considering levee failure, exposure, and vulnerability are used to estimate flood risk. This chapter is based on the research presented during the European Geosciences Union (EGU) conference.

  Mainguenaud, F., Usman T Khan, L. P., Carvajal, C., Beullac, B., & Sharma, J. (2023). Mapping the impact of levee failure on flood risks: A toronto case study. *EGU General Assembly 2023, Vienna, Austria, 24–28 Apr 2023*, (EGU23-3616). https://doi.org/10.5194/egusphere-egu23-3616

- Chapter 6 is the Conclusion that summarizes major conclusions of each chapter, novel contributions to research, and presents future works.

Chapter Two: Literature review

We provide in this section basic information related to the research topic, complementary to the specific methods detailed in chapter and .

Chronology of floods

A flood is usually pictured as static reinforced by flooding maps which represent maximum flood parameters. Far from being static, flood water increase and recede sometime over several weeks. A flood event can be divided in three time sections: before, during, and after the flood.

Before a flood, is a suitable time to improve general knowledge and identify potential threats of an area. Hydrology and geotechnical studies provide essential background information to any flood assessment. Research about fundamental data used in flood assessment: flood triggers, human behavior, meteorology models help reduce the uncertainty of flood modeling. Flood models rely on theoretical water propagation and its interaction with hydraulic structures to model a flood. Assessing flood risk ahead of a flood event provides an opportunity to anticipate and prepare mitigation solution to reduce the risk. Flood risk assessments rely on civil engineering and hydrology knowledge in attempt to raise awareness of areas that require the most attention.

Flood crisis management starts with flood warnings and followed the emergency management plans implemented by local authorities. Real-time tools susceptible to help are: dynamic flood mapping, real-time transportation, amongst others. Flood crisis management relies on engineered tools and knowledge established before the flood. The ability to communicate and coordinate between authorities, technical services, and exposed population must be preserved. Social sciences study the adaptive capacity of local authorities to react to unforeseen circumstances characteristic of any emergency situation.

After a flood, assessing social and economical impacts will help improving emergency management plans. The economic recovery of a territory is usually measured in years by social studies. The data gathered throughout the flood will help calibrate future numerical models. If damages were intense, a study on how to build a more resilient city is necessary, creating a retro-active loop to the first time section.

This PhD dissertation is part of the first time section and focuses on the theoretical study of flood events and how to provide more accurate flood hazard maps as in the first tier of figure 1.

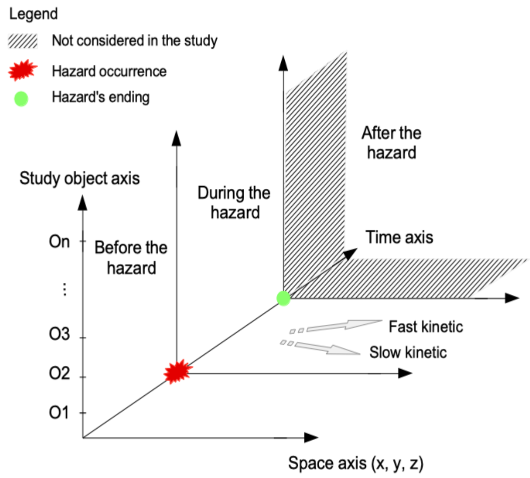

Figure 1: A proposition of perceived flood event temporality

Spatial aspect of floods

An important factor of a flood is the spatial scale of the study: local, regional, or national. Local scale flood management has some drawbacks as a local scale flood model does not cover spatial dependence of hydraulic events (e.g. cumulative effects at confluence of river tributaries), nor large scale implications of adopted mitigation solutions.

When possible, the spatial dependence of hydraulic events near river confluences should be taken into consideration as simultaneous floods events on different tributaries will result in an aggravated flood as in Pomeroy et al., 2016's study of the causes and damages of the combined flood of South Saskatchewan and Elk River basins in 2013 triggered by heavy rainfall. Neal et al., 2013 studied spatial dependence of rivers and tried to generate flood events with realistic spatial dependence between tributaries, while Fischer et al., 2021 proposed a method to assess the probability of simultaneous flood events in a main channel and tributaries.

Rivers may repeatedly cross country boundaries, which add to already existent data acquisition difficulty such as the Rhine River originates in the Switzerland's Alps, stands as a border between France and Germany, flows through Germany to the Netherlands' delta. Bomers et al., 2019 showed that levee breaches, overland flow patterns, and backwater effects must be included in flood safety assessments as they may change downstream flood risk.

A large scale flood modeling should take into account back-effects such as deviating river flow. Emergency flood management plans based on local cale flood maps only provide partial information as in 2011, when the diversion of water from the Assiniboine River to Lake St. Martin ordered to protect downstream cities along the

Assiniboine River resulted in flooding of 17 First Nation communities and displacement of 4,525 First Nations people (Flood Review Task Force, 2013). In response, Martin et al., 2017 proposed developing a joint policy and decision making system in Manitoba, Canada.

A national assessment to showcase weak points as in Keef et al., 2009 study of Great Britain's rivers dependence on extreme river flows and precipitation can guide the choice of the study area scale. They showed that precipitation spatial dependence is weaker in mountainous areas due to high topographic variation and river flow spatial dependence of fast-responding catchments located next to slowly-responding catchments is low. Modeling the full watershed can be an alternative if it does not add too much computation strain. Raining events modeling is highly sensitive to spatial and temporal variability of the rainfall (Winchell et al., 1998; M. B. Smith et al., 2004), hence modeling over several watersheds add to the uncertainties as to know how much water should be allocated to which watershed.

As described by Masseroni et al., 2017, a Rainfall-Runoff (RR) model is a set of equations which estimate runoff from rainfall, evapotranspiration data, and other parameters describing the characteristics of the watershed (e.g. drainage, soil properties, vegetation cover, topography). There are many physical-based RR models, however their accuracy and reliability is still an open topic. The prediction of watershed runoff using Artificial Neural Network (ANN) presented by Zhang et al., 2000 was thoroughly discussed in Sonnen, 2002. Other models using Fuzzy Neural Network (FNN) are used to predict peak flow rate (Khan et al., 2018).

Considering the topography and river confluences, we chose to not consider simultaneous hydraulic events.

Type of floods

Flooding is the submerging of land which is usually dry. A food can be man-made or triggered by natural phenomenon. Natural floods are distinguished by their causes and three categories are identifiable: coastal flood, fluvial flood (a.k.a. riverine flood), and pluvial flood (a.k.a. precipitation flood).

- Coastal floods may originate from storm surge or rise in sea water level. Purvis et al., 2008 present a methodology to estimate the future coastal flooding probabilities considering sea level rise of several high tide events. The resulting brine flooding waters are a threat to infrastructures and soil fertility as explored in Finkl, 2013.

- Fluvial floods can be part of the natural flow variation cycle of a watershed or due to seasonal ice and snow-melts.

- Pluvial floods are triggered by precipitation events, some of which can be intense and short leading to fast kinetics floods (a.k.a. flash floods). Flash floods are usually due to short, high-intensity rainstorms. This type of flood generally occurs in mountainous ranges where slopes are steep and rapid snow melting is more likely. Douvinet et al., 2015 model flash flood in North of France. He et al., 2018 presents an overview of historical flash floods in China showcase rapid surface waters, affected communities have a short response time and may face severe damage due to the high intensity of the flood. Dam breach events lead to flash flood events as it suddenly releases stored waters.

Flooding can be aggravated by external factors such as change in land-use increasing runoff waters, overload of the urban hydraulic network or a combination of flood types.

Rogger et al., 2017 showed that change in land-use has an impact on flooding as impervious soils are known to aggravate flood events by increasing runoff. In response, mitigation measures such as open spaces are implemented. Brody et al., 2013 study the impact open spaces in the United States of America (USA).

Urban areas have tight knitted, complex substructures (e.g. sewage systems) which limit water circulation and evacuation. Runoff can saturate urban systems causing an overload. The initial flood threat from the river flow increase is aggravated by the inability of urban systems to evacuate flooding waters. While sewage systems have been a great invention in its time improving quality of life through waste management and reducing water born diseases, downsides have recently been pointed out. A systemic approach shows issues linked to the 21^{st} century challenges are presented by Esculier et al., 2019 who also proposes a new approach to waste management in answer to those challenges. Flooding aggravation occurs when the hydraulic network systems are saturated, creating flooding due the sewage backwater phenomenon. Sandink, 2013 describes backwater from sewage system as extreme precipitation events exceeding the capacity of urban stormwater management infrastructures, resulting in uncontrolled flows of stormwater entering through windows, doors, or any kind of opening. He explored potential measures to reduce the risk of storm sewer backup aiming to reduce urban flood risk in new homes throughout Canada. Mohammed et al., 2021 used SWMM software to model a 1D sewage system by connecting nodes and applying flow rates resulting from a RR model. They simulated pipe flow, resulting in flooding discharge values ($m^3.s^{-1}$).

Combination of flood types is possible, Naseri et al., 2022 proposes a copula-based Bayesian framework to model compound coastal and fluvial floods.

This PhD dissertation does not cover additional elements to floods and focus on slow kinetic fluvial floods.

Flood defence systems

Flood defence systems include active (permanent and temporary) and passive structures. Permanent active civil engineered structures include dams and coastal levees which hold water back at all times. Whereas temporary active structures include storm surge barriers, removable flood walls and gates that are added when the need arise after a flood warning has been issued. These structures require time to install and, just like engineered structures, they can fail if the food scale is larger than expected or if the structure has not been secured properly. Temporary active structures intervene during the crisis management of a flood event, therefore does not constitute a structure we consider in this dissertation. Passive flood defence structures are permanent by definition and usually multi-purpose (e.g. leisure area becomes a retention basin when needed). A better understanding of river behavior triggered the trend of giving back space to the river by rehabilitating floodplains or create multi-purpose spaces in urban areas along with inviting green spaces back to reduce impervious surfaces and run-off that contributes to saturation of urban sewage systems. With this mindset, ponds, retention basins, flood barriers, and reinforced berms are included in new or renovation construction projects.

The structure carrying the most danger are dams (Brown et al., 1988; Jakob et al., 2013), which are closely monitored and a prolific research field. Piton et al., 2016 designate dams as transversal structures built across streams made from various materials such as logs, gabions, stones, masonry, or reinforced concrete. Dams functions are diverse and include: control sediment hazard for torrents, control water discharge, storing water supply, producing energy, short term terrain stabilization waiting for long term reforestation plans to take effect, or river bed stabilization aiming to stabilize the watershed. ICOLD, 2020 provides a summary of single purpose dams usages: 48% for irrigation, 17% for electricity, 13% for water supply, 10% for flood control, 5% for recreation, < 1% for navigation and fish farming. Frequent dam failure mechanisms include: overtopping, overtopping due to debris blockage or settlement of the dam crest, foundation settlement, slope instability, internal erosion through animal burrows and through cracks, structural failure, and inadequate maintenance.

Like all permanent civil engineered structure, dams have a lasting impact on its surroundings aside from its main purpose (e.g. sediment retention, changes in river flow). Brandt, 2000 confirms that dam sediments retention creates sediment starvation downstream of the dam with multiple consequences on the whole watershed flow behavior. To better understand the consequences, one must understand the basics of geomorphology. Rivers are dynamic entities evolving on a longer time scale than us. Rivers are pathways for water to flow which people rely on for energy, transportation of people and goods. However, in its course, water gather and transport sediments, resulting from erosion processes. The river carries sediments through river and streams from mountains to valleys, ending in the ocean. During the journey, sediment size diminishes in result to friction and shocks.

To understand the dynamic geomorphology of a watershed (i.e. why river shift and meanders), we need the sediment transport equation proposed by Lane, 1954, which describes a dynamic equilibrium between water, soil, and rock as shown in Equation 0.1.

$$Q_S \cdot D_{50} \propto Q_W \cdot S \tag{0.1}$$

Q_S the sediment discharge, D_{50} the median size of the sediment, Q_W the water discharge, S the slope of the stream as in Equation 0.2.

$$S = \frac{\text{Length}}{\Delta\text{Elevation}} \tag{0.2}$$

Consequences of this relationship include:

- Change in the flow (seasonal, precipitation, modification of hydraulic structures) result in either erosion that shifts the river channels or deposition of sediment which can incapacitate a navigation channel or destroy wild life habitats.
- Sediment variation occurs when the flow is strong enough to carry the sediments, it carries it ultimately to the sea, creating deltas. Those added sediments create an unbalance, which steers other parameters to adapt and preserve the equilibrium of Equation 0.1. Soils can be stabilized by plants and trees, diminishing the quantity of soil particles torn from the soil matrix and added to the flow,
- Erosion and deposition of sediments will influence the natural slope of a river,
- Obstacles such as dam retain sediments, specially the large sized ones and carry small sediments downstream of the dam. The deficiency in sediment provokes erosion downstream of the dam.
- A river cannot change the rise or fall between its starting point to its finish, but can change the length of its course by creating meanders. The length increase diminishes the channel slope as defined by Equation 0.2. In addition, curves triggers the flow preferential erosion and deposition mechanisms at specific location, accentuating the curve. When spread too far out, the stream cuts off the meander loop, creating recognizable landscape patterns as in Figure 2.

Figure 2: Meanders of the Nowitna River, in Alaska @Oliver Kurmis

Today's understanding of dam failure and forecast is well documented in literature amongst which, Altarejos-García et al., 2012 propose a methodology to estimate the probability of sliding failure in concrete dams. International Commission on Large Dams (ICOLD) sets standards and guidelines of dam safety.

The second structure of interest are levees. Levees may look alike at first glance but are complex structures coming in many shapes, materials, construction methods, and many mechanisms are involved in its collapse. Jozsef et al., 2015 provide a database of 1,000 levee breaches and develop empirical equations to estimate breaching parameters such as length, depth, and peak discharge. Recent levees construction are documented and their construction usually include a drainage system, and involve various materials (e.g. impervious core materials, porous materials, geotextiles) to prevent against bank erosion. However most levees are old earthen structures, which may have been renovated overtime but building methods and materials are scarcely documented leading to high uncertainties when evaluating their reliability.

This thesis dissertation focuses on earthen levees and provide a method to include levees reliability as part of regular flood hazard assessments.

Flood risk assessment

Flood risk assessments are composite approaches, each step can be identified as deterministic or probabilistic, using analytical or simulation methods. Flood risk assessments consist in four main steps:

1. determination of flood events and their probability,

2. assessment of the flood defence system and the associated failure probability for each element,
3. flood propagation through numerical simulations for every flood scenario,
4. vulnerability assessment and risk attribution.

I will lightly describe each step and focus in particular on levee performance as part of the flood defence system assessment. Finally, I provide an example of operational integrated flood risk assessment.

Flood frequency analysis

The hydrology of an area is an important determinant of flood hazard as either a hyetograph (precipitation over time) or a hydrograph (flow over time) is an input to a flood model as shown in Figure 3.

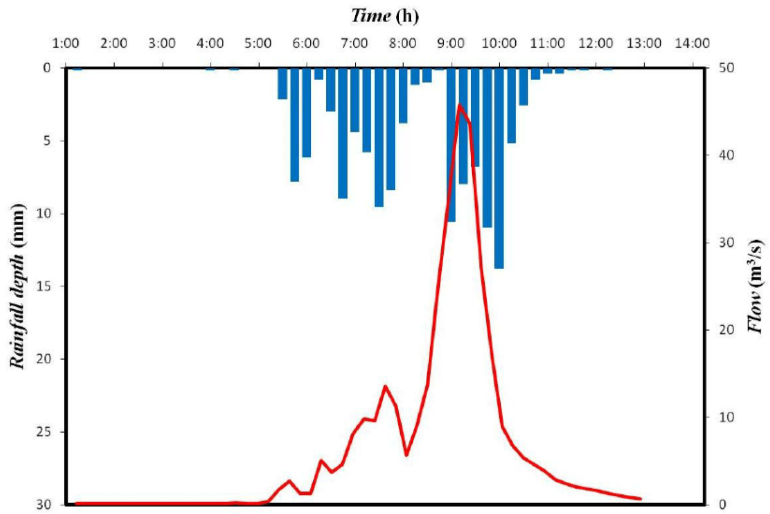

Figure 3: Example of hyetograph and hydrograph from Bellos et al., 2015

For historical flood studies, the flood event and local conditions can be estimated and modeled to the best of available knowledge. However, for generic flood risk assessments, a theoretical flood event must be considered. Flood frequency analysis predict flow values corresponding to return periods. The flood frequency analysis technique consist in a statistical analysis (e.g. mean, standard deviation, skewness) of annual peak flow data. Then, the best fit of the data as a PDF (e.g. Gumbel, Normal, Log-normal, Exponential, Weibull, Pearson, and Log-Pearson) is chosen. As a result, we can plot flood frequency curves to estimate of the intensity of a flood event (Moges et al., 2019).

The selection of a suitable return period is of debate, but typically the 1 in 100 year event is used. The maximum return period considered also has an impact on annual flood risk estimate as shown by Ward et al., 2011 who noticed an increase of the economical risk as the maximum return period used increases.

Levee performance

Among the various flood defence structures found in a watershed, we focus on levees as Bomers et al., 2019 noticed that the effects of levee breaches on downstream discharge are not addressed in flood safety assessments. They estimated the impact of levee failure on a flood assessment and studied how levee breaches and overflow affect flow discharge. Extreme discharges increases flood risk along the river branch, while flood risk along the other river branches is reduced. Therefore, levee breaches should be included in flood safety assessments.

Levees are longitudinal structures that can stretch over several kilometers. CIRIA et al., 2013 details the steps required to assess levee reliability: the division into homogeneous segments of the levee as described in Royet et al., 2012 and the performance assessment of each segment for different failure mechanisms considering the levee structure weaknesses, which results in several failure probabilities (CIRIA et al., 2013). An additional step can be added, which aggregates levee failure probabilities of several mechanisms into one fragility curve for each levee segment (Allard et al., 2012). The method to assess levee performance is displayed in Figure 4 and based on the French National Project “CriTerre” and the ERINOH (Internal Erosion in Hydraulic Earthworks) project. A similar proposal is also included in the Geophysical Monitoring System (GMS) methodology from Zuzana Boukalová, 2008.

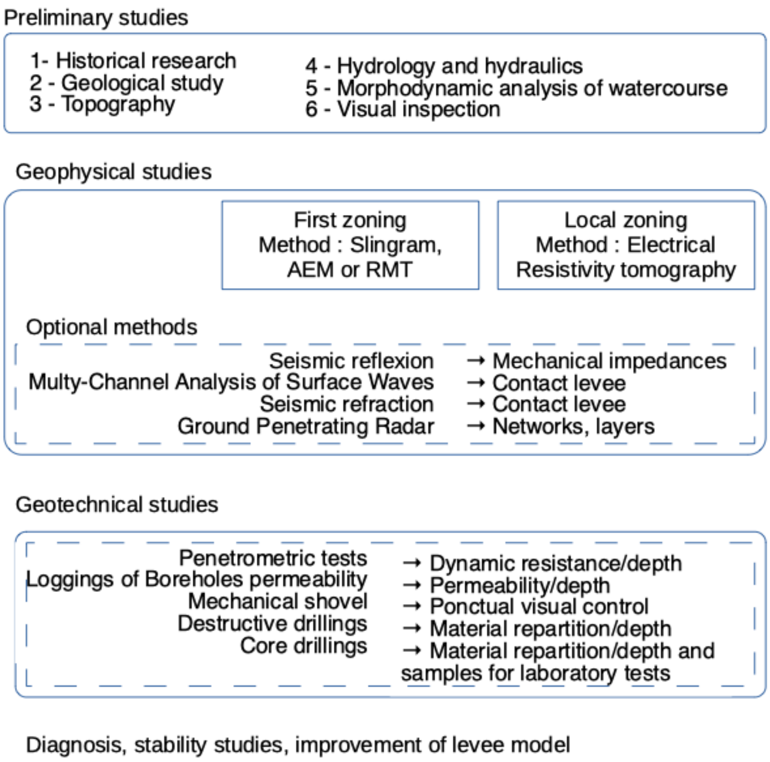

Figure 4: Methods to assess levee systems from Fauchard et al., 2007 and Damien et al., 2008

Levee segmentation

Roscoe et al., 2020 described the length effect phenomenon: as the length increases, there is a larger distance over which a weak spot in the levee can occur, thus a higher probability of failure. They quantified the length effect using the "modified outcrossing method" which relies on a bayesian network. Therefore, it influences levee breach locations, hence flood propagation, and should be carefully considered.
Methods to discretize levee segments either follow constant or variable length, and may consider singularities such as tree covered areas (roots offer a preferential infiltration path to water and weaken levee structures), or pipes going through the levee.

Constant length approach was used by Bowles et al., 2012 in their risk analysis, segmenting the levee every 500 m and assuming that all segments are independent. Or in the Cardigues project presented by Durand et al., 2016. In Japan, a constant length of 1 km levee is assumed, with detailed investigation performed each kilometer. However, geomorphologic data varies within 1 km, therefore Takahara et al., 2016 used expert judgment based on geomorphologic data to segment levees (Figure 5).

The variable length approach can be characterized by either expert judgment or geotechnical data based levee segmentation. Guidance for expert judgment segmentation was proposed by the U.S. Army Corps of Engineers in US Bureau of Reclamation, 2011 and discretize based on statistically independent levee segments.

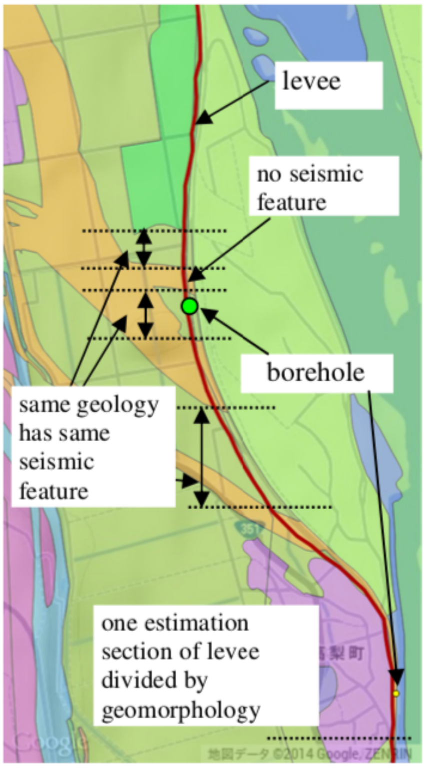

Figure 5: Levee segmentation based on geomorphologic data by Takahara et al., 2016

Picton, 2019 applied the geotechnical data based automatic levee segmentation presented by Vuillet et al., 2012, where levee segments are divided on a scale of 0 to 10 for each performance criteria defined in the study. Vuillet et al., 2012 suggest that a decision-making procedure to split levees into homogeneous sections according to their performance level. The uni-criterion method assess global performance of levee segments using the minimum operator to aggregate all four break mechanism performance levels into one global level criterion (Figure 6).

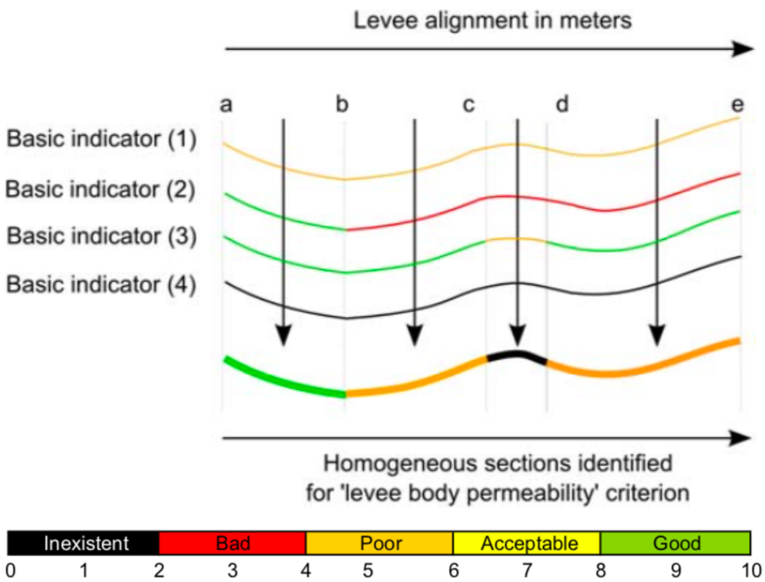

Figure 6: Levee segmentation based on on the permeability criteria by Vuillet et al., 2012

This dissertation, we use variable expert judgment levee length segmentation based on geotechnical parameters and geometry. First, a linear segmentation by type hydraulic structure (levee, storm surge barrier, dam) is based from visuals. Then, geomorphologic classification is used to divide into homogeneous geomorphological segments each levee. Then, geometrical characteristics (e.g. crest height, base angle, slopes) provide an additional level of precision for the levee system segmentation. Finally, the geotechnical layer is considered, discretizing levee segment by soil properties (e.g. cohesion, friction angle) based on investigation reports or literature. For levee segments without any available data, we assume that same geomorphologic classification leads to the same geotechnical properties. If the hereby segmentation results in too many segments, a combination of close segments may be considered.

We suggest the exploration of the concept of "hydrologic segmentation" defined as having a levee system segmentation based on equivalent damage values over the area exposed to a breach of the levee segment. This hydrologic segmentation can be incorporated in a retroactive loop as it requires prior flood assessment knowledge over the designated area. We acknowledge that damage quantification is subject to variations over time triggered by renovations, change in land use, or type of exposure considered.

Levee failure mechanisms

Levee failure mechanisms lead to hydraulic failures such as overtopping or overflowing, and mechanical failures such as external and internal erosion, and slope instability as presented in ERINOH, 2017 (Figure 7).

Overtopping and overflow occur when a flood event water level exceeds the one for which the levee structure was designed. Overtopping is associated with waves and corresponds to coastal levees built perpendicular to the water flow, while overflowing is associated with water levels exceeding the levee crest and correspond to levees parallel to a river or stream.

Levee mechanical failures depend on materials composing the levee, which is determined by a geotechnical assessment. Levee structures are usually made of local soils. Therefore, bulk density γ ($kN.m^{-3}$), soil cohesion c (kPa or $10^{-3}.kg.m^{-1}.s^{-2}$), soil friction angle φ (^{o}), and permeability k ($cm.s^{-1}$) are parameters of interest along with other geotechnical parameters such as the elasticity or Young module E (Pa or $N.m^2$ or $kg.m^{-1}.s^{-2}$) or Poisson's ratio ν ($\emptyset$).

Wave and tide are the main mechanisms initiating external erosion, thus are not considered in this dissertation following the assumption that the impact of waves on a levee structure parallel to a water flow is limited. Internal erosion knowledge of the processes that occur within the soil matrix is still limited, specially the erosion propagation mechanisms. K. T. Lee et al., 2009 uses an analytical method coupled to an infinite slope model to predict landslides. The ERINOH, 2017 research project (2006 – 2012) provided a database of levee failures on the Rhone river caused by breaching from 1993, 1994, 2002, and 2003. Initiating mechanisms identified consisted in 84% due to overtopping and 16% due to internal erosion.

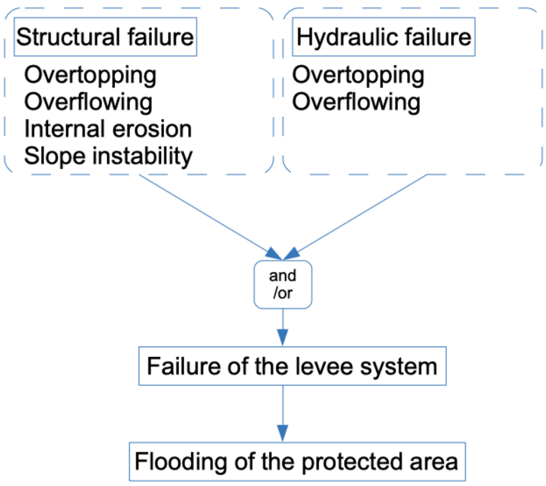

Figure 7: Levee failure mechanisms schematic from ERINOH, 2017

The deterioration or damage threshold is referred to as Service Limit State (SLS) and the breaking threshold to the Ultimate Limit State (ULS). The kinematic of backward erosion mechanisms can be progressive for erosion mechanisms or sudden for the sliding mechanism as in Figure 8. CIRIA et al., 2013 refer to levee breach during a flood event as a fast failure, although preceded by an initiation phase.

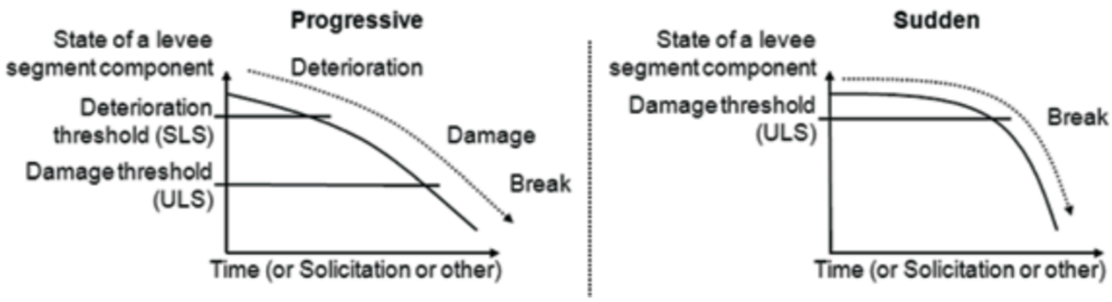

Figure 8: Kinematics of a failure mechanism @ R. Tourment, INRAE and Y. Deniaud, CETMEF)

Each failure mechanism will be presented in more depth along with methods commonly used to quantify them. First the overtopping and overflowing failure, followed by internal erosion mechanisms and finally sliding failure.

Visser, 1998 investigated the breaching process of overtopping, and overflowing structural failure, and associate overtopping with waves, while overflowing refers to water levels higher than the hydraulic structure crest (Figure 9). We must distinguish between overtopping as a hydraulic failure and structural failure. CIRIA et al., 2013, describes overtopping and overflowing hydraulic failure as the levee being overflown before reaching the designed protection level. On the other hand, overtopping and overflowing as a structural failure consist in surface erosion of the levee material on the protected-side of the levee, potentially leading to breaching of the levee.

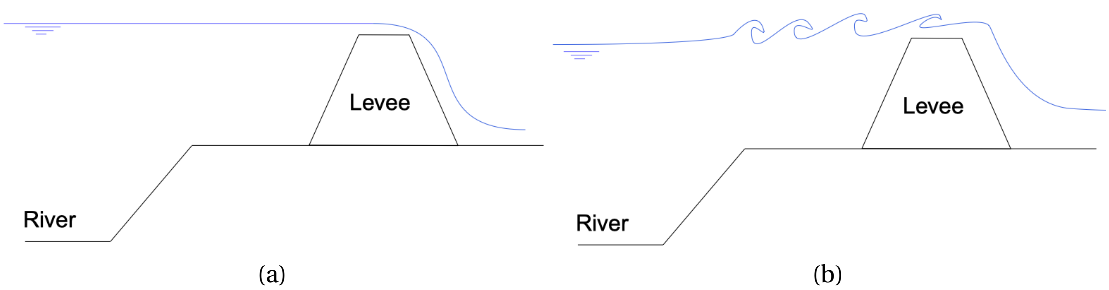

Figure 9: (a) Overflow mechanism; (b) Overtopping mechanism

When considering levee failure due to overtopping or overflow, there are two component to the hydraulic discharge: the regular overflow of the levee structure, and the flow through the breach opening. Formentin et al., 2018 proposed a prediction model to estimate average overtopping levee discharge valid for over-washed and fully breached levees, but the hydraulic discharge computation is usually dictated by the software used for flood propagation. The parameter which influences hydraulic discharge is the breach opening in itself, statistical and modeling approaches are available in literature for both overtopping and overflowing induced levee failures.

A simple method to assess the discharge for random waves was developed for smooth slopes by Hydraulics Research Station, 1980 and presented in Equation 0.3.

$$Q^* = Ae^{-B\frac{R^*}{r}} \tag{0.3}$$

With the dimensionless parameters of the wave discharge $Q^* = \frac{q}{gT_mH_s}$ and the freeboard $R^* = \frac{R_c}{T_m(gH_s)^{0.5}}$, R_c the freeboard, H_s and T_m wave parameters. r correspond to the roughness coefficient, and A, B to the slope angle coefficients found in Table 1.

Slope	A	B
1:1.0	0.0079	20.1
1:1.5	0.0102	20.1
1:2.0	0.0125	22.1
1:3.0	0.0163	31.9
1:4.0	0.0192	47.0

Table 1: from Hydraulics Research Station, 1980

Alhasan et al., 2016 presented a probabilistic overtopping breaching of a river levee, the overtopping breaching mechanism presented in Figure 10. Overtopping was simulated using simple surface hydraulics equations (Equations 0.4 and 0.5), while the levee erosion model consisted in soil transport equations used with erosion parameters calibrated with historical data.

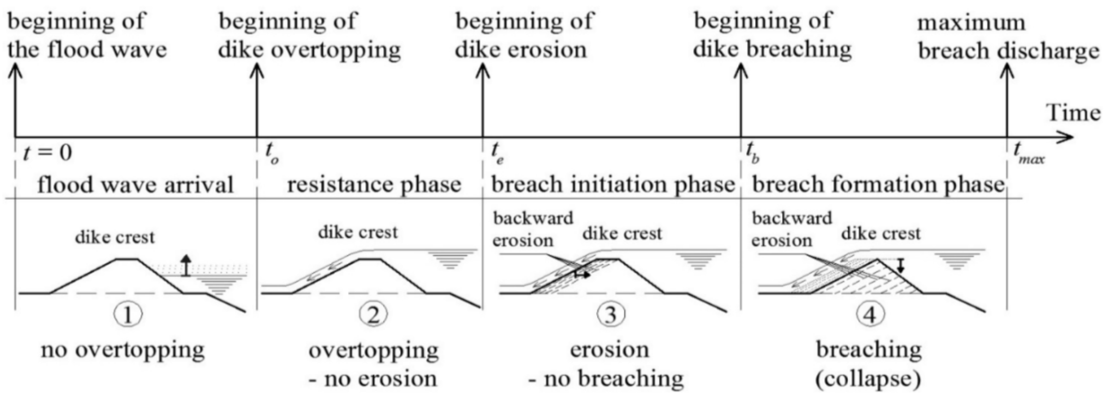

Figure 10: Breach by overtopping mechanism by Alhasan et al., 2016

They describe water flow during levee overtopping with the overflow head $h(t)$ as the difference between the water level in the river $h_s(t)$ (a constant along the breach opening) and the elevation of levee crest Z_c (or the elevation of breach opening bottom $Z(t)$ during the erosion process).

$$h(t) = h_s(t) - Z_c \tag{0.4}$$

$$Q_b = m \cdot b \cdot h^{\frac{3}{2}} \cdot \sqrt{2g} \tag{0.5}$$

Q_b the flow discharge over or through the levee breach, $b(t)$ the breach width, m the discharge coefficient for a broad crested weir, and g the gravity acceleration.
On the other hand, ERINOH, 2017 provides an average breach width due to overtopping failure as $190m$ long for a maximum of $740m$.

A levee failure due to overflow consist in flow of water eroding the inner slope, which initiate breaching as described by Fujisawa et al., 2007 who proposed experimental levee observations to understand the failure due to overflow.

A hydraulic levee failure by overflow as described by CIRIA et al., 2013 provides a simplified method to estimate uniform overflow discharge of a broad-crested levee with Equation 0.6.

$$Q = q \cdot L = C_d H^{\frac{3}{2}} L \tag{0.6}$$

With $Q(m^3.s^{-1})$ the total discharge, and $q(m^3.s^{-1}.m^{-1})$ the unit discharge per length of overtopped levee, $L(m)$ the overflow length, $H(m)$ the head above the crest of the levee, and C_d the weir discharge coefficient for which Hager, 1987 developed an estimation method but other approximation such as Bazin Equation 0.7 and Rahbock Equation 0.8 are commonly used.

$$C_d = 0.405 + \frac{0.003}{H + H_a} \tag{0.7}$$

With $H(m)$ the head of water above the levee crest and H_a the additional water head due to velocity of approach.

$$C_d = 0.605 + 0.08\frac{H}{z} + \frac{0.001}{H} \tag{0.8}$$

With $H(m)$ the head of water above the levee crest and $z(m)$ the crest height.

Internal erosion is the transport of soil particles detached by seepage flow within a structure as in Figure 12. CIRIA et al., 2013 and Bonelli, 2012 identify piping or backward erosion, concentrated leak erosion, contact erosion, and suffusion as the main internal erosion mechanisms. Backward erosion (a.k.a. piping) begins at the exit point of seepage through the levee and drills a continuous passage as the seepage hydraulic gradient exceeds the flotation gradient of the soil as in Figure 11.a. Concentrated leak erosion requires an open channel for water to seep through the levee body. The erosion occurs on the sides of the channel when the shear stress induced by the flow velocity exceeds a critical value as in Figure 11.b. Contact erosion requires a fine soil and coarse soil boundary. This erosion mechanism consist in fine soil being washed into coarse soil by horizontal water flow as in Figure 11.c. Suffusion consist in fine soils being washed away by seepage leading only coarse soil matrix behind as in Figure 11.d.

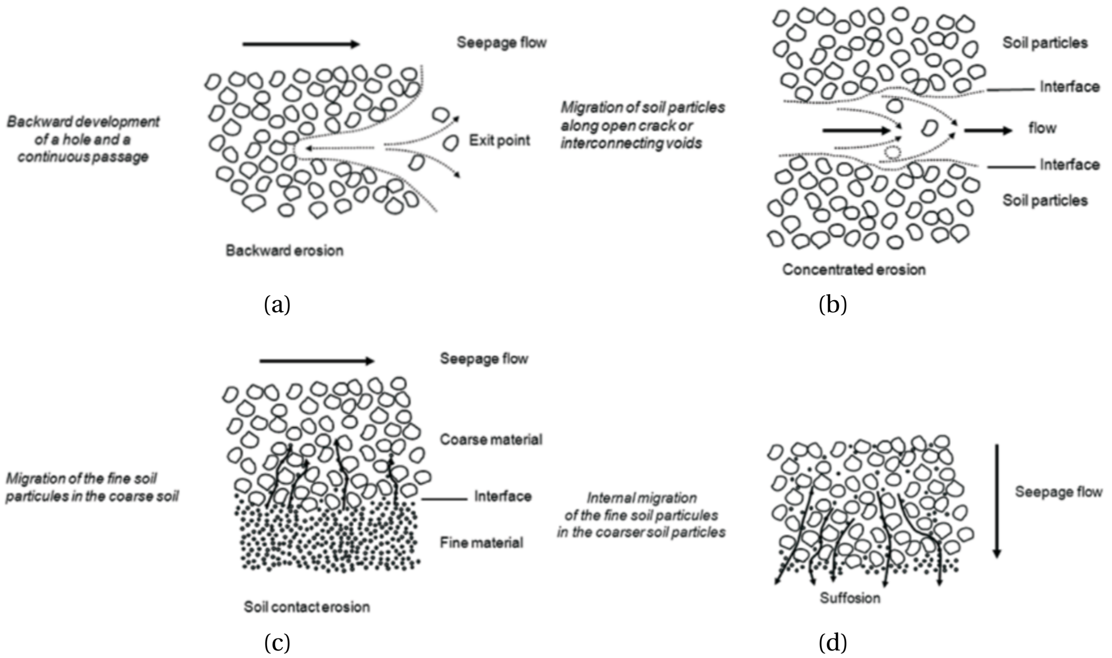

Figure 11: (a) Backward erosion, (b) Concentrated leak erosion, (c) Contact erosion, and (d) Suffusion internal erosion mechanisms from CIRIA et al., 2013 and Bonelli, 2012

Initially aiming to consider all internal erosion mechanisms, available data and current knowledge turned the focus to backward erosion as statistical data from ERINOH, 2017 showed that some mechanisms may be more prevalent than others.
Moreover, due to the lack of models on internal erosion evolution over time and no consensus within the research community. We consider a conservative hypothesis once the critical gradient is reached, the breach suddenly opens.

Though engineering guidance considers that gradients less than 1.0 are generally safe, particle transport can occurs before reaching this critical gradient (K. S. Richards et al., 2007, Skempton et al., 1994, Van Beek et al., 2014). For instance, Skempton et al., 1994 showed that for homogeneous unstable sandy gravels, backward erosion can be initiated for hydraulic gradients one third to one fifth of the theoretical critical gradient. In future works, a study considering a percentage of the critical gradient value could be interesting. As a first approach, we could consider around 50-60% of the critical gradient.

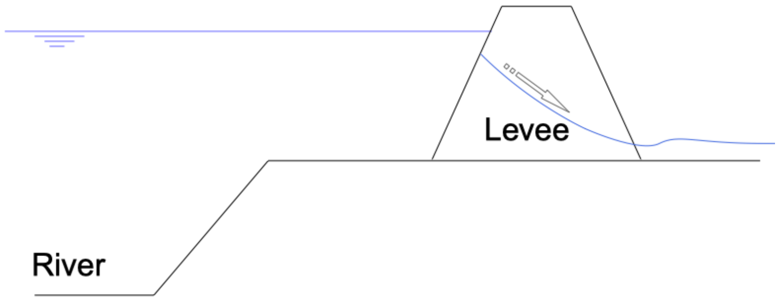

Figure 12: Internal erosion: backward erosion mechanism

The criteria for the initiation and progression of backward erosion can be estimated through a local hydraulic gradient or a global hydraulic gradient averaged along the flow path.
Heave is a special case of local backward erosion for a horizontal pervious soil layer combined with a vertical upward flow. The upward seepage due to differential head equals the overlying buoyant weight of soil as shown in Equation 0.9.

$$\beta \leq \varphi' - \sin^{-1}\left(\frac{i}{i_{cr}}\sin\left(\varphi' + \lambda\right)\right) \tag{0.9}$$

Where $i_{cr} = \frac{\gamma'}{\gamma_w}$ Terzaghi's critical gradient. $\beta = 0$ corresponding to a horizontal soil layer, and $\lambda = 0$ corresponding to a vertical upward flow.

Uplift is a special case of local backward erosion for an impervious soil layer in which cracks develop, described by the equation 0.10.

$$\sigma_v > u \tag{0.10}$$

Where $\sigma_v(kPa)$ correspond to the vertical stress, and $u(kPa)$ the pore water pressure underneath the imperious soil layer.

Global criteria models only apply to backward erosion in a sandy layer below an impermeable roof. The concept of length of the path travelled by seeping water $L_h(m)$ led to creep factors C_x, and $h_t(m)$ the top layer thickness as shown in Figure 13.

Other models to estimate backward erosion failure considering a global gradient. Bligh, 1927 propose the Equation 0.11 as a criteria for backward erosion failure.

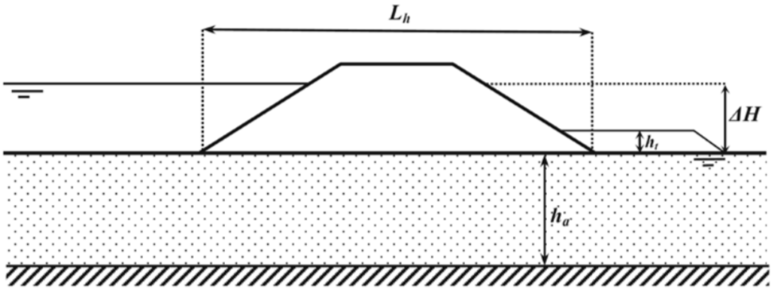

Figure 13: Global gradient parameters required for the determination of backward erosion from CIRIA et al., 2013

$$\Delta H - 0.3h_t > \frac{L_h}{C_{Bligh}} \tag{0.11}$$

With $\Delta H(m)$ the hydraulic head over the levee, C_{Blight} the creep factor of Bligh.

Lane, 1935 adapted the Bligh model to Equation 0.12 fitting the presence of an extra structure of length $L_v(m)$, which would cause a barrier for the seepage path. C_{Lane} depending on the type of soil.

$$\Delta H - 0.3h_t > \frac{\frac{L_h}{3} + L_v}{C_{Lane}} \tag{0.12}$$

Other models such as J. B. Sellmeijer et al., 1991, Hoffmans, 2022 or Schmertmann, 2000's also provide backward erosion estimation methods.

In ERINOH, 2017, breach width due to internal erosion vary from 3 m to 65 m with an average of 21 m, while in Özer et al., 2020, failures due to instability and internal erosion are less frequent but lead to larger breaches. Statistically, studies do not account for the risk associated with breaching as a less frequent occurrence is assumed being balanced by the bigger impact a breach have on its surroundings.

To go further, it is possible to consider other internal erosion failure mechanisms such as concentrated leak erosion by considering an additional safety coefficient for contributing factors such as animal burrows, tree roots, pipes due to human activity or other structures going through the levee. These data need to be collected on-site.

Slope instability (a.k.a. sliding) mechanism can be triggered by gravity or external actions when the shear stress applied on the levee slopes exceed the shear strength to levee materials. Engineers calculate the safety factor as the ratio between resistance forces over the stresses as shown in Equation 0.13, $F_s \leq 1$ implying a structure failure.

$$F_s = \frac{Resistance}{Stress} = \frac{\tau}{\tau_{eq}} \tag{0.13}$$

With τ the shear stress. Sliding mechanisms are linked to the geometry of a levee cross-section (Figure 14) and can be divided into: shallow sliding, deep rotational sliding, and translational sliding as described in CIRIA et al., 2013.

- Shallow sliding is dependent on the side slopes. The shear strength depends on: characteristics of the material (e.g. clay), moisture content, and compaction degree. Over time, the soil can dry or crack during the summer months forming a preferential pathway for water in the autumn or winter and rendering slopes vulnerable to wave erosion. For steep slopes, this seasonal process reduce the factor of safety against shallow slip failure.

- Deep rotational failure can be triggered by high groundwater pressures acting in a permeable layer beneath the levee or initiated by changes to the levee (e.g. load, water level, local excavation, drainage).

- Translational sliding consist in a horizontal movement of a levee due to weak surface layers in the foundation or the levee. This situation occurs when undrained shear strength of the surface layer can not resist hydraulic forces applied to the levee.

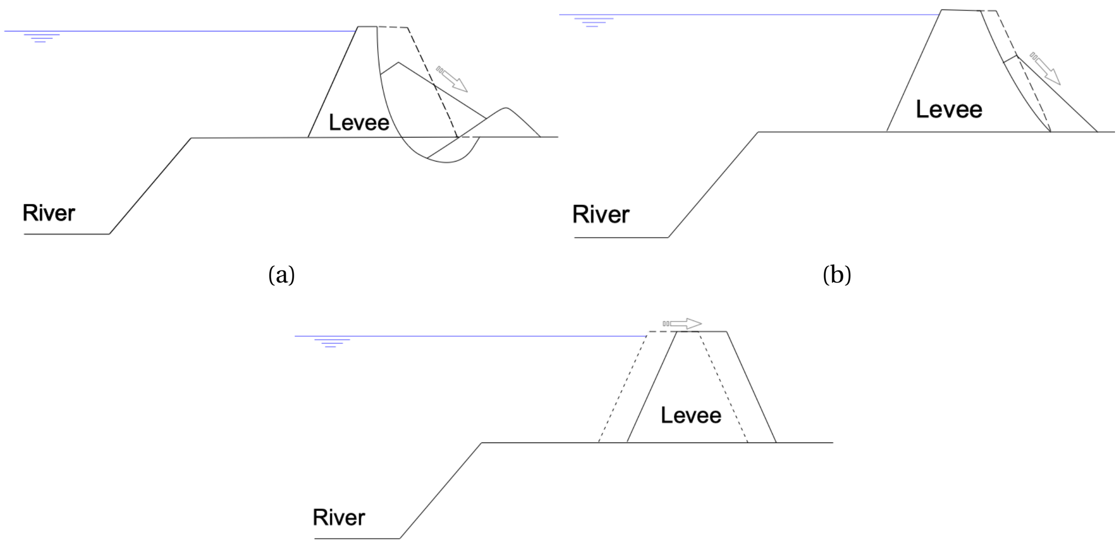

(a) (b) (c)

Figure 14: Slope instability mechanisms: (a) shallow sliding, (b) deep rotational sliding, (c) translational sliding schematics

Contributing factors to slope instability include: load variation, human activity, tree roots, animal activity, and seismicity. Load variation such as soil saturation may cause an increase in weight and decreases the shear strength resistance of the levee, hence, poorly compacted soils seem at higher risk of failure due to the volume of void the water can fill. Human activity such as construction activity near a levee may steepen slopes, add singularities such as pipes, liquefaction of the soil may be triggered by vibrations, and loss of vegetation increase external erosion. Animal activity such as burrows can induce piping, so does tree roots once decayed may result in instabilities or preferential flow routes. Seismic activity can induce soil liquefaction.

Static slope stability analyses use the well-established limit equilibrium method. Other methods such as slope stability design charts developed by Janbu et al., 1973 can be used for preliminary analyses but need to be completed by a more complete analysis. Uncertainties of such methods stems mainly from the accuracy of geometry, pore water pressure, and soil properties rather than from the approximations of analytical method.
The limit equilibrium approach is adaptable to various soil and loading conditions. The limit equilibrium method is considered in a 2D plane where the soil slides on a slip surface using the Mohr-Coulomb criteria. A factor of safety is computed based on force or moment equilibrium equations. There are three types of limit equilibrium assessment methods:

1. Graphic methods are based on a single shape of slip surface and useful for first approximations.
2. Slices and blocks methods divide the slope into slices and require inter-slice forces assumptions to solve the force and moment equilibrium equations.
3. Perturbations methods require assumptions of the normal stress distribution along the slip surface.

The methods of slices divides the sliding area into n vertical slices (Figure 15). The mechanical equilibrium is written using the Mohr-Coulomb criteria (Equation 0.14). Solving the vertical and horizontal forces Equations 0.15 complemented by the moment equilibrium Equation 0.16 require many assumptions which is what the different slice methods differ in.

$$\tau = c' + (\sigma - u)\,tan\varphi' \tag{0.14}$$

With τ shear strength, c the cohesion, σ normal forces, φ the angle of friction, and u the interstitial pressure.

$$F_{S,f} = \frac{\sum_{i=1}^{n} cos\alpha_i (c_i b_i + (N_i - U_i)\,tan\varphi_i)}{\sum_{i=1}^{n} k_c W_i + N_i sin\alpha_i} \tag{0.15}$$

$$F_{S,m} = \frac{\sum_{i=1}^{n} (y_{Pi} cos\alpha_i + x_{Pi} sin\alpha_i)(c_i b_i + (N_i - U_i)\,tan\varphi_i)}{\sum_{i=1}^{n} W_i (x_{Gi} + k_c y_{Gi}) + N_i (x_{Pi} cos\alpha_i - y_{Pi} sin\alpha_i)} \tag{0.16}$$

With X_i the vertical inter-slice forces, E_i the horizontal inter-slice forces, N_i the normal reaction on the slice base, and T_i the tangential reaction.

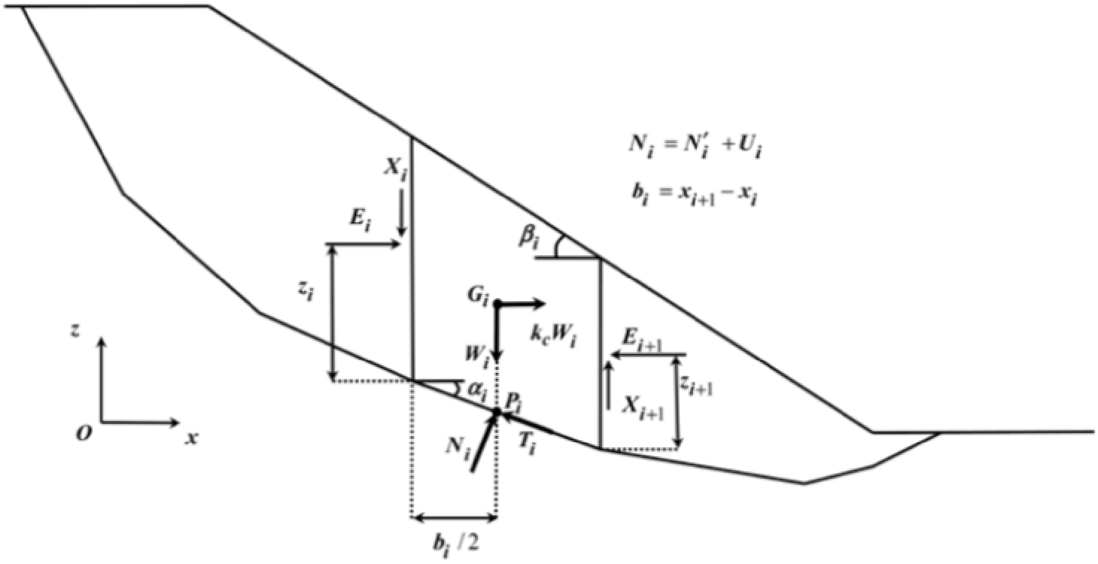

Figure 15: Slice method schematics from CIRIA et al., 2013

Simplification methods to solve static equations include Fellenius, Bishop simplified, Carter, Janbu simplified, USACE, Lowe-Karafiath, Spencer, Morgenstern-Price, Janbu rigorous, and General multi-block described in Table 2 as referenced in GeoStudio, 2021a and CIRIA et al., 2013.
In geotechnical engineering, limit equilibrium methods have shown great accuracy and guidelines are provided. Slice limit equilibrium methods drawbacks are described by Griffiths et al., 1999, listing hypotheses taken on the number of slices, the security factor, which is considered identical along the sliding surface and not physically accurate, the circular sliding surface assumption, and the soil variability that is not taken into account (see section).

Soil saturation impacts levee failure probability estimations. The conservative approach consist in considering saturated soils for which water circulates sooner than for unsaturated soils. Soil is a three phase material (Figure 16) containing solid, liquid, and gaseous. The soil discretize between soil particle, adhesion water, cohesion water, free water, and air pores. Free water refers to water under the phreatic table which is not bounded to any particle. Cohesion water refers to water in partially saturated soils and mets an equilibrium brought by gravity and tension forces.

Slice methods	**Assumptions to solve force and moment equilibriums**
Fellenius	Inter-slice forces neglected
Bishop simplified	Resultant of inter-slice forces horizontal
Carter	Resultant of inter-slice forces horizontal
Janbu simplified	Resultant of inter-slice forces horizontal and correction factor to account inter-slice shear force
USACE	Direction of resultant inter-slice forces parallel to the ground surface
Lowe-Karafiath	Direction of resultant inter-slice forces equal to the average of the ground surface and slope of the base of the slip surface
Spencer	Resultant inter-slice forces are of constant slope throughout the sliding mass
Morgenstern-Price	Direction of the inter-slice forces defined using an arbitrary function
Janbu rigorous	Location of the horizontal inter-slice force is defined by an assumed line of thrust
General multi-block	The shear strength is mobilized on the sides of all inclined slices

Table 2: Limit equilibrium method simplification methods (CIRIA et al., 2013)

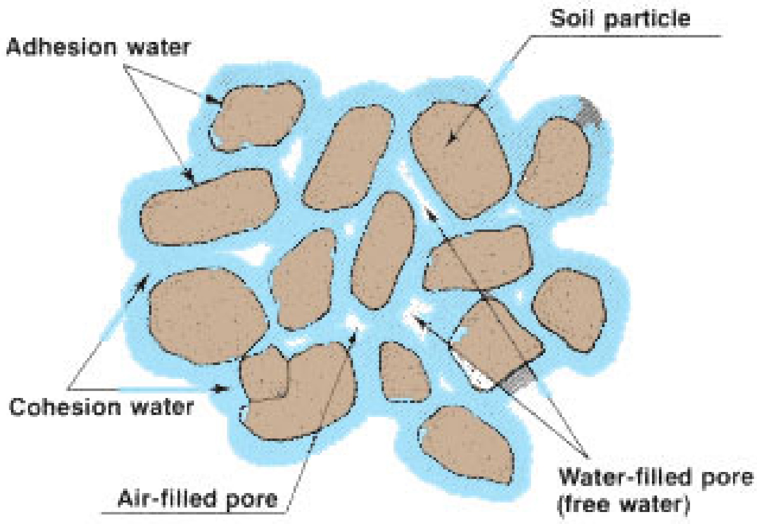

Figure 16: Type of water

Flow equations for saturated and unsaturated soils are described following Darcy's law shown in Equation 0.17.

$$\underline{v} = k \cdot \underline{i} \tag{0.17}$$

With the tensor $\underline{v}$ representing flow velocity, k the hydraulic conductivity (or permeability) coefficient, and the tensor $\underline{i} = -grad(H)$, H being the hydraulic gradient described in Equation 0.18.

$$H = \frac{u}{\gamma_w} + z \tag{0.18}$$

With u the pore pressure based on the water height z, and γ_w the water bulk density.

To model the transient flow of water in unsaturated soils, Darcy's law is adapted to Richard's Equation 0.19 (L. A. Richards, 1931).

$$C(u)\frac{\partial H}{\partial t} = -div(\underline{v}) = -div(-k(u).grad H) \tag{0.19}$$

With k, now a variable, is dependent on pore pressure, $C(u)$ is the capillary capacity.

Uncertainty in soil properties

Taking into account soil variability is difficult. We can consider 2 types of soil variability: the vertical variability and the one in the length of the levee. First, the vertical soil variability, represented by the anisotropy parameter. Anisotropy refers to a material property with different properties in different directions. For an earthen levee, the permeability, shear strength, or compressibility of the soil may vary depending on the direction. This anisotropy can be influenced by the arrangement of soil particles, the loading or consolidation history. This is particularly relevant when records show that the levee was raised over the years by adding material to the existing levee. Farshid et al., 2020 shows that climate change, thus changing environmental conditions, has an impact on material behavior. Other studies such as Abdulazim et al., 2009 characterize anisotropic properties to better understand how they contribute to failure scenarios.

Second, the spatial variability represented in the length of the levee. A first approach to consider spatial variability is to divide a levee into homogeneous segments. By so doing, different soil parameters can be attributed to each segment (Elenas et al., 2013). However, there is a limit to how finely the soil model can be discretized. Therefore, we can use probabilistic methods to account for soil variability as in Zhan et al., 2023, Ji et al., 2014, or Sibley et al., 2017.

Flood propagation

A flood propagation simulation consist in a numerical hydraulic model, usually running for supercritical water flow, and resulting in flood maps named in this dissertation flood *hazard* maps to avoid the confusion with flood *risk* maps as this dissertation covers several research fields.

To better understand flood propagation, Teng et al., 2017 provides a substantial review of flood models and distinguish between: empirical methods, hydrodynamic models, and simplified conceptual models. Empirical methods include surveys, remote sensing, and statistical models. They are data-based methods, which requires a heavy amount of reliable data and are specific to a given location. Hydrodynamic models solve physics equations to compute water propagation. Depending on the floodplain terrain and the water flow, those models are divided into 1D, 2D, or 3D models. The choice of which model to use depends on the scale and objective. Many research fields (e.g. civil engineering, hydrology, hydraulic) make use of these these models. Simplified conceptual models are simplified hydrodynamic models with shorter run times and preferred for large scale study areas, data sparse regions, stochastic modeling, and showed a recent increase in popularity. Maranzoni et al., 2023 provides a review of flood hazard assessment methods, dividing them into heuristic, conceptual, and empirical approaches, while flood maps can be either deterministic or probabilistic. Maranzoni et al., 2022 considers the probabilistic flood hazard for multiple levee breaches. Classic softwares such as in Table 3 are available for flood modeling.

Software	Modeling capacities	Status	Developers
TUFLOW ($-Classic$, $-FV$)	1D, 2D, 3D, 1D/2D	Commercial	BMT WBM
SOBEK Suite	1D, 2D, 1D/2D	Commercial	DELTARES
MIKE ($-+$, -11, -21, -3, $-Flood$)	1D, 2D, 3D, 1D/2D	Commercial	DHI
TELEMAC ($-2D$, $-3D$, MASCARET, ARTEMIS, TOMAWAC)	1D, 2D, 3D	Open source	EDF
HEC-RAS ($-2D$, $GEO-$)	1D, 2D, 1D/2D, 2D/3D	Free	US Army Corps of Engineers
LISFLOOD-FP	2D, 1D/2D	Research	University of Bristol
Flood Modeler ($-Pro$)	1D, 2D, Simplified conceptual	Commercial	CH2M Hill
DELFT 3D	2D, 3D	Open source	DELTARES
XPS ($-2D$, $-SWMM$, $-STORM$)	2D, 1D/2D	Commercial	XP Solutions
OpenFlows FLOOD	1D, 2D, 1D/2D	Commercial	Bentley

Table 3: List of flood modeling softwares with their characteristics

To quantify the flood, several parameters can be taken into account, water depth being the most common but other include water velocity, flooding duration, flood arrival time, return period, flow discharge, sediments transportation, hydraulic structure breaching, scenario probability, flowing debris, and people behavior (e.g. evacuation time, traffic modeling, building occupancy).
This dissertation uses a physics-based model providing depth and velocity values with the HEC-RAS software.

Vulnerability assessments and risk attribution

The concept of flood risk can be formalized in many ways each involving the concept of hazard and vulnerability with sometime additional elements (e.g. resilience, consequences, exposure, preparedness) to fit the research field that uses it (Thywissen, 2006, Solin et al., 2013, Meyer et al., 2009, Soldati et al., 2022). In this dissertation, we will consider flood risk as the combination of flood hazard, exposure, and vulnerability (Equation 0.20).

$$\text{risk} = \text{hazard}x(\text{exposure x vulnerability}) \tag{0.20}$$

Flood hazard refers to the potential for flooding to occur in a given area. Flood is a dynamic phenomenon influenced by rainfall intensity, river discharge, climate change, and topography. Assessing a flood consist in 2 main steps (Solin et al., 2013): (i) assess annual maximum discharges and their corresponding water levels (see section), (ii) model and propagate the flood to estimate the extent of the flood and the value of flood parameters such as flood depth or flow velocity (see section). Exposure refers to the quantity or assets impacted by a flood hazard: population density, number of people's dwellings, businesses, national heritage buildings (cultural assets), transportation (e.g. roads, bridges) and communication means (e.g. electric lines), critical infrastructures (e.g. hospitals, utilities) as referred by Solin et al., 2013, El Bilali et al., 2022, and Cardona et al., 2012. This type of data can be sorted in 3 categories: social, economic, and environmental. Exposure datasets are derived from population and household census databases, urban planning documents, or satellite imagery.

There are many definition of vulnerability depending on the field and context, some of which are listed in Table 4 (Chan et al., 2022, Nasiri et al., 2016). As exposure, the concept of vulnerability is divided in 3 types: economical, social, and environmental.

In this dissertation, the vulnerability represents the damage extent to which an exposed element is subjected when a hazardous event occurs (Samuels, Gouldby, et al., 2009). Therefore, a vulnerability assessment consist in estimating the potential damage to exposed elements (social, economic, or environmental) and their ability to withstand flood hazard. Vulnerability qualitative methods relies on interviews and surveys to explore the social and economical component of flood vulnerability. In this sense, it builds up data for quantitative assessments of flood vulnerability. The toolshed for qualitative assessment include:

- Interviewing local authorities and stakeholders to gather firsthand information on flooding perceptions
- Group discussions or community survey to gather local knowledge regarding flood vulnerability and estimate population awareness.
- Cultural heritage assessment (i.e. explore traditional knowledge and indigenous practices around flood resilience)
- Ethnographic studies to analyze the effectiveness of policies and understand social and governance structure dynamics
- Develop vulnerability indexes

There are many vulnerability criteria, some of which include: population age, income level, household type, building economic value (Tanoue et al., 2016), natural resources indicators, Population At Risk (PAR) which can be estimated by a Agent-Based Model (ABM) (El Bilali et al., 2022), or buildings structural integrity and their resistance to flood damage (based on construction materials), which is often assessed using land-use data when a detailed survey is not available. An application of vulnerability comes

Source	Vulnerability definition
United Nations, 1984	Vulnerability is a degree of damage to a certain objects at flood risk with specified amount and present in a scale from 0 to 1 (no damage to full damage)
Watson et al., 1996	Vulnerability is the extent to which climate change may damage or harm a system. It depends not only on a system's sensitivity but also on its ability to adapt to new climatic conditions
Menoni et al., 1996	Vulnerability term is damage goods, people, buildings, infrastructures and activities in hazard condition
Blaikie et al., 2004	Vulnerability is an assessment of a person's or a group's exposure to the consequences of a threat, as well as their ability to recover from the event's impact
Naess et al., 2006	A function of exposure, sensitivity, and adaptive capacity, generated by multiple factors and processes
Balica et al., 2010	Vulnerability is defined with interaction between exposure, susceptibility and resilience of each community in risk condition
Jongman et al., 2015	Vulnerability are efforts made to reduce the impact of the natural flood hazard (e.g. flood defences, early-warning systems, health care, communication facilities)
Tanoue et al., 2016	Vulnerability is the mortality rate or economic loss rate.

Table 4: Vulnerability definitions in literature

from the Netherlands, where a unique vision of social vulnerability was presented by Jonkman et al., 2010. They defined separately Individual and Societal risk as part of their vulnerability assessment.

Nasiri et al., 2016 provides a review of vulnerability assessment methods applied to flooding. Methods to assess vulnerability include: vulnerability curve method, using indicator based method, analytical hierarchy process, mapping method using Geographic Information System (GIS) (Ebert et al., 2009, Abid et al., 2021). Scussolini et al., 2017 quantify economic impacts with the indicator of direct damage to buildings and their content using the Damage Scanner model, also applied in Koks et al., 2015 and Lasage et al., 2014. Estimating quantitatively damages in in $US\$$ requires land use maps, economic value per unit of area, and depth-damage curves for each land use type. They compute annual damage for flood maps of different return periods, the damages are weighted according to the flood event probability of occurrence. Jonkman, Kok, et al., 2008 analyze flooding risks for the levee ring area South Holland in the Netherlands and estimate of number of fatalities as an annual probability of death due to flooding. Jonkman et al., 2011 identify societal risk as the probability of a flood event with many fatalities. As such, simultaneous flooding events and multiple levee breaching have a significant impact on the societal risk. Scussolini et al., 2017 quantify societal impacts with the indicator of potential casualties (number of people facing life-threatening situations).

A limitation of vulnerability assessment is presented in Nepal Aksha et al., 2018 used the DesInventar database to examine the spatial and temporal patterns of natural hazard mortality. This an approach provides an insight on how the flood events changed. As a result, comparing previous vulnerability assessments with new ones are usually not relevant as cities expand, or climate changes over time. Klijn et al., 2015 pinpoints an interesting misconception about vulnerability and exposure concepts. To some, vulnerability equally refers to persons and property, regardless of the location (in or out of the floodplain). While in Marchand, 2009, vulnerability refers to an entire area including its characteristics like terrain elevation. This approach excludes areas above maximum flood level, swallowing the concept of exposure into vulnerability. Environmental vulnerability as disruption of local fauna and flora is not considered, being part of a different field of study and also due to the difficulties associated with globally applicable criteria and data availability. National Heritage buildings are sometimes considered separately from economic and social vulnerability as in Figueiredo et al., 2021 and Stephenson et al., 2014.

Integrated Flood Risk Management

The elemental bricks that constitute flood risk assessments are well identified and common to all flood risk assessment projects. However, the process covers several specialization fields and is usually handled by different actors. Therefore hypotheses taken during each step of the process adds up to the assessment uncertainties throughout the project. Also, flood risk management stakeholders is fragmented into national, local governments, and private companies, which aims may not be congruent R. Dawson et al., 2008. To ensure coherent management decision on a national scale, UK and the Netherlands centralized flood risk assessments and use integrated flood risk assessment methods. This enables them to better manage data access, uncertainties, and focus on national interests.

In the United Kingdom

In the UK, flood risk management is based on the Flood and Water Management Act of 2010 Parliament of the United Kingdom, 2010, which relate to England and Wales. UK flood risk institutions oversee national scale flood risk management. The governmental strategy is developed by the Department for Environment, Food and Rural Affairs (DEFRA) and the Environment Agency (EA) (Flikweert et al., 2015). DEFRA is a ministerial department aiming to increase the resilience to foods by reducing the likelihood and impact of flooding and coastal erosion on people, businesses, communities, and the environment. DEFRA oversees rainfall levels, imminent flooding, flood warnings, while different services are responsible for flooding in Wales, Scotland, and Northern Ireland. Nevertheless, DEFRA also assesses long term flood risk in England and possible causes of flooding. EA is an executive non-departmental public structure responsible for managing the risk of flooding from main rivers, reservoirs, estuaries, and the sea. while Lead Local Flood Authoritys (LLFAs) are responsible for managing flood risk from surface water, groundwater and ordinary watercourses, and lead on community recovery.

As Hall et al., 2003 outlined challenges to national-scale flood risk assessment were data acquisition, numerical computation, and presentation of results. A decade later, in accordance to their national policy, three Climate Change Risk Assessment (CCRA) reports have been published including flood risk analysis that identify flood risks considering people, property, societies, infrastructure, and nature in the UK (e.g. Sayers et al., 2020). The next National Adaptation Programme (NAP) for England due in 2023, as well as the National Adaptation Program of Scotland, Wales and Northern Ireland.

The UK integrated flood risk assessment is made using the Future Flood Explorer (FFE) model which model flood risk analysis for the UK (England, Wales, Scotland, and Northern Ireland) in regards to coastal, fluvial, surface water, and groundwater flooding. Sayers et al., 2016 describes how the FFE model differs from computation extensive traditional modeling approaches by learning from past national scale studies. The FFE model follows the source, pathway, receptor model and uses nationally available datasets to simulate the flood risk and model future flood risks. Adaptation measures such as flood defence or catchment storage are integrated in the FFE model as well as potential adaptation scenario. Following the floodplain division into cells methodology from Gouldby et al., 2008, FFE Calculation Areas are determined based on the river network, floodplain, and coastline. Outside of floodplains, Calculation Areas are divided into $1km^2$ squares (Penning-Rowsell, 2015) as in Figure 17. The FFE model generates Impact Curves (return period in relation to potential damage based on nationally available data and flood modeling) for each Calculation Area. The FFE model results in annual average damage maps taking into account the influence of climate change and adaption measures through modification of Impact Curves.

Examples of the FFE model is provided by Russell et al., 2022 who modeled several climate change and adaptation scenario showcasing how efficient measures vary depending on location making difficult to find an effective uniform national representation of the risk. Or Sayers et al., 2020 who used the FFE to provide an estimate of future flood risk across the UK using the latest climate projections (UKCP18). Rudd et al., 2017 used the national-scale gridded hydrological model to investigate droughts across Great Britain over the last century, it showed spatial and temporal variability but no changes through time.

Economical flood risk assessment of England and Wales of 2002 is illustrated in Figure 17, and Expected Annual Damages in England and Wales in 2020 and future scenario in 2050 and 2080. The future scenarios are based on a 4^{o}C rise in Global Mean Surface Temperature (GMST) by 2100 relative to pre-industrial times and a high population growth as described in Sayers et al., 2020 and illustrated in Figure 18.

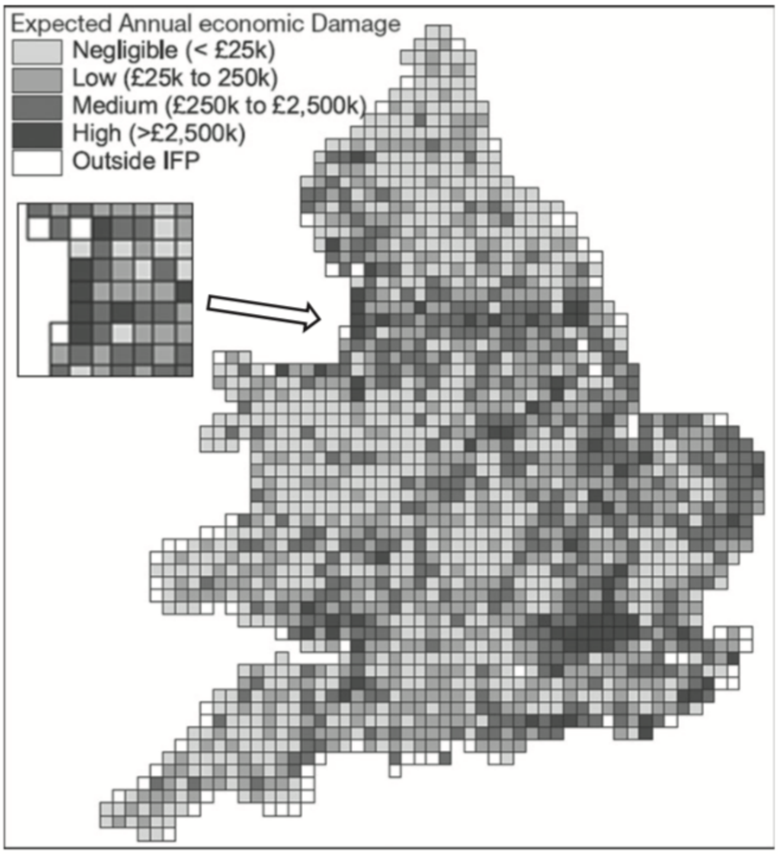

Figure 17: England and Wales economical flood risk assessment for year 2002 from Penning-Rowsell, 2015

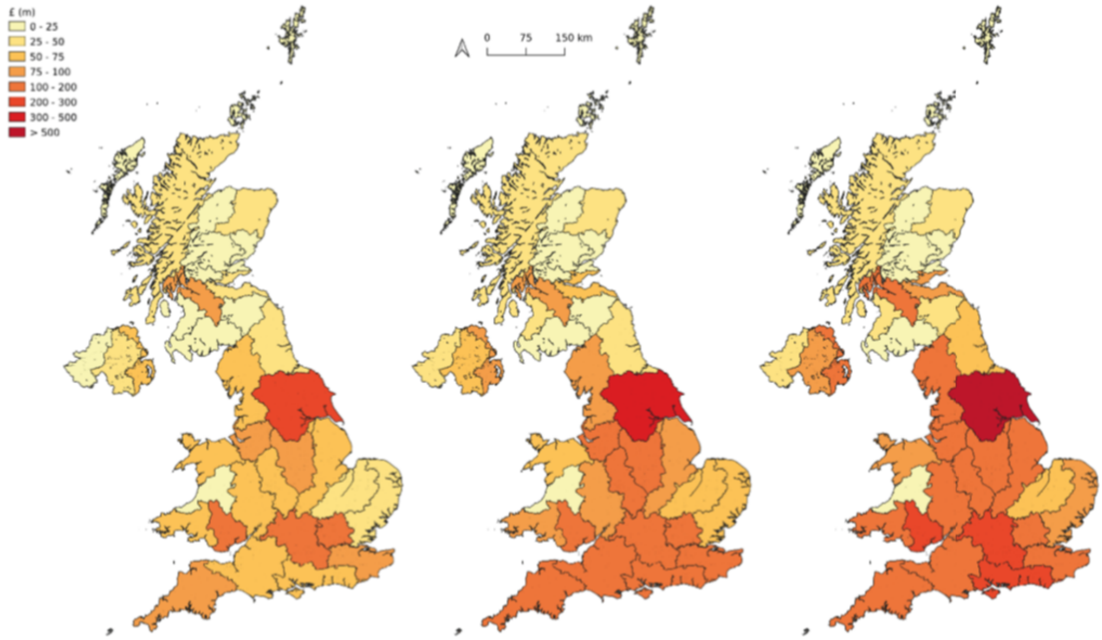

Figure 18: Expected Annual Damages in England and Wales from left to right: 2020, 2050, 2080. Future scenario considering +4^{o}C in GMST by 2100 and high population growth from Sayers et al., 2020

Some limitations of the integrated flood risk assessment method include its applicability is limited to countries with governmental flood risk institutions or other system that ensure data sharing and cooperation between stakeholders. National Audit Office, 2011 showed preliminary obstacles to identify flood risk on a national scale such as: inconsistency in flood mapping representations, risk level categorization, percentage probability to quantify the risk, local knowledge otherwise considered is not easily transferable to national flood risk assessment model, and lack of data about existing defence infrastructures.

In the Netherlands

The Netherlands Ministry of Infrastructure and Water Management is in charge of water safety and flood risk management. The Delta Committee work from 2008 to 2010 to establish a preliminary work to build a robust integrated approach to flood risk management. Since 2011, the Delta Programme directed by an independent Delta Programme Commissioner focus on flood risk management. The governmental institution adapt its strategy to suit recently acquired knowledge. Currently, Delta Programme is involved in fresh water availability and flood protection from sea level rise and extreme weather through strengthening flood defences and lower water levels by launching programs such as Room for the River (RftR). Each year, a report is available and relates any advancement made during the year. Such as in 2018 when

Delta Programme included for the first time Spatial Adaptation as according to KNMI's 14 climate scenario. Or in 2020 when Delta Programme showed insights into the potential acceleration in sea level rise added to the uncertainties of measures beyond 2050.

The Netherlands is located in a delta where the rivers Rhine, Meuse, Scheldt, and Eems drain into the North Sea (Figure 19). The country has low lying coastal areas subject to sea level rise and facing an increase of extreme river discharge expected from climate change. As a result, the country developed a significant amount of flood defences including circular levees, floodgates, sand dunes, and dams. However the in 2007, Hurricane Katrina triggered made the scientific community reflect on the consequences of the "complete flooding protection" approach commonly assumed at the time (Jonkman, Stive, et al., 2009). As response, the flood safety program RftR transitioned to a large-scale to be implemented into IFRM as described in van Herk et al., 2015. However, the Netherlands had no major flood since 1953, hence flood risk awareness of the general public is relatively low (OECD, 2014).

Figure 19: Water systems in the Netherlands from Geerse et al., 2011

In 2015, the Dutch flood risk protection policy evolved from semi-quantitative flood risk approach to a risk-based approach (Van Alphen, 2015).

Prinsen et al., 2015 presents the Delta Model as a set of models used for analyzing fresh water supplies and flood risk management of the Netherlands. The Delta model is computationally demanding but enabled possible adaptation measures (e.g. levee height and strength, making room for the river) and analyses of present and future scenarios (2050 and 2100). The Delta model is used in national and regional analyses.

Hydraulic loads are determined with the probabilistic model Hydra-Zoet described in Geerse et al., 2011, which provides the probability of flooding. Hydrodynamic models such as Delft FLS or SOBEK 1D-2D are combined with probabilistic models to provide flooding probabilities, water depth, and velocities.

The Delta model computes "safety tasks" corresponding to the difference between local hydraulic load (water level or required crest level) and local strength level. The required crest level is the crest level needed to meet a critical wave overtopping discharge. The strength level is characterized by critical water levels for piping or sliding. The effectiveness of adaptation measures is estimated by comparing "safety tasks". Improvements of flood defences are determined based on waves and water levels to estimate a new minimal design for flood defences. Slomp et al., 2014 presented a more detailed explanation of the Delta model's climate change scenario and integrated models used in flood risk management.

Economic vulnerability is estimated using a damage function to determine the total cost per flood scenario including an estimation of the cost of flood defence improvements. For example, Ward et al., 2011 estimated potential direct economic damage using the Damage scanner model. The indicator to estimate social vulnerability is described by Van Alphen, 2015 as the Local Individual Risk (LIR) being the probability of drowning due to a flood of every inhabitant should be no more than 10^{-5} per year. Another indicator is the societal risk described that consist in the probability of a flood disaster with many fatalities or so called exposed population based on the time available before flooding and the time required for evacuation.

Jongejan et al., 2015 presents the methodology and results of a large scale probabilistic risk assessment of levee systems in the Netherlands taking into consideration levee failures (Figure 20). The VNK2 project assess economic and fatality risks. Jonkman, Kok, et al., 2008 describes a probabilistic flood risk assessment to estimate the fatalities due to a flood considering levee breaches (Figure 21).

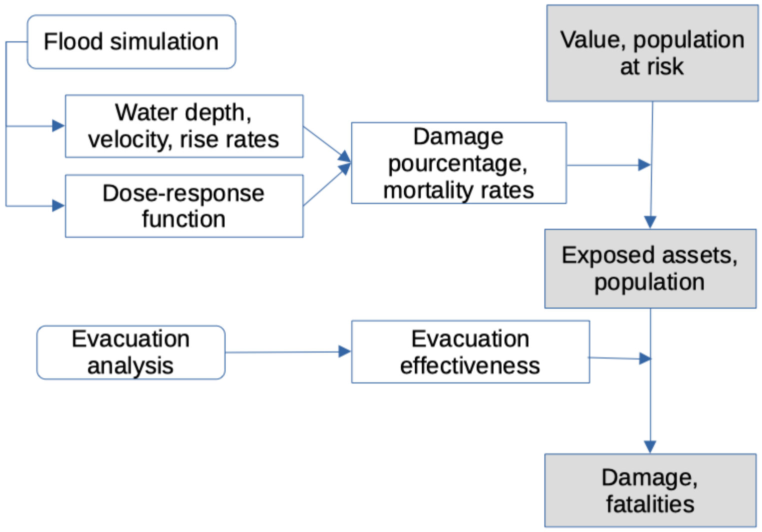

(a)

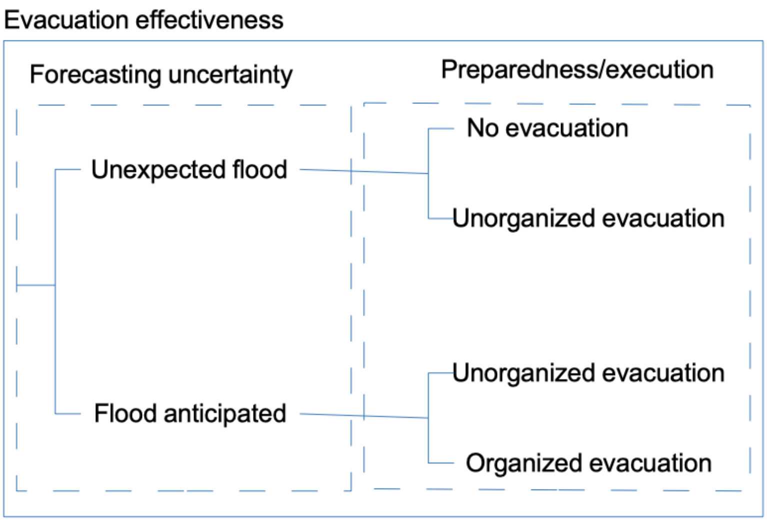

(b)

Figure 20: Flood scenario consequences of the Netherlands Integrated Flood Risk Management initially presented in Jongejan et al., 2015

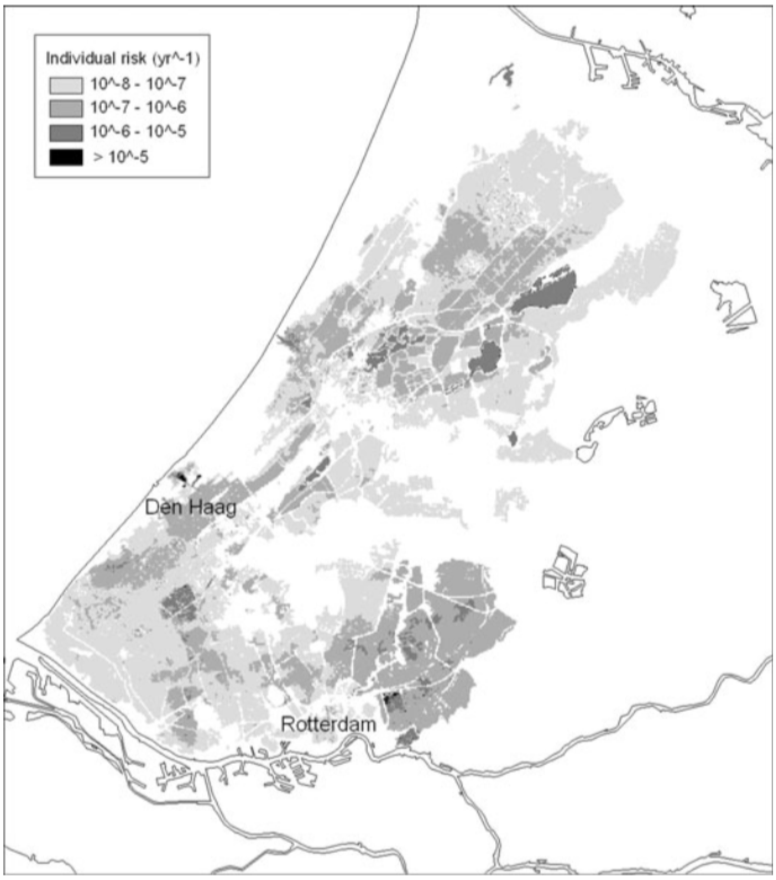

Figure 21: Individual risk for South Holland from Jonkman, Kok, et al., 2008

The Delta Programme main challenge was to assess all flood defences in accordance with new standards that were defined. Upgrade flood defences to those standards is still ongoing.

Risk analysis of levee protected areas

Risk analysis identify and quantify potential risks to devise strategies to mitigate or eliminate them. Tourment et al., 2016 present risk analysis of levee systems following the Source-Pathway-Receptor model as illustrated in Figure 22. The risk analysis process includes the following steps:

- identification of the risk (e.g. levee failure),
- estimation of the event probability which determines the water load
- levee failure analysis (e.g. levee failure scenario and associated probability)
- flood modelling (e.g. water depth and velocity)

- exposure and vulnerability assessment including mitigation solutions
- estimation of the flood risk level (probabilities or qualifying term)
- retroactive loop to assess the remaining gaps in knowledge
- risk attribution to the flood defence system (e.g. levee segments)

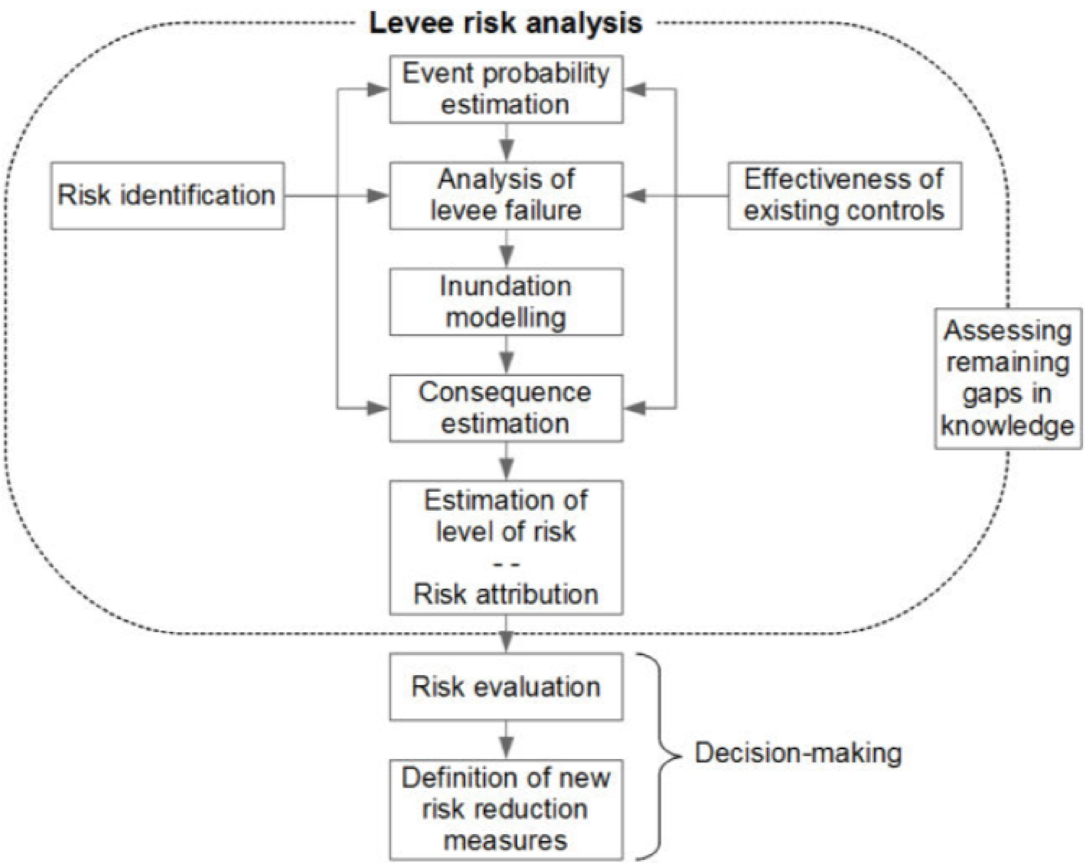

Figure 22: Steps of risk analysis from Tourment et al., 2016

Risks can be assessed qualitatively, quantitatively, or with a holistic approach which combine quantitative and qualitative methods such as Vojinovic et al., 2016.

Methods to qualitative risk analysis include: (i) one-dimensional scale system and (ii) a combination approach which uses a two-dimensional system to rate the risk likelihood and its consequences.

Kotek et al., 2012 present the one-dimensional, HAZard and OPerability study (HAZOP) qualitative method applicable to complex processes, which identify potential hazards and propose preventing actions. The qualitative risk analysis qualify each event with a double-criterion qualitative method. The risks are evaluated by Equation 0.21. For P and S, a 5 level qualitative scale is defined respectively: (Very low, Low, Middle, High, Very high) and (No injury, Minor injuries, Serious injuries, 1 deadly injury, > 1 deadly injury). Resulting in a 3 level qualitative scale (Non-significant, Low significant, Significant).

$$\text{Risks} = \text{Probability of occurrence x Severity of consequences} \tag{0.21}$$

Weerasinghe et al., 2018 use aone-dimensional approach by performing a qualitative approach with statistical hazard, exposure, and vulnerability combined to express a level of flood risk. Risk indexes are computed using Equation 0.22. The qualitative scale chosen to represent the risk include 5 levels: Very Low, Low, Medium, High, and Very High.

$$\text{Risk Index} = \text{Hazard Index x Exposure Index x Vulnerability Index} \tag{0.22}$$

Leitão et al., 2013 use a combination approach with a risk matrix which considers consequences and likelihood each estimated on a scale from 1 to 5 respectively: (Insignificant, Low, Moderate, High, Severe) and (Rare, Unlikely, Moderate, Likely, Almost certain). A risk acceptance criteria was defined for the study range by stakeholders on a scale from 1 to 3 (Low, Medium, High). The main advantage of this risk matrix approach is its easy and effective implementation. The risk matrix helping reduce the subjectivity of results compared to a linear qualitative approach.

Scorzini et al., 2017 present the results of a qualitative flood risk assessment using a risk matrix which considers potential damage and likelihood each estimated on a scale from 1 to 4: (Low, Moderate, High, Very high). The qualitative flood risk assessment process is represented in Figure 23.

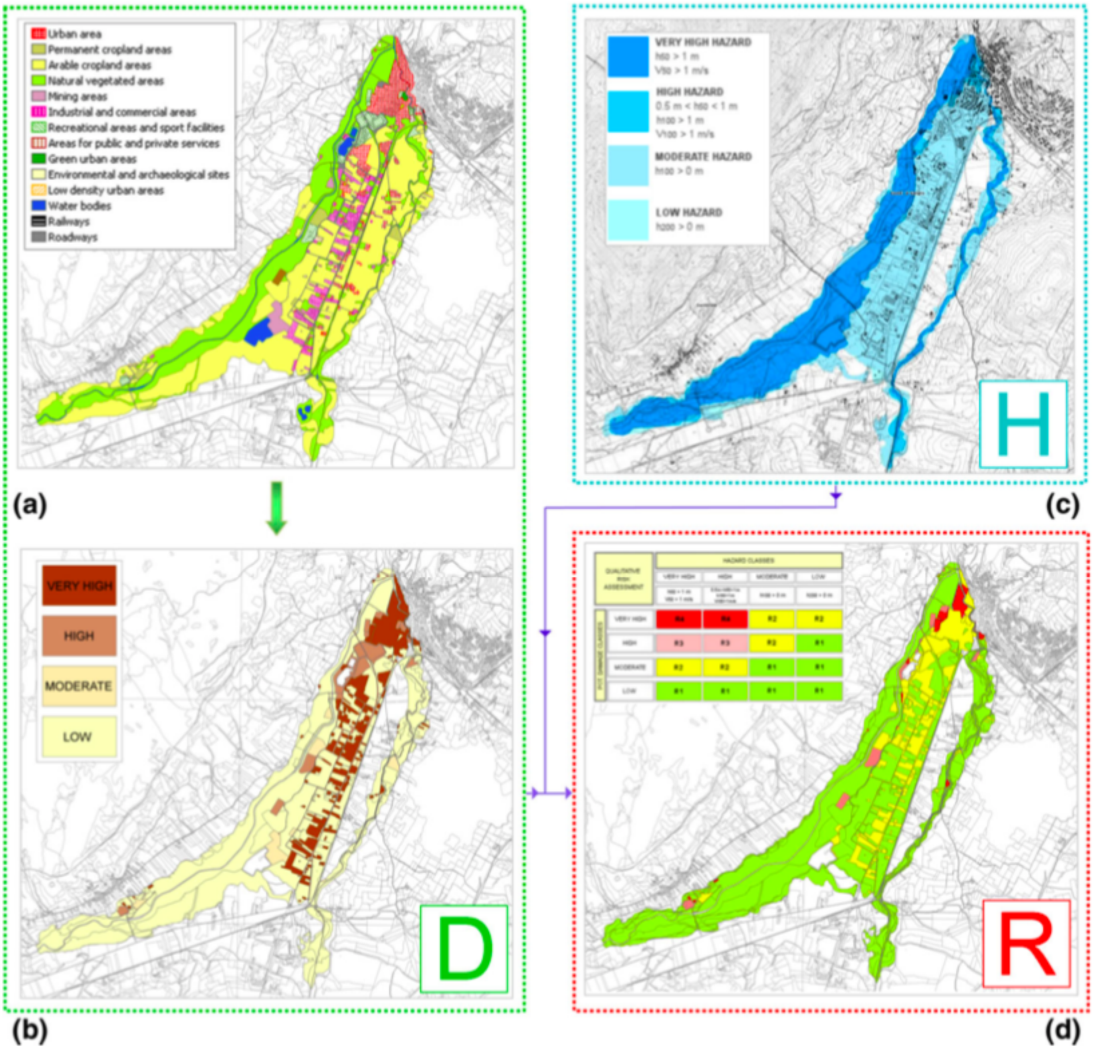

Figure 23: Qualitative flood risk assessment process from Scorzini et al., 2017

Risk analysis of a same structure can reach different conclusions (Emblemsvøag et al., 2006). Those differences in results can be due to the perception of the risk and the different scales used. In addition to which Emblemsvøag et al., 2006 points out that organisation strength and weaknesses are not considered and that there is little to no quantification of the quality of the data used.

Quantitative risk analysis consist in numerical estimation of the risk based on available data. Approaches to quantitative risk analysis include Failure Modes and Effect Analysis (FMEA) (including fault trees (Escuder-Bueno et al., 2012, ten Veldhuis et al., 2011), sensitivity analysis) and simulations methods (Monte Carlo analysis). Peyras et al., 2012 proposed a dam safety probabilistic assessment combining risk analysis and reliability methods. Flood susceptibility estimation using machine learning models are a growing trend (Diaconu et al., 2021, Santos et al., 2019). FMEA are inductive methods that analyse potential failures in a system (Modarres et al., 2016). They are limit-state approximation methods which anticipate every potential failures and can be subdivided into Fist Order Reliability Method (FORM) and Second Order Reliability Method (SORM).

The FORM method is a linear approximation of the limit-state on a standardized plan. An iso-probabilist transformation (T) of the physical variables (X_i) into gaussian, standardized, centered, and independent variables (U_i). The performance function $G(\{T\})$ is written $H(\{U\}) = G(T^{-1}\{U\})$ in the standardized plan (ERINOH, 2017). FORM method steps are detailed in Lemaire et al., 2005.

SORM method objective follows the same steps as the FORM method but instead of approximate the limit state surface by a hyperplan, it approximates the limit state surface by a hyper-surface of the second order.

Simulation methods estimate failure probabilities based on the law of large numbers Lemaire et al., 2005. The objective is to sample statistical variables over a physical or space distribution.
In case of flood in levee protected areas, levee failure mechanisms can be identified, assigned a probability and modeled, hence a simulation approach seems the most appropriate to spatially quantify risk.

To assess levee failure probabilities, numerical simulation are either based on limit state functions or Monte-Carlo simulations.

Numerical simulation can be used based on limit state function, which assess for each sample if the failure is in the area of interest and the probability of failure based on the number of sample which are within the failure area. Limit state function (Z) is a function of strength (R) and load (S) for a given failure mode. $Z = R - S$ with $Z > 0 \Rightarrow$ the failure mode does not occur; $Z = 0 \Rightarrow$ is at the limit state, and $Z < 0 \Rightarrow$ indicates a failure. R and S are stochastic variables defined by a probability distribution and a probability density function. as described in van Gelder et al., 2008.

A common simulation method is the Monte-Carlo simulation. Other simulation methods such as directional simulation, importance sampling, and conditional sampling are derived from Monte-Carlo simulation and detailed in Lemaire et al., 2005. Monte-Carlo simulation considers a sample $\{\underline{x_1}, \underline{x_2}, ..., \underline{x_n}\}$ build on N drawings, independent of the random vector $\{X\}$. The probability of failure P_f is estimated by Equation 0.23.

$$P_f = \frac{1}{N}\sum_{j=1}^{N} {I_{Df}}^{(j)} \tag{0.23}$$

${I_{Df}}^{(j)}$ represents the failure indicator. The failure indicator equals 1 if the drawing $\underline{x_j}$ falls in the failure zone or at its limit $G(\{X\}) \leq 0$ and equals to 0 otherwise.

Directional simulation random draws are made within standard space following radial direction until limit state is reached. Then the probability of failure is estimated by the mean of the calculated probabilities estimated in different directions.

Importance sampling consist in samples around the failure area. This is intended as a more efficient method to estimate the failure probabilities but is relevant only if the conception point p^* is well identified. Be careful of secondary extremums.

Conditional sampling requires knowledge of the conception point p^* estimation. All draw are made outside the hypersphere centered in the origin and with a radius equal to reliability index β_{HL}.

Some limitations and hypotheses to a simulation risk analysis approach are worth noting such as: the dependance on the quality of the pseudo-random number generator used for the numerical simulation. The computational burden for reliable systems: to estimate a failure probability of 10^{-n}, 10^{n+2} to 10^{n+3} Monte-Carlo simulation are needed. Details directional simulation, importance sampling, and conditional sampling simulation methods were introduced to lessen the computational burden.

For example, Jongejan et al., 2015 uses a probabilistic qualitative flood risk analysis for the VNK2 project. Flood risk is quantified by Equation 0.24 in which a set of probabilities and consequences for a flood event (i.e. scenario). The resulting Individual risk considering the levee system failure is presented in Figure 24.

$$\text{Risk} = \{\text{Scenario(i)}, \text{Probability (scenario}_i), \text{Consequences (scenario}_i)\} \tag{0.24}$$

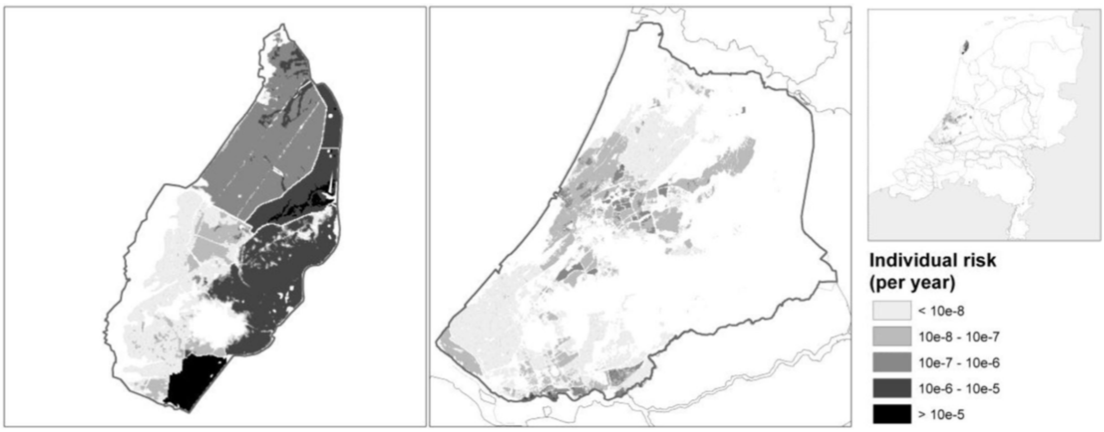

Figure 24: Quantitative Individual risk from Jongejan et al., 2015

PhD dissertation proposal

Scientific questions

Flood risk assessments require the contribution of different fields such as geotechnics, hydrology, hydraulics, and safety engineering. For each step of the assessment, assumptions, simplifications, uncertainties are carried out to the next.

The literature review of each key component of flood risk assessment exposed many gaps in the flood risk assessment engineering practice as one could expect.

In this context, the research provided in this PhD dissertation aims to propose a new probabilistic representation of flood risk that would incite the consideration of levee failure to become a standard in engineering practices.

The main scientific issues of the PhD proposal are the following:

- The development of a probabilistic assessment methods of hydraulic actions acting against levees,
- The development of spatialized methods to assess levee failure probabilities and taking into account the various failure mechanisms occurring in levees,
- The development of methods able to simulate a large number of levee break scenarios, including wave propagation and flooding scenarios in the protected areas,
- The development of spatial and probabilistic methods, crossing the intensity of the flood hazard due to levee break and the vulnerability of the territories, at any point in the area protected by the levees.

The main global issues of this research are the optimization of the methods to lighten the computation time of numerical simulations and maintain a satisfying accuracy level for decision making.

Overview of methods used in the PhD dissertation

The main steps of the aimed process are presented below.

1. Hydrological and hydraulic analysis

   Hydrologic study, using water stage, discharge and climatic data, to determine river water discharge for a range of flood event frequencies, from unexceptional to extreme events

   Hydraulic simulations of flood events, using hydrologic study results and topographic and bathymetric data, to determine the river flood water level along levees segments, according to the different flood event frequencies and including a quantification of uncertainties on water levels

2. Structural analysis

   Characterization of levee system properties and identification of homogeneous levee segments: according to the nature and geometry of levee structural components.

   Identification of possible structural failure scenarios for each homogeneous levee segment using reliability methods.

Determination of probabilistic distributions of safety factors for each failure scenario, for each homogeneous levee segment (according to probabilistic distributions of geotechnical parameters and using Monte-Carlo simulation) and for the different flood event frequencies.

Determination of fragility curves (probability of failure according to probability of flood loading conditions) for each levee segment, for each failure scenario and for an aggregation of all failure scenarios.

3. Flood assessment and risk attribution

   Determination of properties of inundations in the protected area, to obtain inundation maps, resulting from each levee segment structural failure (according to breaches hydrographs and geometries) and from the normal running of the levee system (overflowing without levee failure), for the different flood event frequencies.

   Multicriteria analysis to define the vulnerability of assets in the protected area, to obtain a map for social and economic vulnerabilities.

   Assessment of inundations consequences, by crossing inundation maps and vulnerability map, for the different flood event frequencies, for each levee segment failure and for the normal running of the levee system.

   Flood risk estimation and attribution to each levee segment of the levee system, to improve decision making about levee management, and to each part of the protected area, to improve decision making about protected area and assets vulnerability management

The way these different steps interact to finally produce flood risk attribution is presented in Figure 25.

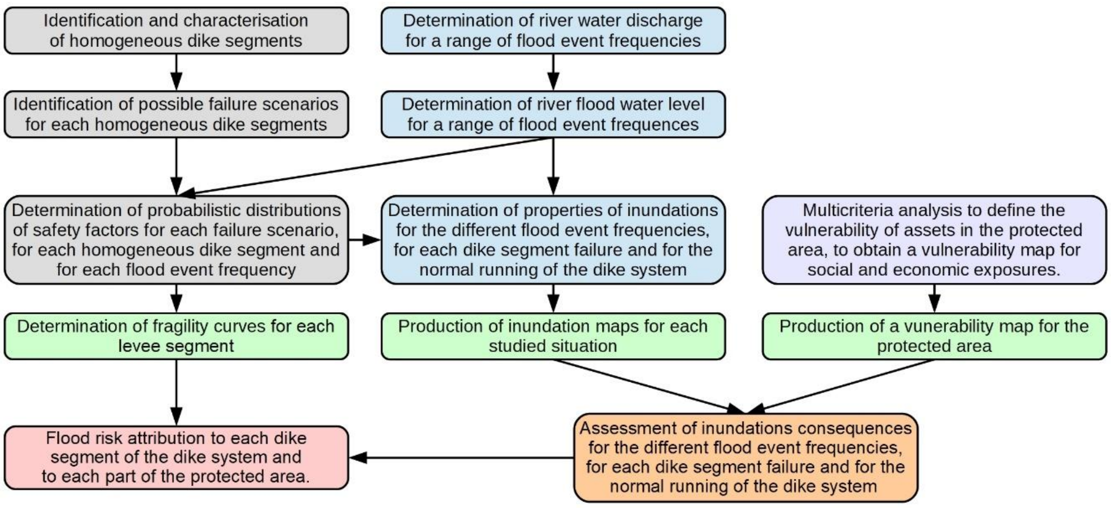

Figure 25: Process for flood risk analysis of levee systems

PhD dissertation outline

This PhD report is an article based report thesis, hence some chapter of this dissertation are constituted by a journal or conference article, adapted to the format of a PhD dissertation manuscript. Those chapters have their own introduction, literature review, methods, results, and discussions. References for the entire dissertation, including previously published articles, are included at the end of the dissertation.

Chapter present the case studies in Canada used for our PhD: the first is located in Calgary, Canada were the Bow an Elbow Rivers flow through the city, the second is located in the GTA, focusing on a local levee which protects a residential area.

Chapter presents a probabilistic method to estimate levee failure for several failure mechanisms and aggregate those into a fragility curve representing failure occurrence probability and associated to a levee segment. Literature review of failure mechanism and an introduction to estimation of the failure probabilities of the instability, backward erosion, and overflowing failure mechanism is provided. The method is applied to a case study located in Calgary, Canada. This chapter is based on the article published in JFRM: Mainguenaud, F., Peyras, L., Khan, U. T., Carvajal, C., Sharma, J., & Beullac, B. (2023). A probabilistic approach to levee reliability based on sliding, backward erosion and overflowing mechanisms: Application to an inspired canadian case study. *Journal of Flood Risk Management*, e12921. https://doi.org/10.1111/jfr3.12921

Chapter presents a probabilistic flood hazard assessment method taking into consideration levee failure on different location for backward erosion and overflowing failure mechanisms. Literature review of flood assessments is provided with a focus on assumptions of hydraulic models. The method is applied to a local case study in the GTA, Canada. This chapter is based on the article submitted in JFRM: Mainguenaud, F., Khan, U. T., Peyras, L., Carvajal, C., Beullac, B., & Sharma, J. (2024). Probabilistic assessment of flood hazard of a levee protected area considering different breaching scenarios. application to a levee on etobicoke creek river. *Journal of Flood Risk Management*

Chapter 0.0.0.1 presents anew the steps of a flood risk assessment. We present vulnerability assessment methods and an application of a flood risk assessment: building from previous chapters, we use flood hazard considering levee failure, exposure, and vulnerability to estimate flood risk. This chapter 0.0.0.1 is based on the article published in EGU: Mainguenaud, F., Usman T Khan, L. P., Carvajal, C., Beullac, B., & Sharma, J. (2023). Mapping the impact of levee failure on flood risks: A toronto case study. *EGU General Assembly 2023, Vienna, Austria, 24–28 Apr 2023*, (EGU23-3616). https://doi.org/10.5194/egusphere-egu23-3616

Chapter Three: Case studies

In this chapter data related to two case studies used in this PhD dissertation are presented, one located on the Bow River in the City of Calgary and the other on the Etobicoke Creek in the Greater Toronto Area (GTA). Each case study is lightly described in chapter and , this chapter provides additional data.

Historical case studies are used to calibrate numerical models. Numerical models are but simplifications of complex, dynamic processes which try to replicate physical mechanisms. The reliability of a flood assessment depends on the precision of the input data. Therefore, the more detailed the case study, the more accurate a numerical model result will be.

An extensive description of hydrology and geotechnical data of the Bow River in the City of Calgary and the Etobicoke Creek in the GTA is presented below.

Bow River, City of Calgary, Canada

Description of the watershed

Located in southern Alberta, the Bow River basin area measure approximatively $25,123 km^2$. The Bow River begins from the Bow Lake in the Rocky Mountains, and flows through Banff and Calgary. The City of Calgary distinguish the Bow River, Elbow River, and Nose Creeks watersheds as shown on Figure 26.a. The Calgary city center is located at the junction between the Bow and Elbow Rivers (Figure 26.b). The Bow River average slope is 0.4% over its $645 km$ length (Khan et al., 2018). The average width of the River is $124 m$ for the case study location, and an average elevation of $1,042 m$ above sea level (City of Calgary, 2013).

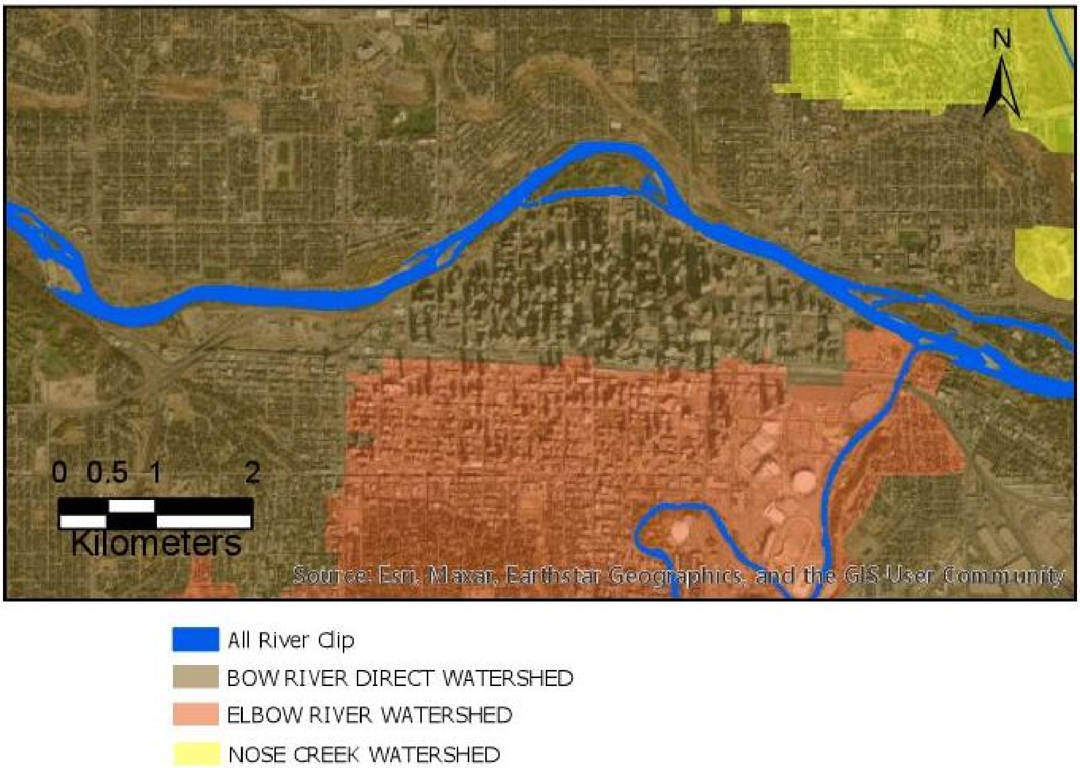

(a)

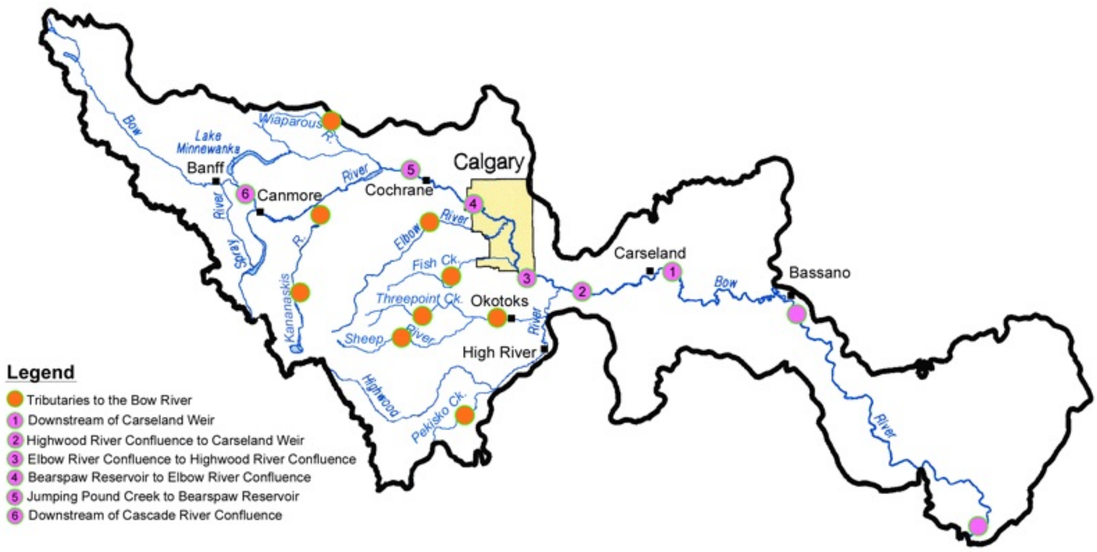

(b)

Figure 26: (a) Watersheds of the City of Calgary; (b) Junction of Bow & Elbow Rivers from Alberta Environment and Parks, 2023

The City of Calgary has a dry climate close to the mountains, resulting in unpredictable sudden weather changes which can result in droughts or floods due to intense thunderstorms.

Description of the hydrology of the City of Calgary

Pomeroy et al., 2016 points out that peak flows occur between May and June due to snowmelt, but these seasonal patterns are likely to evolve due to climate change. Nevertheless, the hydraulic data used for the case study comes from the hydraulic station $05BH004$ (Government of Canada, 2022). Flow values based on historical data (City of Calgary, 2020) from 1933 to 2015 registered 172 to $1,840 m^3.s^{-1}$ annual peak discharge.

Historical flood of the area

During the 19^{th} to the 21^{st} of June 2013, heavy precipitations in Southern Alberta lead to one of their worst flood in 2013 when heavy rainfall combined to snowmelt from the Rocky Mountains resulting in severe run-off.

The Bow River at Calgary observed hydrograph showed an increase in streamflow from around $200 m^3.s^{-1}$ on the 19^{th} of June to over $1,700 m^3.s^{-1}$ at the peak discharge on the 21^{st} of June as shown on Figure 27.

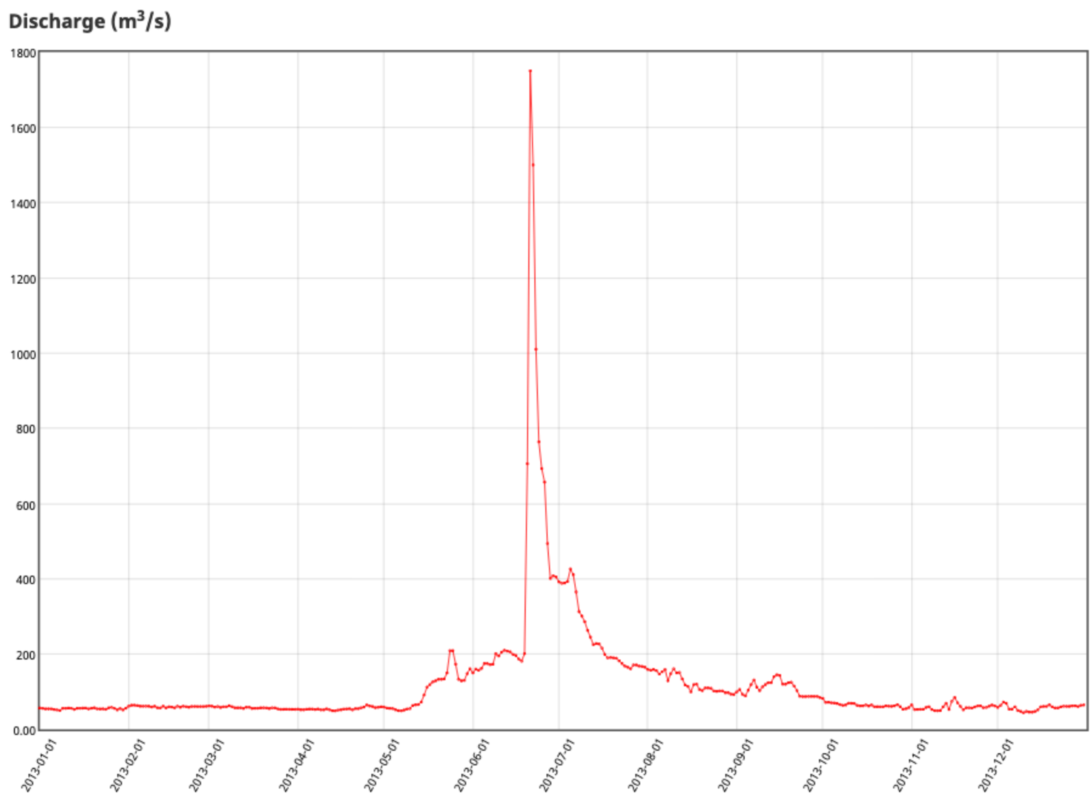

Figure 27: Hydrograph of the flood of 2013 at Calgary from station 05BH004 (Government of Canada, 2013)

The disaster resulted in an estimated $6 billion in damage, evacuations, and several deaths. The Bow and Elbow Rivers both overtopped their natural banks as well as flood control barriers along the rivers during the flood of 2013 as can be seen in Figure 28.

Figure 28: City of Calgary in 2013 @Wilson Hui

Description of the levee of interest

Bow and Elbow Rivers house bridges in close proximity to each other due to the high density populated area (Picton, 2019). Figure 29 shows the location of levee cross-sections from which Cocaign et al., 2020 defined 11 homogeneous levee segments of average length 192m to study. We inspired our levee cross-section from the ones available in Cocaign et al., 2020, raising the crest height while retaining the overall shape of Calgary's levees resulting in Figure 36.

Figure 29: Levee cross-sections in the City of Calgary extracted from an HEC RAS model used by Cocaign et al., 2020

Calgary's levees are composed of clay with supporting grounds composed of silts (Picton, 2019). Agricultural Regions of Alberta Soil Inventory Database (AGRASID) gives a more precise description and classify Calgary's levees as loamy clay to clay with little sand. We considered the soil porosity $n \in [0.3; 0.45]$ (Hough, 1969), the solid particle density $\gamma_s \in [2,600; 2,800]\ kg.m^{-3}$, and $\gamma_w = 1,000 kg.m^{-3}$.

The Etobicoke Creek, Greater Toronto Area, Canada

Description of the watershed

Figure 30 shows the Etobicoke Creek watersheds and the study area located in Meadowland Park in Brampton, Ontario, Canada. The study area was identified as one of the flood vulnerable clusters by Toronto Region Conservation Area, 2023.

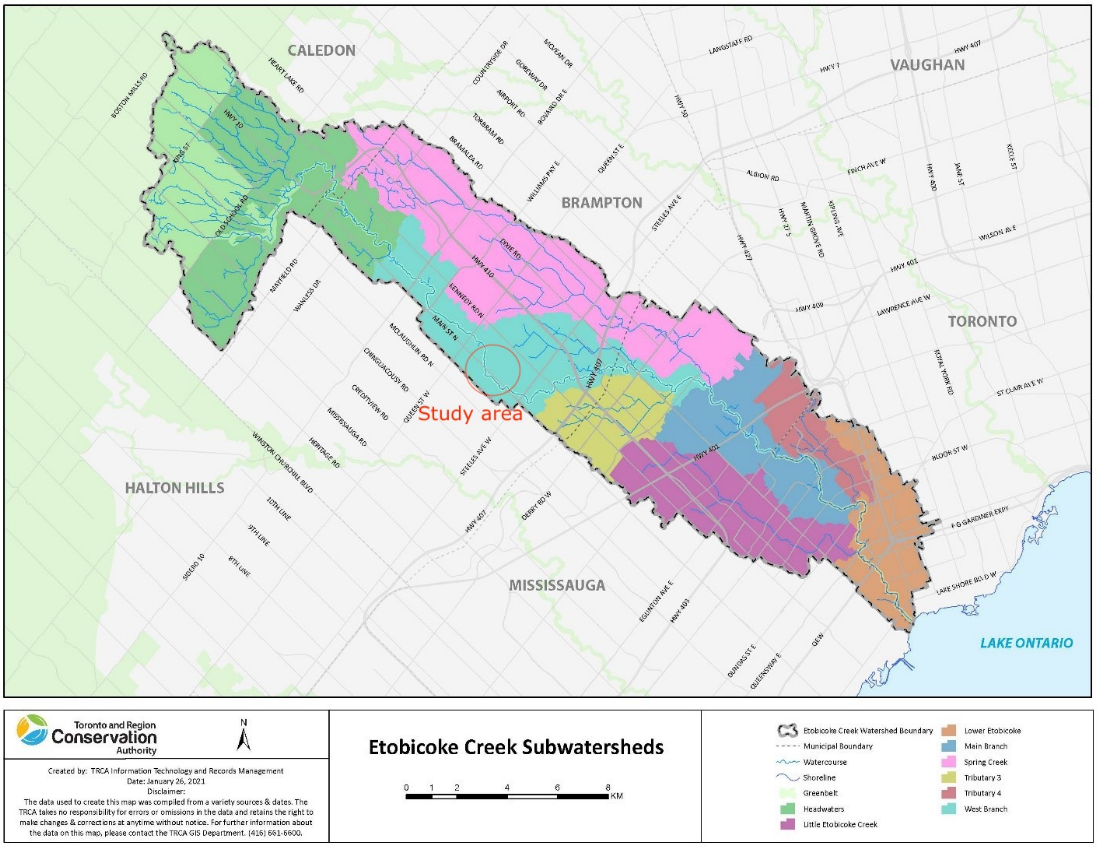

Figure 30: Etobicoke Creek sub-watersheds from TRCA from TRCA Information Technology and Recordq Management, 2021, modified by addition the location of the study area in red

Toronto Region Conservation Area, 2010 provides spatial land-use map (Figure 31), which indicates that for the Etobicoke Creek watershed: industrial land is concentrated in the central part of the watershed, the headwater area is located in Caledon, is a mostly rural area, and residential areas are located in Toronto, Brampton, and Mississauga. Globally, the Etobicoke Creek watershed land-uses are: 60% urban, 28% rural, 12% natural land, and impervious surfaces 48%. Toronto Region Conservation Area, 2023 noted a 5% increase in urban area and impervious surfaces with the loss of 9% of rural areas in 7 years. The study area consists in Residential, Commercial, Institutional, and Urban open spaces (e.g. parks)

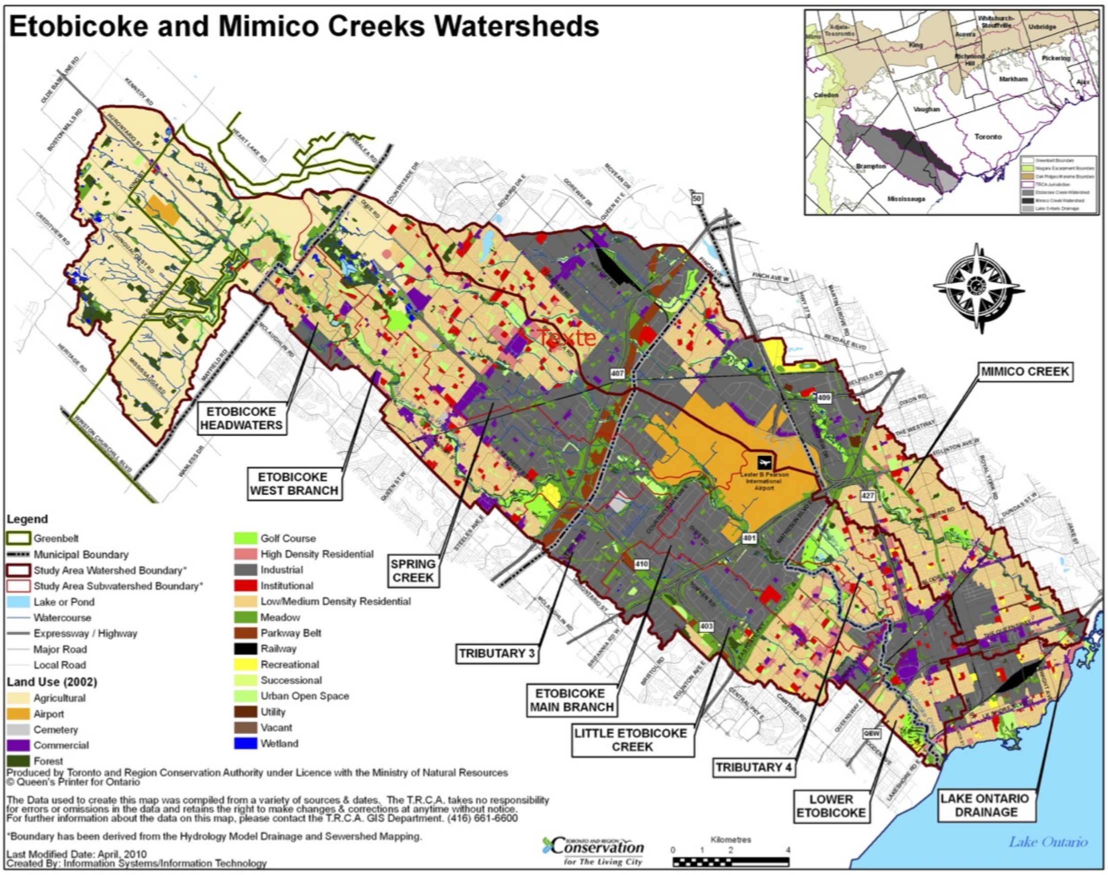

Figure 31: Etobicoke Creek land-use from Toronto Region Conservation Area, 2010

Toronto Region Conservation Area, 2010 noticed that temperatures near the lake are slightly warmer due to the moderating effects of Lake Ontario and high urbanization in the lower portions of the watersheds. Average temperatures vary between 18 to $20^{o}C$ in summer and $-3.5^{o}C$ in winter. Therefore, precipitations are composed of approximatively 85% rainfall and 15% snowfall.

Description of the hydrology of the GTA

The Etobicoke watershed drains $211 km^2$ with a mean slope of 0.005. Etobicoke Creek flows southward to Ontario Lake (Figure 32). Flow values and shape of hydraulic events were estimated based on the Water Office historical database (Government of Canada, 2023), which provides water levels and flow values. The hydraulic station $02HC017$ is located in our study area provided the data for the flood frequency analysis which determined peak flow values, ranging from 85 to $530 m^3.s^{-1}$. We simulated flood events associated with return periods 100, 200, 350, 500, 750, and $1,000$ year.

Figure 32: Etobicoke Creek levee extension used for the case study

Historical flood of the area

The historical flood and regional storm of the Southern Ontario area is Hurricane Hazel which occurred on the 15^{th} of October 1954.

Prior to Hurricane Hazel's arrival, the Toronto area had experienced above average rainfall, which saturated the ground, preventing further soil infiltration. Then came Hurricane Hazel with $285mm$ of rain in 48 hours causing major flooding. The Etobicoke Creek overflowed its banks, damaging houses, evacuating four hundred people, and killed 81.

In the Brampton area, Hurricane Hazel reached $124km.h^{-1}$, $183mm$ of rain in 24 hours to $210mm$ in 48 hours resulting in water depth of 6 to $9m$.

Description of the levee of interest

The study case levee is located along the Etobicoke Creek, on the east side of Main Street South. The levee was constructed in the mid-1960's to provide flood protection to the adjacent residential area. The levee is approximatively $2m$ high and $550m$ long, with a $2m$ wide asphalt trail on its crest. The original levee was extended in 1967 with a storm drain built to facilitate drainage behind the levee. Information for the original levee design and construction is not available except for the limited information regarding the 1967 upgrade as shown in Figure 33.

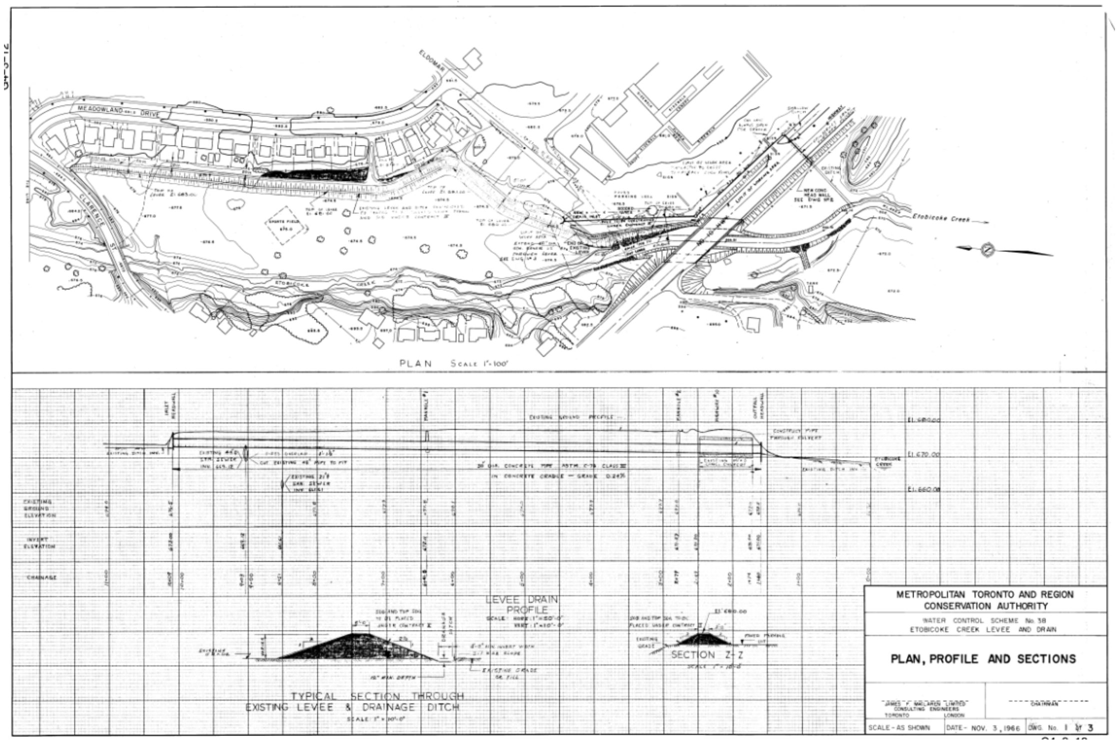

Figure 33: Meadowland park's levee profile from Toronto and Region Conservation Authority (TRCA)

We chose to model another extension to the levee southwards as shown in Figure 32. The levee slopes considered consist of 3 : 1 (horizontal:vertical) for the water side and 2 : 1 for the protected area side of the levee as shown on Figure 46. This extended levee is able to withstand a 100 year flood return period without overtopping.

It is important to point out that the Etobicoke Creek levee is not directly located on the river bank but approximately 80m away from the river stream, hence leaving space for a floodplain. The Etobicoke Creek River banks show significant vegetation cover during the summer months as shown in Figure 34.

(a) (b)

Figure 34: Etobicoke Creek River banks at Clarence's Bridge

Terraprobe Inc., 2023 indicates that the levee is homogeneous. The levee side slopes are grassed on both sides and well maintained by the City of Brampton. The levee appears visually to be in a good condition with no conspicuous deficiencies. The geotechnical report (Terraprobe Inc., 2023) describes the levee cross-section from the top as a layer of asphaltic concrete (about 50mm thick) at the ground surface, an earth fill is located beneath the asphaltic concrete layer and extended to 3.0m of depth on the original levee and to 6.0m at the extension location of the case study levee.

Toronto Region Conservation Area, 2010 describes the Etobicoke Creek watershed soils as composed of low permeability silt and clay as shown in Figure 35.

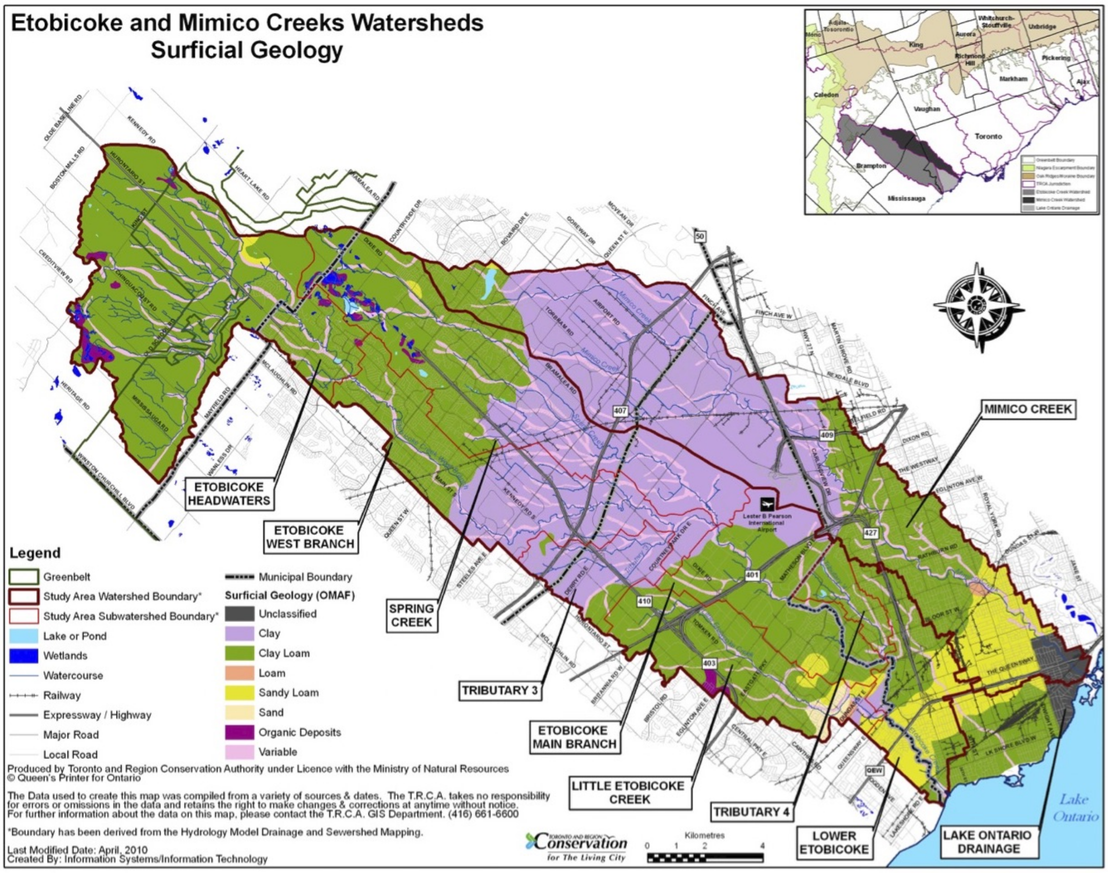

Figure 35: Etobicoke Creek soils from Toronto Region Conservation Area, 2010

Terraprobe Inc., 2023 described the levee earth fill material as clayey to sandy silt matrix with sand and silt pockets. The silty soil contains 10% gravel, 41% sand, 31% silt, and 18% clay for $0.3m^3.m^{-3}$ water content, $10^{-8}m.s^{-1}$ levee permeability, $10^{-6}m.s^{-1}$ foundation permeability, a finished soil settlement, and an estimated earth fill cohesion of $0kPa$ for an angle of internal friction of 28^o.

Chapter Four: Performance of levee defence systems

Summary

Preface

This chapter focuses on estimation of levee failure probability. Section presents a literature review on different approaches to flood risk management in several countries (), and state of the art of levee failure mechanisms and the subsequent failure probability estimations at the time of writing. Section details probabilistic methods to assess a levee failure probability and engineering standard practices. Section proposes a case study application of previously introduced levee failure probability methods. Section presents a discussion of hypothesis validity range, the impact of parameters, and advantages of aggregating levee failure probabilities of several failure mechanisms into a single value.

The content of this chapter was published as Mainguenaud, Peyras, et al., 2023 in Journal of Flood Risk Management in 2023. The contributions of each co-authors in the current chapter are as follows:
Florence Mainguenaud conducted the literature review, and wrote the original manuscript of this publication. Laurent Peyras, Claudio Carvajal, Bruno Beullac, Usman T. Khan, and Jitendra Sharma supervised the research and contributed to the writing and editing the manuscript.

Abstract

Improving protection against fluvial floods requires a better estimation of levee failure. We developed an assessment method of levee failure probabilities for sliding, backward erosion, and overflowing each represented by fragility curves. We tested two approaches to aggregate those fragility curves into a global fragility curve respectively using: an envelop curve and Monte-Carlo simulations. We implemented this approach to earthen levee reliability for several flood return periods to the Bow River in Calgary, Canada. We used limit equilibrium method to estimate the safety factor of the levee segment and Monte-Carlo simulations to estimate sliding probabilities. We used Terzaghi's critical hydraulic gradient to estimate backward erosion failure probabilities. The estimation of overflowing probabilities required expert judgement. We discussed how the choice of the hydraulic gradient area and the consideration of a steady state or transient model impact backward erosion failure probabilities. The results showed for our study case that, even though the transient model is a closer representation of reality, the levee saturation parameter has little impact on hydraulic gradient values, by extension, on sliding and backward erosion failure probabilities. The Monte-Carlo aggregated fragility curve is more realistic than the envelop curve of the failure mechanisms for an equivalent computation time.

Introduction

Flooding is a worldwide threat: the Intergovernmental Panel on Climate Change (IPCC) warns that floods will increase in frequency and intensity with climate change (Field et al., 2014). Recent floods in British Columbia (Canada) and Toulouse (France) in November 2021 and January 2022, respectively, highlight that floods are a global issue Our case study, the City of Calgary, experienced its largest flood since 1932 in June 2013 (City of Calgary, 2013). This flood was due to three days of heavy rainfall on the melting snowpack in the Rocky Mountains, leading to overflow of the Bow and Elbow Rivers, resulting in rapid and intense flooding in Southern Alberta watersheds (Pomeroy et al., 2016; Tanner et al., 2018). The $6 billion in financial losses and property damage across Southern Alberta highlights the need for better flood mitigation and risk assessment (City of Calgary, 2013; Khan et al., 2018; Snieder et al., 2020).

Flood risk management procedures were theorized in response to severe floods (Beffa, 2000). In Europe, flood risk management is regulated under the directive 2007/60/EC, implementation of which is detailed in European Environment Agency, 2007, Klijn et al., 2008, and Dráb et al., 2010. The first step of flood risk management is flood risk assessment, which includes developing of prediction models and mitigations strategies. Modeling flood hazard refers to defining hydraulic events and the system performance analysis such as event and fault trees (Rosqvist et al., 2013, CIRIA et al., 2013, Van et al., 2022). Flood mitigation attempts to limit the extent of flood damage and loss of life (Snieder et al., 2020) using structural elements (e.g., levees, dunes, sea walls, dams) and non-structural elements (e.g., risk assessment, risk management, governance, and early flood warning systems) as described in Tasseff et al., 2019 and Conitz et al., 2021. The second step of flood risk management is to map flood hazard and assets of the area (material properties, economic damages, casualties, immaterial values). The consideration of levee failure may have, depending on the area, a significant effect on the flood risk map. Our research focuses on flood risk assessment, specifically evaluating the resilience of flood defence systems of fluvial levees. One approach to flood risk assessment is quantitative risk analysis, which require time and availability of data (CIRIA et al., 2013). Another widely used approach is probabilistic risk analysis, described in the following literature. Kubal et al., 2009 describe integrated flood risk based on the concept of multicriteria assessment as it was developed in Europe and Vuik et al., 2017 describes the national scaled integrated flood risk method such as used in United Kingdom (UK) (Hall et al., 2003) or the Netherlands (Vrijling, 2001). However, national scaled integrated flood risk assessment method have issues related to the geographic scale for analysis that stem from the transition of local to national-scaled assessments. At a national scale, it is considered that local uncertainties cancel each other out and some study do not consider uncertainties in detail. Therefore, issues include data availability and consistency, developing or adapting new flood forecasting tools, and selecting the appropriate failure mechanisms for flood defence infrastructures. Lendering, Kasper, 2016 and Gouldby et al., 2008 propose a method for flood risk assessment at an intermediate or regional-scale. This scale presents its own set of challenges: the uncertainties made at a national scale may not apply at a regional scale, and the choice of failure mechanism may differ due to regional conditions. Vuik et al., 2017 present a semi-probabilistic approach with probabilistic hydraulic loads and deterministic levees and dunes strength.

For any approach, deterministic or probabilistic, the choice of levee failure mechanism is an important component of flood risk assessment as the resulting flood hazard may change with the collapse of a levee. We outline three failure mechanisms commonly studied: sliding, internal erosion, and overflowing. To evaluate the reliability of a levee in a probabilistic framework, event or fault tree methods are often used to take into account complex scenarios. Then, these scenarios occurrence is evaluated with a probabilistic or a semi-probabilistic approach (Peyras et al., 2012). Probabilistic analysis on slope stability has been widely documented in literature with limit equilibrium method or numerical methods. Cho, 2007 applies to a fluvial levee a limit equilibrium method based on Spencer's slope stability model and performs probabilistic stability assessments with Monte-Carlo simulations to study the variations of critical surfaces due to spatial variability of soil properties. Their study shows the importance of considering the soil properties spatial variability in probabilistic assessments. Mouyeaux et al., 2018 provide an example of a probabilistic slope stability analysis on earthen embankment using finite element method.

Levee internal erosion includes four mechanisms: backward erosion, suffusion, concentrated leak erosion, and contact erosion, described in Hall et al., 2003 and International Commission on Large Dams, 2017. The evaluation of internal erosion mechanism is not completely understood and their deterministic assessment methods are still in development. Probabilistic models for internal erosion are not as mature as the ones available for sliding, leading to fewer probabilistic studies on internal erosion. The following literature describes a probabilistic approach for each internal erosion mechanism. S. Lee et al., 2017 propose a probabilistic model to evaluate backward erosion and suffusion. van Noortwijk et al., 1999 calculated the failure probability of uplift failure using the directional sampling simulation and concluded it provided close results with the Fist Order Reliability Method (FORM) approach. Julínek et al., 2020 provided an application of uplift failure mapping and described uplift failure downstream of the levee as a mode of failure that occurs mainly in the presence of a permeable layer in the foundation topped by a layer of more impermeable materials of small thickness. Vuik et al., 2017 describe the assessment of sea levees considering overflow and overtopping. Fry, 2016 shows that concentrated leak erosion is the most dangerous internal erosion mechanism for dams. However, levee failure studies mostly consider backward erosion or suffusion. The estimation of levee backward erosion failure relies on comparison of hydraulic gradients to a critical gradient value. Říha et al., 2020 proposed a statistical analysis of experimental critical hydraulic gradients for heave. Many critical gradient estimation methods consider global gradient in opposition to local gradient. H. Sellmeijer et al., 2011 use global gradient at hydraulic structure scale, whereas Terzaghi, 1943 considers local hydraulic gradient to evaluate internal erosion.

Overtopping implies dealing with waves that go over the levee crest, whereas overflowing relates to a consistently higher water level than the. levee crest. Little literature is available on the mechanical modeling of levee overflowing. Formentin et al., 2018 propose a new method to predict water discharge for over-washed and fully breached levees. However, extensive literature is available for wave overtopping which can be estimated using deterministic or probabilistic models. Pickert et al., 2011 detail the process of overtopping for a homogeneous non-cohesive levee. Deterministic models include: empirical models (Hydraulics Research Station, 1980, Waal et al., 1992, Hedges et al., 1998), stochastic models as in Sharafati et al., 2020, or mechanical models as in Pohl et al., 2008 who use failure equations to describe damage and wave overtopping. Probabilistic models on are used in the following literature. Aguilar-Lopez et al., 2018 propose a method to quantify grass cover erosion failure by wave overtopping. Alhasan et al., 2019 use a random sampling procedure to evaluate the probability of levee breach by overtopping and study the impact of the surface lining that protects the levee. Overall, models to estimate failure by overflowing are either scarce or specific to a given location. These approaches either concern wave induced overtopping (i.e., not overflowing) or require extensive historical data. An alternative approach, when such detailed data is unavailable, is to use expert judgement to estimate failure by overflowing, as done by Hathout et al., 2020 and Rongen et al., 2022.

To evaluate the reliability of a levee in a probabilistic framework, one can use fragility curves, which is a function of probability of failure for a mechanism over a conditioning load (water level or water discharge). Hall et al., 2003 assume that probability of hydraulic load correspond to a given flood return period and developed fragility curves for overtopping. R. J. Dawson et al., 2005 extend the use of fragility curves to fluvial wall instability and piping. Vorogushyn et al., 2009 study piping, overtopping, and micro-instability fragility curves. Wojciechowska et al., 2015 gives a general framework to combine piping, macro-stability, and overtopping fragility curves.

Our research aims to provide global failure probabilities tailored for flood risk assessment purposes on regional to national scales. We focus on fluvial earthen levees, which are a common occurrence in cities. The aggregation of failure probabilities provides a more understandable levee failure map for flood management organizations

Materials and methods

In this study, we propose a probabilistic method to assess a levee failure probability integrating three failure mechanisms relevant to fluvial levees (CIRIA et al., 2013): sliding, internal erosion, and overflowing. We selected failure probability methods for each mechanism according to the current state-of-the-art related to the limit-state conditions of these mechanisms. Although we consider those mechanisms independent from each other as done in research to study and understand each mechanism as well as in engineering for simplification purposes, they are intertwined. It is difficult to attribute levee failure to a single mechanism as failure tends to result from a combination of several mechanisms. The probability of occurrence of the flood (expressed in return period) is associated with the water level of the river. A previous statistical study on water discharge of the river and hydraulic study provided water flow and peak water levels of the river for each return period (Picton, 2019).

This study proposes to use the fragility curve method as a probabilistic framework for all three failure mechanisms, and to estimate the overall probability of failure by aggregating these fragility curves into a single global fragility curve. The aggregation of failure probabilities provides a single failure probability value for flood propagation and avoids making a biased interpretation of the results due to distinct fragility curves for a same levee segment.

Failure mechanism

Sliding

Assessing the failure probabilities of levees with a minimum computation time is essential to enable its effective use in flood risk management. To meet the required level of precision for our study, which is intended for several levee segments, the most efficient approach is to use the limit equilibrium method (in 2D) for the stability analysis. Limit equilibrium method defines the safety factor (F_s) as the ratio between the shear strength over the shear stress required for equilibrium. If F_s is below 1, it is considered a failure. Among the different methods of limit equilibrium analysis, this study adopts the Morgenstern-Price method (Morgenstern et al., 1965) since it considers shear forces, normal inter-slice forces, and moment and force equilibriums (GeoStudio, 2021b).

We performed the probabilistic analysis using GeoStudio's SLOPE/W module to model the slope stability combined with a Monte-Carlo simulation method to obtain the sliding failure probability (see section). Sliding failure mechanism complexity partially stems from uncertainties associated with assumptions required about the type of material used to build the levee. In this study, to address soil type uncertainties, we treated the material properties in a stochastic manner. We considered cohesion $c(kPa)$ and friction angle $\varphi(°)$ as random variables in accordance to the sensitivity analysis results of Picton, 2019, which showed they had the most influence on failure probabilities. We carried out Monte-Carlo simulations on these random variables to obtain a probabilistic distribution of F_s. We evaluated the probability of failure as the probability of $F_s < 1$ and repeated for each flood return period.

To model the sliding failure in GeoStudio, we listed in Table 5 the soil properties of the Mohr-Coulomb model and the cohesion and angle of friction sampled with normal distributions truncated to 0 to avoid physically non-coherent values and enable us to put a lower and upper limit value to the distribution. We based the mean values of cohesion and friction angle on literature (Peck et al., 1991, Dysli, 2000, Government of Alberta, 2022) and the standard deviation on expertise covering all the range of values we extracted from the literature. The unit weight in Table 5 refers to the total density of the soil.

	Levee (Silty clay)			Foundation (Loam silt / Silt)		
	$\varphi(^o)$	Cohesion (kPa)	Unit weight $(kN.m^{-3})$	$\varphi(^o)$	Cohesion (kPa)	Unit weight $(kN.m^{-3})$
Mean value	20	15	18	25	10	19
Standard deviation	4	6	–	5	5	–
Variation coefficient C_v	0.2	0.4	–	0.2	0.5	–

Table 5: Mohr-Coulomb soil model data

Internal erosion

Among the different mechanisms of internal erosion, and in the absence of drains or through structures in a levee section, backward erosion is commonly used as the design criteria for levees. Thus, this study focuses on estimating backward erosion initiation (not taking into account the erosion progression until the levee failure). The resulting probability of failure corresponds to the probability of erosion initiation, which is a safe approximation, as erosion does not always lead to failure such as when the process is interrupted (e.g., filtration of eroded particles, limited flood duration). Backward erosion analysis can be performed comparing hydraulic gradients to a critical gradient fitted to the soil type. H. Sellmeijer et al., 2011 and CIRIA et al., 2013 demonstrate empirical methods where the seepage flow in the levee is approximated by a global hydraulic gradient. However, finite element hydraulic models provide local hydraulic gradients with a better accuracy than the global gradient, therefore we decided to use local hydraulic gradients for our backward erosion analysis. The evaluation of hydraulic gradients is a source of uncertainty related to the type of hydraulic modeling (steady-state or transient model) and to numerical aspects (e.g. mesh size). We discuss these elements respectively in sections and . A local hydraulic gradient require a local critical gradient, thus we used the model of Terzaghi to evaluate the critical gradient. Equation 0.25 defines the local critical hydraulic gradient of Terzaghi, 1943.

$$i_{cr} = (1-n)(G_s - 1) \tag{0.25}$$

With i_c the critical gradient, n the porosity, and G_s the specific gravity. Terzaghi's model is defined for ascendant laminar flows, horizontal soil layers, and applicable to fine and loose soils.

The evaluation of the critical gradient is a significant source of uncertainty. For the probabilistic analysis of backward erosion, this study considers the uncertainty in the critical gradient by modeling it as a random variable. We computed hydraulic gradients using GeoStudio's SEEP/W module. Initiation of backward erosion occurs at the foot of the levee (land-side), hence the selection of nodes from the hydraulic analysis as shown in Figure 36 and Figure 37. For each return period, after running the hydraulic model presented in section , we considered the maximum hydraulic gradient within the node selection. We defined the parameters of the probability distribution of the critical gradient based on expert judgment and literature (Hager, 1987).

We evaluated the probability of failure as the probability that the critical gradient is less than the hydraulic gradient obtained by the numerical seepage analysis model. Local hydraulic gradients vary depending on the area of interest within the levee. For backward erosion, the most relevant local gradients are located on the land-side around the foot of the levee. The local gradient considered in this study is the maximum observed gradient within a $1m^2$ buffer area around the foot of the levee as illustrated in Figure 36 and Figure 37.

Overflowing

Levees have some resistance to overflowing failure, but available models cannot determine this resistance without a significant margin of uncertainty. Thus, engineering practice conservatively considers the occurrence of the overflowing scenario where overflowing water erodes the levee crest until the levee breaches. The Bow River does not create significant waves that could overflow the levee, hence in this study we do not consider waves. In those conditions, the levee is able to withstand a 35 years flood return period. Overflowing as a type of external erosion is a time dependent mechanism. Visser et al., 1995 describes overflowing erosion in three phases: the beginning of the overflow and erosion, the progression of the erosion at various speeds, which is

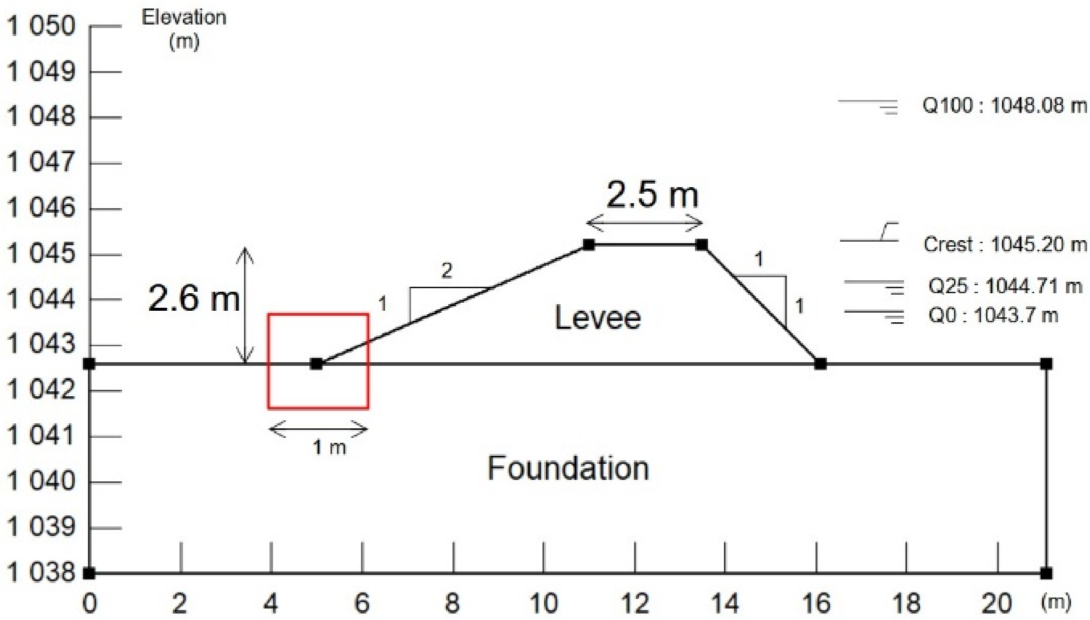

Figure 36: An idealized cross-section of the Inglewood levee system along the Bow River in Calgary, Canada from Cocaign, 2018; in red the location of the gradients of interest for backward erosion.

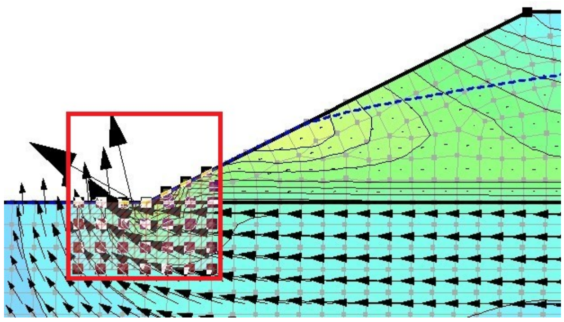

Figure 37: Node selection around the foot of the land-side levee for the estimation of backward erosion probability

the most complex part of erosion estimation, and the collapse of the structure. We chose to consider that the failure by overflowing equals the beginning of a severe erosion of the hydraulic structure for hydraulic peak conditions, meaning the end of the progression phase.

Estimation of overflowing probability based on expert judgement required a group of specialist engineers including at least one specialized in risk analysis. In addition to this condition, each expert in the panel must have knowledge of the geotechnical or hydraulic fields. Each expert independently provided an expert judgement of the probability of failure considering the water level, the soil type, the geometry, the mechanical parameters, and the overflow duration of the levee segment. They estimated the failure probability due to overflow on a qualitative scale from "not probable" to "almost certain probability" (7 grades). Then, a group discussion followed, where misunderstanding of questions and biases were addressed, and the experts selected together in a consensual way the final qualitative scale of failure. Finally, we transposed the qualitative assessment to a quantitative scale using Table 6 as defined in the approach of Peyras et al., 2010.

Qualitative expert judgement	Transposed quantitative probability
Almost certain probability	0.99
Very high probability	0.6
High probability	0.4
Medium probability	0.2
Low probability	0.1
Very low probability	0.01
Not probable	0.001

Table 6: Extended transposition grid of qualitative expert judgement into quantitative 7 probabilities from Peyras et al., 2010

Seepage analysis

The seepage analysis in the studied levee was performed with a numerical model based on the finite elements method. This hydraulic model was used on the one hand to evaluate pore water pressures in the sliding mechanism analysis, and on the other hand, to evaluate hydraulic gradients in internal erosion analysis. We adopted Equation 0.26 for the analysis of flow through the levee, which assumes that the flow follows Darcy's law regardless of the degree of soil saturation (L. A. Richards, 1931):

$$\frac{\partial h}{\partial x}\left(\frac{\partial K_x}{\partial x}\right)+\frac{\partial h}{\partial y}\left(\frac{\partial K_y}{\partial y}\right)=0 \tag{0.26}$$

Where h is the total head, and K_x and K_y are hydraulic conductivity in the horizontal and vertical directions, respectively.

This study assumes steady-state flow conditions, as prolonged exposure to the maximum water level creates conditions for the worst case effects on the levee. As a complementary approach, a transient analysis allowed us to consider the duration of the flood and the evolution of the river level during the flood period but required more computation time compared to the steady-state analysis (see section). The consideration of partially saturated soil conditions in the transient model required additional data corresponding to the volumetric water content and hydraulic conductivity curves. Van Genuchten, 1980, Fredlund et al., 1994, and Aubertin et al., 2003 propose methods to estimate the volumetric water content. We chose Van Genuchten's model for its classical use in the field and used the following non-saturated material model:

$$\theta_w = \theta_{res} + \frac{\theta_{sat} - \theta_{res}}{[1 + (a'\varphi)^n]^m} \tag{0.27}$$

In Equation 0.27, θ_w represents the water retention curve and ϕ the suction pressure. The parameters a', n, and m are the curve fitting parameters which control the shape of the volumetric water content function. θ_{sat} is the saturated volumetric water content and θ_{res} is the residual volumetric water content.

$$K_w = K_{sat} + \frac{[1 - (a'\varphi)^{n-1}[1 + (a'\varphi)^n]^{-m}]^2}{[1 + (a'\varphi)^n]^{\frac{m}{2}}} \tag{0.28}$$

In Equation 0.28, K_w represents the hydraulic conductivity curve. The parameter K_{sat} represents the saturated hydraulic conductivity and the rest of the parameters a', n, m are the fitting parameters of the volumetric water content function.

Monte-Carlo simulations

As defined by Cho, 2007, the Monte-Carlo simulation method is widely used in reliability analysis studies and consist in sampling random variables following a probability distribution. In this study, we integrated cohesion and angle of friction random variables into the slope stability analysis model to compute the output safety factor (F_s). We repeated this process to evaluate the statistical properties (mean and standard deviation) of the safety factor. In the Monte-Carlo approach, the number of simulations must be large enough to achieve convergence of the random variables and ensure that the failure probability (P_f), defined as the ratio of the number of failures to the total number of simulations, has a sufficient precision. However, the disadvantage is that the lower the P_f value, the larger the number of simulations. For a P_f with an order of magnitude of 10^n, an equivalent of 10^{n+2} simulations would be required. In order to limit the number of simulations, we considered the mean and standard deviation of the safety factor, which converge quickly, to define a probability distribution of the safety factor. Therefore, the failure probability was evaluated directly from the safety factor distribution as the probability that $F_s < 1$.

In this study, for each return period, we used 10,000 Monte-Carlo simulations to determine the distribution of the safety factor. We calculated the probability of sliding failure as the number of $F_s < 1$. By plotting the results as a function of the failure probability over the flood return period associated with peak water levels, we constructed the sliding fragility curve.

Aggregation of fragility curves

Wojciechowska et al., 2015 describe the construction, application of fragility curves, and derivation of fragility curves to combine them. To be able to aggregate fragility curves, a shared range of flood return periods associated with peak water level of the river should be covered. After obtaining fragility curves, we considered two approaches distinct from Wojciechowska et al., 2015 to aggregate them: one that uses the maximum function to produce an envelope curve and one that uses Monte-Carlo simulation.

For the envelope curve, we applied the maximum function to all fragility curves. For each flood return period, only the highest probability of failure will contribute to create the global aggregated fragility curve. For the Monte-Carlo simulation method, we generated a random value ranging from 0 to 1. When the sample value was over the probability of failure of the failure mechanism considered, we considered the levee to have failed. We repeated this process for all three failure mechanisms. Then, we aggregated those three results by considering a global levee failure when one of the mechanism failed. We repeated this process 10,000 times to obtain an aggregated probability of failure: the number of global failure over the number of simulations. The Monte-Carlo aggregation attempts to improve flood risk assessment by suggesting a more realistic and more statistically robust failure probability aggregation method for our case study. We discuss the accuracy of our Monte-Carlo simulation method in section .

Case study

We applied the proposed method to the Inglewood levee system, along the Bow River, in southeast Calgary, Canada. The Bow River has an average slope of 0.4% over its 645km length (Khan et al., 2018), and an average width of 124m at the case study location, for an average elevation of 1,042m above sea level (City of Calgary, 2013). Precipitation is highest in June and July in Calgary and the area is prone to short but intense thunderstorms. More details about the Bow River's hydrology properties are available in Pomeroy et al., 2016. Figure 36 shows the idealized levee we used based on the Inglewood levee system. We adapted the levee segment, raising its height while retaining its overall shape. This adaptation lead to non-negligible failure probabilities for each mechanism, which allowed us to better demonstrate our method. 7 lists the hydraulic parameters adopted for a specific levee cross-section and Table 5 lists the geotechnical parameters. We used the collected hydraulic data from Government of Canada, 2022 for the station $05BH004$ from 1933 to 2015 and which registered 172 to $1,840 m^3.s^{-1}$ of annual peak discharge according to City of Calgary, 2020. Agricultural Regions of Alberta Soil Inventory Database (AGRASID) from Government of Alberta, 2022 classify the levee soil from loamy clay to clay with little sand for which we assumed a homogeneous levee.

		Water levels (m) by flood return period (yrs)							
Levee elevation (m)	Length (m)	25	30	35	40	45	50	75	100
1045.20	199. 25	1044.71	1044.96	1045.22	1045.49	1045.75	1046.01	1047.25	1048.08

Table 7: Water levels of the Bow River obtained by statistical analysis, built on Picton, 2019

The seepage analysis model was designed for eight flood return periods (25, 30, 35, 40, 45, 50, 75, and 100years) for peak water levels (Table 7). We chose a $0.3 m$ mesh with triangular and rectangular shapes for the finite element model used in seepage analysis (see section). We chose an anisotropic coefficient to consider the construction of the levee by horizontal layers of soil, which created a higher permeability at the interface between layers: $\frac{K_y}{K_x}$

For the transient analysis, the parameters adopted for Equation 0.27 and 0.28 are: $K_{sat} = 5.10^{-7} m.s^{-1}$, $\theta_{sat} = 0.5$, $\phi = 20^o$, $a' = 6.1 kPa$, $n = 1.37$, $M_v = 4.10^{-5} kPa^{-1}$, and a residual water content of $\theta_{res} = 0.005$. The initial soil moisture content considered was $0.05 m^3.m^{-3}$ for an initial water level of $1,043.6 m$. We selected the following boundary conditions: the water level was applied on the river's ground and river side of the levee and we attributed for the levee crest and land side of the levee a potential infiltration condition of $0 m^3.s^{-1}$.

For the estimation of the backward erosion probabilities, we calculated a mean critical gradient value of 1.06 using Terzaghi's Equation 0.25 for values obtained by expert judgment based on data found in literature: $n \in [0.3; 0.45]$, and for the specific gravity, the solid particle density $\gamma_s \in [2,600; 2,800]\ kg.m^{-3}$ and $\gamma_w = 1,000 kg.m^{-3}$. The parameters range provided critical gradient extremum values with a standard deviation of 0.27. Therefore, to estimate backward erosion failure probabilities, we assumed a critical gradient curve following a normal distribution $N(1.06; 0.27)$ represented in Figure 38.

Results

Fragility curve for each failure mechanism

The probability failure of each mechanism is conditioned by the probability of occurrence of the considered flood. Fragility curves represent the probability of failure

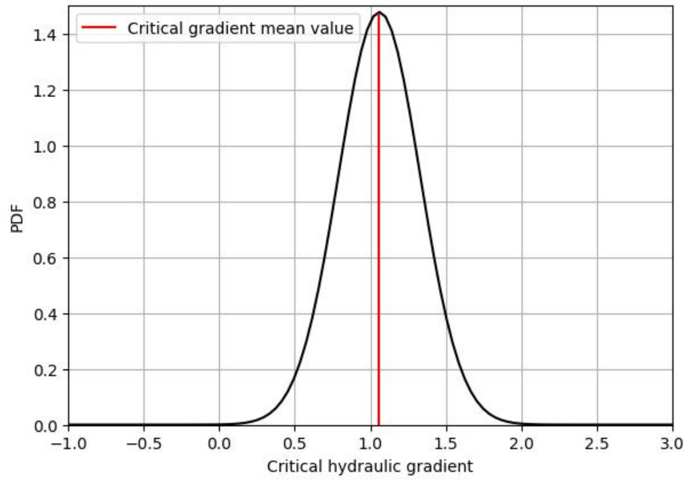

Figure 38: Critical gradient probability density function (PDF) assumed for backward erosion using Terzaghi's model; red line shows the mean value of the critical gradient

as a function of the return period of the considered flood. The slope stability was modeled with GeoStudio as described in section and section . This analysis resulted in Figure 39.a, which shows low sliding failure probabilities for a saturated levee. We plotted the backward erosion fragility curve in Figure 39.b with backward erosion failure probabilities over flood return periods. We observed the main increase of backward erosion failure probabilities between 25 and 50 years flood return periods. Table 8 shows the chosen overflowing failure probabilities by the experts, which resulted in the overflowing fragility curve shown in Figure 39.c. The main increase in failure probability for the overflow fragility curve occurs between the 35 and 45 years flood return periods.

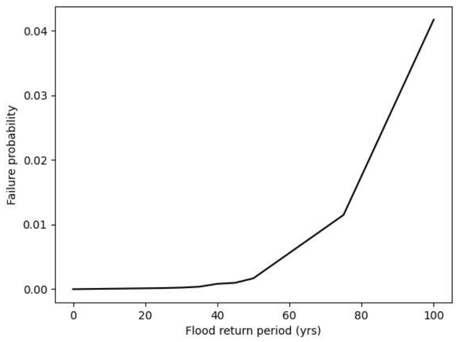

(a)

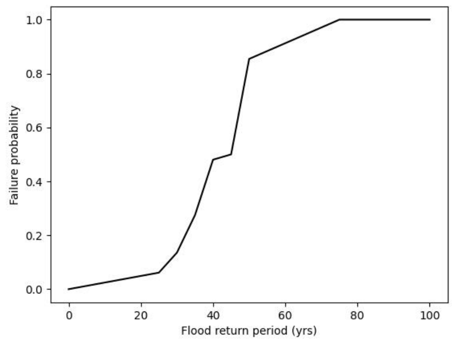

(b)

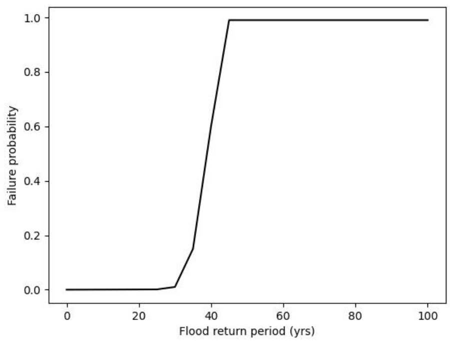

(c)

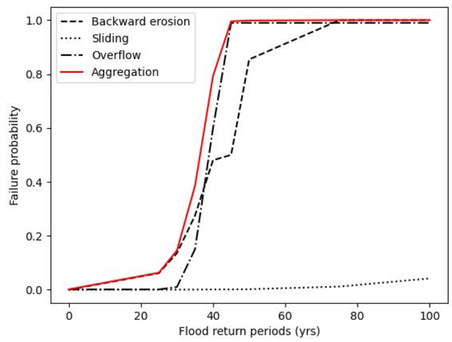

(d)

Figure 39: (a) Slope instability fragility curve; (b) Fragility curve for backward erosion; (c) Overflowing fragility curve; (d) Aggregated fragility curve of the case study levee

Flood return period (yrs)	Overflow water height (m)	Probability of failure by overflowing, conditional on water levels
100	> 1	0.99
75	> 1	0.99
50	0.81	0.99
45	0.55	0.99
40	0.29	0.6
35	0.03	0.15
30	0.00	0.01
25	0.00	0.001
2	0.00	0.001

Table 8: Expert estimation of overflowing failure probabilities conditional on water levels

Aggregation fragility curves

We ran 10,000 Monte-Carlo simulations as described in section to obtain an aggregated probability of failure. We repeated this process for all return period associated with peak water levels, which resulted in the Monte-Carlo aggregated failure probability curve as shown in Figure 39.d. We discuss the comparison of the maximum function (=envelop) and the Monte-Carlo simulation in section .

Discussion

Fragility curve for each failure mechanism

For the Bow River levee segment, the sliding mechanism is not critical, since its fragility curve has the lowest probability amongst all mechanisms. The design of the levee with a low height is the main reason for the low sliding failure probabilities. Backward erosion and overflowing are the most significant failure mechanisms as shown in Figure 39. Internal erosion is a time dependent mechanism, however the current model does not account for this, which may result in overestimated backward erosion failure probabilities. Contributing factors to backward erosion initiation such as animal burrows, vegetation roots, pipes, or other structures going through the levee are not accounted for either, which could balance our previous statement as such factors may increase backward erosion failure probabilities. Complementary work on including time and contributing factors to the backward erosion would improve the erosion fragility curve accuracy. Based on the overflowing mechanism probability assessment method used, we observed that overflowing failure probability is highly dependent on the water level applied to the levee and the overflow duration. Moreover, expert judgement is prone to over- and underestimation of failure probabilities as shown in Hathout et al., 2019, which may explain why the overflowing fragility curve has the steepest increase in this case study.

Steady-state and transient models

We ran both steady-state and transient hydraulic models to investigate the effect of non-saturated soil conditions related to the limited duration of the flood on backward erosion failure mechanism. For the transient model, we used a saturated/non-saturated soil model, which lead to different values and location of hydraulic gradients by the seepage analysis. We built theoretical hydrographs by taking into account a flood duration of $7days$ as shown in Figure 40, which provides the water levels of the river over time for all return periods (see section). These hydrographs are an attempt to include soil water content variation in our backward erosion model. We compared both hydraulic models on several criteria: the value of hydraulic gradient, the localization of highest gradients, the influence of the levee saturation parameter, and the time frame at which the gradients are observed. Because the hydraulic gradient is the value of interest for backward erosion, we only discuss the hydraulic model effect on backward erosion.

We observed in Figure 41 that hydraulic gradients location for saturated and non-saturated models differ. Hydraulic gradient values ranged for all flood return periods from 0 to 8. As expected, the steady-state model provided the highest hydraulic gradient values for a given water load with the hypothesis of fully saturated soils. For information, the transient model last time frame of $t = 7$ days would present hydraulic gradients location to be similar to the stationary model, knowing that the corresponding time frame for the flood was $t = 2.5$ days. In contrast, the transient model is a closer representation of reality since it takes into account the change in water level and in soil water content during the flood event. The results showed that for this case study, the levee saturation parameter has very little influence on hydraulic gradient values and location.

Selection of the local hydraulic gradient

Backward erosion starts at the land-side foot of the levee and therefore, local hydraulic gradients in this area are of interest (Figure 37). The size and shape of the area is worth further investigation because it has a large influence on the failure probabilities. To investigate this further, we considered four possibilities regarding the choice of the hydraulic gradient in the area of interest around the foot of the levee: (i) maximum

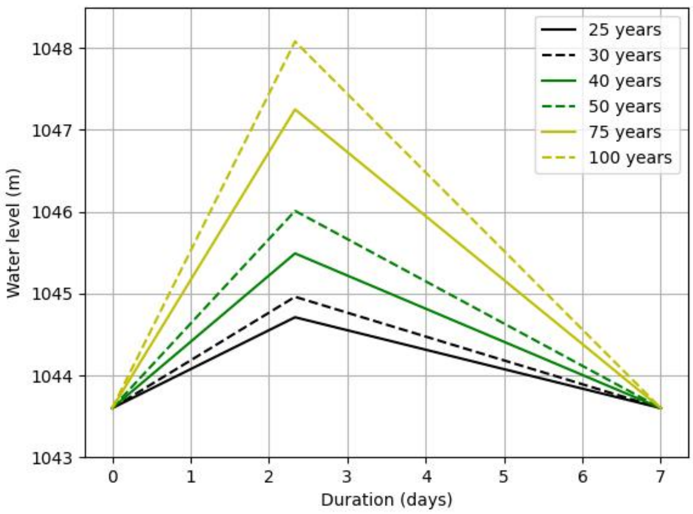

Figure 40: Water level curves for the transient model for selected flood return periods in the Bow River

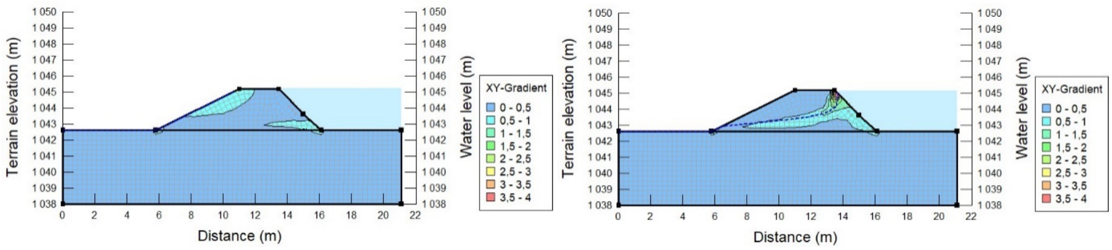

(a) (b)

Figure 41: (a) Levee hydraulic gradients for steady-state model, saturated levee for a flood return period of 35 years (peak flow rate); (b) Levee hydraulic gradients for transient model at peak flow rate ($t = 2.5$ days), non-saturated levee for a flood return period of 35 years

gradient, (ii) mean gradient, (iii) levee mean gradient, (iv) foundation mean gradient. Figure 42 showed that selecting mean gradient values lower significantly the resulting failure probabilities: the mean gradient values reached a 0.75 probability of failure for a 100 years flood return period, whereas the maximum gradient reached it for a 45 years flood return period. We selected a conservative hydraulic gradient for the construction of the internal erosion fragility curve corresponding to the maximum value of the hydraulic gradient around the foot of the levee.

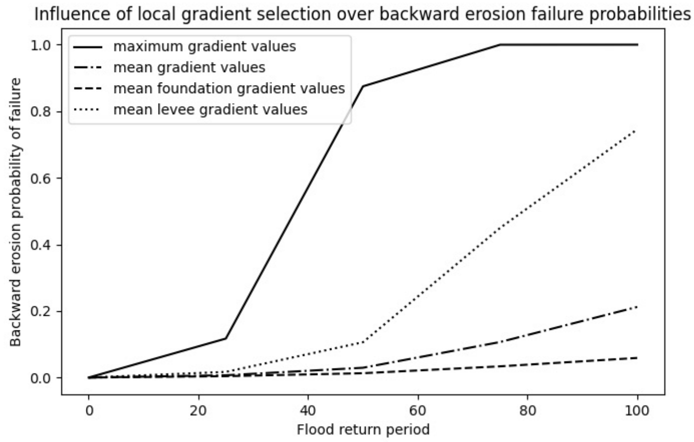

Figure 42: Fragility curves of backward erosion failure depending on the selection of the local gradient in the area of interest around the foot of the levee

Comparison of fragility curve aggregation method

We aggregated four fragility curves, each associated with a different failure mechanism to create a global fragility curve. This is an important step to improve the quantification of levee failure during flood events.

In this research, we investigated two approaches to aggregate fragility curves. The first and most common approach was to consider an envelope curve as described in section . For the second approach, we proposed a new method, which uses the Monte-Carlo method to simulate 10,000 potential failures for each mechanism. As shown in Figure 43, the maximum function curve lays slightly under the Monte-Carlo curve for the return periods between 25 years and 50 years. All individual fragility curves rise during this specific interval; it is therefore the most interesting area of the global fragility curve.

There is no significant change in accuracy from the envelop curve to the Monte-Carlo aggregation we propose. The improvement in flood risk lies in the fact it is more realistic and more statistically robust. The main drawback of any aggregation process is the loss of knowledge of which failure mechanism is predominant.

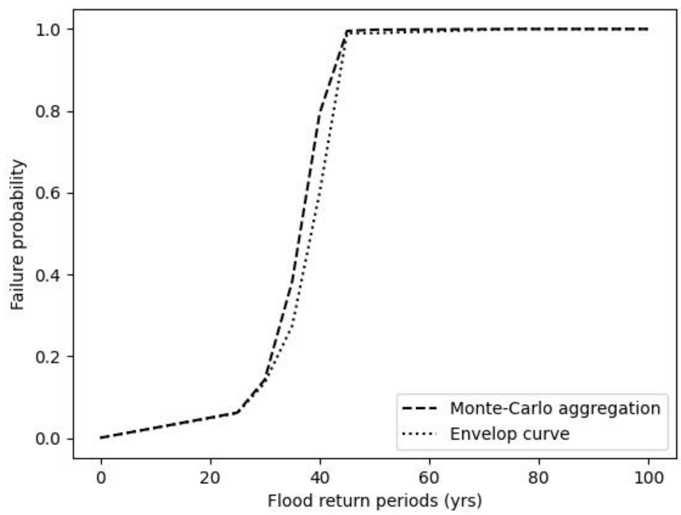

Figure 43: Failure probability aggregation curves using Monte-Carlo or envelop approach for a steady-state, saturated levee segment

Conclusion

Accurate flood risk assessments are a central element toward resilience to flood hazards. With the intent of being part of an integrated flood risk assessment, we proposed a probabilistic method to assess levee failure probability, which integrates three failure mechanisms. With this objective, the evaluation of a flood defence system's failure probability should maintain a satisfactory level of accuracy since the uncertainties at this point in the flood risk assessment process will persist throughout the flood risk assessment. This study proposed an easily implementable method with an acceptable accuracy level meant for medium scale defence systems (e.g., the area of a city), and therefore, the models used should be kept as efficient as possible for it to be applicable to real case structures.

The scientific question we tackle in this study is to develop an assessment method of levee failure probabilities taking into account various failure mechanisms. We have selected sliding, backward erosion, and overflowing failure mechanisms as the main potential failure modes of fluvial levees. For each mechanism, we have selected a method based on the current state of art to estimate the failure probabilities. We applied this method to an idealized levee built using one of Calgary's levee segment on the Bow River. The case study has shown that the sliding mechanism is the failure mode with the lowest occurrence probability of this particular levee segment. The main threat to the studied levee are backward erosion and overflowing.

Finally, we discuss novel interesting effects brought up by our model such as the different impacts the transient and steady-state models have on fragility curves and the value of taking the localization of hydraulic gradients into account. The transient model provides a temporal parameter, which is coherent with the study of flood, which occurs over a designated period of time. However, it also requires longer computation times and additional hypotheses on flood duration and theoretical hydrographs. The selection of the area of interest for hydraulic gradients has an influence on the probability results.

We recommend the use of Monte-Carlo aggregated fragility curves. Our resulting aggregated fragility curve is more realistic than the envelop curve of the failure mechanisms. Having a single aggregated fragility curve can improve the interpretation of the levee failure probability by operators, city staff, and civilians. The aggregated curve also simplifies flood risk analysis and probabilistic flood extent scenarios with only one failure probability to consider instead of several.

In future work, we will extend this analysis from estimating levee failure to estimating the overall flood risk over the entire flood duration. This process will allow including levee breaching and receding of waters from the flood protected area.

Chapter Five: Probabilistic assessment of flood hazard of a levee protected area

Summary

Preface

This chapter focuses on probabilistic flood hazard assessment in an area protected by a levee. Section presents a literature review on flood hazard assessment approaches. Section details levee failure probability assessment methods, the hydraulic model used to simulate flooding scenario, and the computation of occurrence probability of each scenario. Section 0.0.0.1 details the application to the Etobicoke Creek case study. Section 0.0.0.1 presents a discussion of flood depth and velocity probability results.

The content of this chapter was submitted as Mainguenaud et al., 2024 to the Journal of Flood Risk Management in October 2023. The contributions of each co-authors in the current chapter are as follows:
Florence Mainguenaud conducted the literature review, and wrote the original manuscript of this publication. Laurent Peyras, Claudio Carvajal, Bruno Beullac, Usman T. Khan, and Jitendra Sharma supervised the research and contributed to the writing and editing the manuscript.

Abstract

A flood assessment results in one or several flood maps, each dependent on a single hydraulic event, past, present, or future. The resulting flood depends on the intensity and duration of the modeled hydraulic event. As such, the choice of which hydraulic events to consider is carefully made: they must be relevant to the location, not too many to remain understandable for city officials and other decision makers. However a discrete approach such as this one leaves gaps in the flood assessment like hydraulic structure breaching events or combined events from different water tributaries.

We chose a residential area protected by a levee along Etobicoke Creek in the Greater Toronto Area (GTA), Canada. The hydraulic events include backward erosion and overflowing levee breach scenarios, and cover the Ontario regional event. The levee is divided into segments, for each one the backward erosion and overflowing failure probabilities are estimated. Then, for each return period, we simulate flood scenarios by breaching each segment individually for a single failure mechanism at the time. The resulting floods maps are associated with a flood event probability and a levee failure probability, which are combined into one event probability conditional to the flood probability. For every pixel of the study area, we have a cumulative probability curve for depth and velocity. This paper presents a probabilistic method for flood hazard mapping, which considers breach location, and overflowing and backward erosion failure mechanisms.

Multiplying discrete flood maps will increase potential misinterpretation, hence we propose a different approach with a single probabilistic flood map covering several hydraulic events at once.

Introduction

Flood hazard assessment is the first step in flood risk analysis to flood risk analysis Oliver et al., 2018, and includes flood propagation modeling for which Teng et al., 2017 provided a complete review of methods and flood mapping for one or multiple events and scenarios. Flooding assessments improved over time with better understanding of flood triggers and increase of computing capacity for numerical models. A flood assessment requires modeling existing hydraulic structures (e.g. levees, dams, storm surge, channels, artificial river streams, and detention basins non exhaustively). Any modification, removal, addition, or failure of hydraulic structures influences water flow propagation. Building flood defence structures is a natural response to protect populations and properties against water level fluctuations (Baldassarre et al., 2013) making fluvial levees a common feature in urban areas. However levees can reduce flood risk awareness of nearby communities, triggering the levee effect (Ferdous et al., 2019). A flood assessment results in one or several flood maps, each depending on a single hydraulic event be it historical or issued from hydraulic modelization. The resulting flood extent depends on the intensity and duration of hydraulic events modeled. As such, the choice of which hydraulic events to consider must be carefully made to remain understandable for city officials and other decision makers. Flood assessments considering levee failure help in decision making as one of the components to establish emergency plans, flood mitigation strategies and improve urban resilience.

In this context, Maranzoni et al., 2023 provided a comprehensive review of quantitative flood hazard assessment methods carried out in literature sorting them between heuristic, conceptual, or empirical approaches. It highlights that flood parameters include the type of flood, depth, velocity, duration of the flood event, flood arrival time, return period, flow discharge, sediments transportation, hydraulic structure breaching, scenario probability, flowing debris, and people behavior (e.g. evacuation time, traffic modeling, building occupancy). Each flood assessment chose which flood parameter to focus on depending on the objective of the study. Merz et al., 2007 identified water depth and velocity as the most influential flood parameters, hence they are the most commonly used in literature. Flood assessment maps can be either deterministic or probabilistic (D'Oria et al., 2019). Deterministic flood mapping is calibrated on historical flood events to simulate flood propagation of various event magnitudes (Baldassarre et al., 2010; Mazzorana et al., 2011). The uncertainties associated with such flood assessments are due to model inputs and parameters and can be assessed using sensitivity analysis (Hall et al., 2005). Ferrari et al., 2020 is an interesting example of deterministic flood mapping, and present a methodology to numerically simulate levee-breach-induced flooding in wide areas protected by river levees. Probabilistic flood mapping has the advantage to integrate flood hazard assessment uncertainties addressing the problem of lack of flood hazard model validation as it integrates various scenarios at once (Maranzoni et al., 2023). Many probabilistic flood mapping methods are proposed in literature such as Vorogushyn et al., 2010 who introduced the Inundation Hazard Assessment Model (IHAM) which considers overtopping, piping, and micro-instability levee breaches. D'Oria et al., 2019 considers backward erosion fragility functions to characterize levee breaches combined with a 1D-2D hydraulic model. Maranzoni et al., 2022 considered multiple breaching occurring throughout a single flood event. Baldassarre et al., 2010 compared deterministic and probabilistic flood mapping approaches, recommending probabilistic approaches.

One of the main gap in literature is integrated methods that cover (i) flood propagation models of rivers, (ii) levee reliability assessment for different failure mechanisms, (iii) flood propagation in relation to the breach modeling, (iv) spatialized flood hazard risk assessment obtained by statistical and probabilistic analysis and aggregation. Flood propagation models of rivers include: 1D, 2D, 3D, and 1D-2D models. In 1D models, calculations are made for each section and are suited for river channels and floodplains modeled with storage areas. But it needs significant post-processing to generate flood maps. Beilicci et al., 2012 compared of Muskingum method and DUFLOW 1D models and Meire et al., 2010 presented the STReam RIVer Ecosystem (STRIVE) model interaction with the storage modeled floodplain. 2D models solve flow equations across a predefined mesh on ground elevation from a Digital Terrain Model (DTM) and are used for modeling rainfall and complex floodplains. However the run time can be long and the in-channel hydraulic is not accurate. Li et al., 2013 proposed a 2D model based on finite proximate method. Lavoie et al., 2017 compare 2D models SRH-2D and $Hydro_AS-2D$. Morales-Hernandez et al., 2013 proposed a conservative 1D-2D coupled model for solving the Shallow Water Equations. 3D models are suited for specific local hydraulic problems like studying structure and water flow interactions.

Levee reliability can be estimated for different failure mechanisms such as internal erosion, overtopping or overflowing, and slope instability. CIRIA et al., 2013 presents earthen levees main internal erosion mechanisms: concentrated leak erosion, backward erosion, suffusion, and contact erosion. Concerning internal erosion, concentrated leak erosion in levees may be triggered by animal burrows connecting waterside and land-side as presented by Ceccato et al., 2022. Backward erosion failure estimation consists in a comparison of hydraulic gradients to a local or global critical gradient value respectively in Terzaghi, 1943 and H. Sellmeijer et al., 2011. Concerning overtopping or overflowing, Aguilar-Lopez et al., 2018 propose a probabilistic wave overtopping model to quantify grass cover erosion failure by wave overtopping. Vuik et al., 2017 estimate overflow and wave overtopping levee failure probabilities for levees and sand dunes with the Fist Order Reliability Method (FORM) and Monte-Carlo simulations. Mainguenaud, Peyras, et al., 2023 estimated overflow induced failure by using expert judgement as described in Hathout et al., 2020 and Rongen et al., 2022. Concerning slope instability, Mainguenaud, Peyras, et al., 2023 estimate slope instability, taking into account also backward erosion, and overflowing failure probabilities for a levee.

Breach modeling and flood propagation through the breach into the protected area require breaching models integrated into flood propagation softwares. Related to breach modeling, Mazzoleni et al., 2014 modeled a flood hazard with levee piping (aka. backward erosion) breaching in the Po river in Italy. Rifai et al., 2018 points out limitations of fluvial levee breach models that are transposed from dams studies and rely on empirical formulas and tested for dam breach cases like Mohamed et al., 2002. For flood propagation equations used in the 2D area, Costabile et al., 2017 presented the limitations of the diffusive approximation compared to Shallow Water Equation (SWE) and concluded that diffusive-type models should be avoided when simulating urban areas due to the poor results around building. Yilmaz et al., 2017 used both SWE and Diffuse Wave Equation (DWE) to assess flood hazards considering dam overtopping and piping using Froehlich equations for breaching parameter values. They determined that maximum depth, velocity, and arrival time should be calculated by SWE, while flood extent can be accurately determined by DWE.

Spatialized flood hazard assessment consists in assessing the flood parameters in the areas impacted by the flood. One of the main deliverable could be to provide large-scale flooding maps from a mosaic of local flood maps. This process was initiated by the European Environment Agency, 2007 which prompted the formation of large-scaled flood maps. Scaling up comes with its own challenges but a good example is presented by Dottori et al., 2016. In this field, Tufano et al., 2023 combined flood hazard maps of different flood events by overlaying them, making visually appealing and comprehensible flood hazard maps destined to stakeholders, city officials, or insurance companies. Maranzoni et al., 2022 proposed a probabilistic distribution of the flood hazard levels.

Our research aims to build up an integrated method to assess flood risk in levee protected areas and in a probabilistic framework. This article covers the different stages aiming to provide a probabilistic assessment of flood hazard in areas protected by levees, considering different breaching scenarios. Concerning the hydraulic model, we consider depth and velocity flood parameters, and we use a 1D-2D model for our study. Amongst the softwares that enable 1D-2D hydrodynamic models like TUFLOW, HEC-RAS, or MIKE FLOOD, we chose HEC-RAS which has an integrated levee breaching option and we use SWE to propagate flooding in the levee protected area. Concerning the failure modes of the levees, we consider backward erosion and overflowing failures.

We apply our method to the Etobicoke Creek levee (Canada), which was well documented thanks to data provided by local authorities.

Finally, the objective of this study is to provide a probabilistic flood assessment method that incorporates levee failure for several return periods. To this end, we estimate levee failure probabilities for overflowing and backward erosion failure mechanisms. Then, we model flood propagation and simulate extensive flood events and breaching scenarios. For each simulation, we compute a global flood exceedance probability, plot and analyze flood parameters versus the global flood exceedance probability in different locations of the flooded area.

Materials and methods

Levee failure probabilistic assessment

We use the probabilistic method presented in Mainguenaud, Peyras, et al., 2023 to estimate backward erosion failure probabilities and overflowing failure probabilities. Here we summarize the main hypotheses and results of this work useful for this study.

Backward erosion probability assessment

Among the different mechanisms of internal erosion, backward erosion is commonly used as the design criteria for levees. In this study we consider backward erosion initiation (not taking into account the erosion progression until the levee failure). The resulting probability of failure corresponds to the probability of erosion initiation, which is a safe approximation, as erosion does not always lead to failure such as when the process is interrupted. Backward erosion analysis can be performed by comparing hydraulic gradients to a critical gradient fitted to the soil type. We compare local hydraulic gradients obtained from a finite element model based on a seepage analysis to the critical gradient of Terzaghi, 1943. Using the seepage module from the software GeoStudio, we computed hydraulic gradients through the levee and foundation assuming steady-state as a conservative approximation. The soil model parameters used for the seepage analysis are presented in the study case section

0.0.0.1. We selected the maximum gradient located on a $1 m^2$ area centered on the foot of the levee where backward erosion starts. To integrate the uncertainty of the critical gradient, we considered it as a random variable normally distributed and defined the distribution parameters from expert judgement and literature to fit the study case (Mainguenaud, Peyras, et al., 2023). Applying this approach, we estimated the backward erosion probability of each levee segment for our case study on Etobicoke Creek River and represented the corresponding fragility curve in Figure 44.

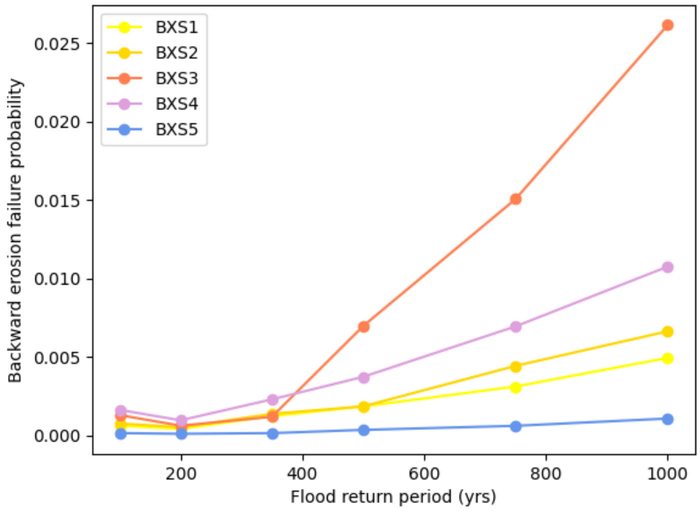

Figure 44: Backward erosion fragility curves for Etobicoke Creek River

Overflowing probability assessment

As described by Visser et al., 1995, overflowing is a time dependent mechanism that can be fractioned in three phases: the beginning of the overflowing and erosion, the progression of the erosion at various speeds, and the collapse of the structure. The progression of the erosion at various speeds being the most complex part of erosion estimation, and without a surefire method to estimate it, we chose to consider overflowing failure as the beginning of a severe erosion of the hydraulic structure for peak flow conditions. To estimate overflowing failure probability, we rely on expert judgement (Mainguenaud, Peyras, et al., 2023). We constituted a panel of specialist engineers with knowledge of the geotechnical or hydraulic fields including at least one specialized in risk analysis. These experts qualitatively assessed each failure scenario. The qualitative scale ranges from “not probable” to “almost certain probability” with a total of 7 grades matching with an annual probability. Then, we use Mainguenaud, Peyras, et al., 2023’s method to transpose qualitative expert judgement into quantitative probabilities, resulting in overflowing failure probabilities for each levee segment of our study case and we represented the corresponding fragility curve in Figure 45.

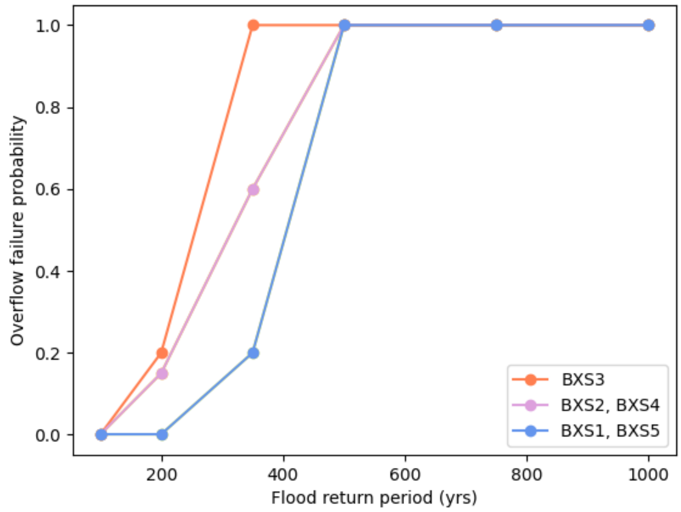

Figure 45: Overflowing failure fragility curves

Hydraulic model

0.0.0.1 Water propagation model

We use HEC-RAS's 1D-2D model to compute the river water surface for a subcritical flow regime in the 1D area, and SWE in the 2D area. SWE are simplified Saint-Venant Equations, themselves being a simplification of Navier-Stokes Equations. SWE assume incompressible flow, negligible vertical velocity and vertical derivative terms. A trial run on our study case showed that this simplification fits the flood propagation conditions in the levee protected 2D area. We use unsteady flow with theoretical triangular hydrographs. For each simulation, we kept the highest depth and velocity values reached during the flood event for each pixel of the protected area.

Levee breaching model

HEC-RAS integrates two breaching mechanism options: (i) piping or (ii) overtopping (Hydrologic Engineering Center, 2023). The piping breach option (i) opens from the bottom of the levee, and the erosion will begin on the protected side of the levee as a result of seepage flow carrying soil particles. As the pipe grows larger, material will detach and fall into the moving water slowly resulting in an open breach. The overtopping breach erosion option (ii) starts on the downstream side of the levee, and was deemed satisfying to model the overflow failure mechanism.

HEC-RAS includes three models that can be used to model the breach: (i) the parametric breach model, (ii) the "simplified physical" breaching method which requires an input of velocity versus erosion rates and breach widening relationships, and (iii) the DL Breach model developed by Wu, 2016. Considering available data, we chose to use the parametric breach (i) model for which we calibrated the breach final width, slopes, and time of breach opening using Froehlich, 1995 empirical equations provided in Table 9. The final breach depth parameter was chosen by expert judgement presented in section 0.0.0.1. The backward erosion breaches are deep with steep slopes, whereas overtopping breaches tend to have a wider bottom section and gentler slopes than breaches due to backward erosion.

Breach final width	Breach slopes	Breach opening time
$B = 0.1803K_o(V_w)^{0.32}(h_b)^{0.19}$ K_o = 1.4 for overtopping, 1 otherwise; V_w the reservoir volume at time of failure h_b breach final height	$Z = 1.4$ for overtopping Z = 0.9 for other failure modes	$t_f = 0.00254(V_w)^{0.53}(h_b)^{-0.90}$ V_w the reservoir volume at time of failure h_b breach final height

Table 9: Froehlich, 1995 empirical breach parameter equations

Paquier et al., 2016 reminds that breaching starting time and final breach dimensions greatly influence the water discharge in the protected area. The faster a breach opens, the more water flow goes through the breach during the flood event, resulting in higher depths or velocity values in the flooded area.

We did not consider simultaneous, nor successive breach failures as we assumed that when a breach occurs, it liberates some of the pressure forces on the structure and should be less likely to breach on nearby downstream segments, which is relevant knowing that our case study is not a long levee. The consideration of multiple breach may be relevant for long levees of several kms.

Cumulative global probability of flood depth and velocity

This section aims to obtain the global flood exceedance probability of each simulation conditional on a flood event and based on a statistical analysis of depth and velocity flood parameters. The appendix presents the global flood exceedance probability values of the 350 year return period.

The general process is as follows: for a given return period, we compute the complementary no breach event probability for each breach simulation, which sum constitutes the no breach simulation event probability for the return period. The levee failure probabilities are obtained as described in section . Then, we use Equation 0.29 to compute the global flood exceedance probability conditional on the flood return period by pondering the failure or non-failure probability by the number of levee segments considered for the return period, and the number of failure mechanisms considered for a designated return period and breach location. Hence, we assume that failure mechanisms are independent. For each return period, the sum of each simulation probability equals 1.

$$P_{(global \mid flood)} = \frac{P_{(\text{failure / nonfailure})}}{(\text{nb failure mechanism}) \cdot (\text{nb segment})} \tag{0.29}$$

Finally, we compute the global flood exceedance probability for each simulation using Equation 0.30.

$$P_{global} = P_{(global \mid flood)} \cdot P_{flood} = \frac{P_{(global \mid flood)}}{T} \tag{0.30}$$

The frequency T corresponds to the return period in years.

We propose two representations of those probabilities for each point described in section 0.0.0.1 using a log scaled probability axis.

- the cumulated global flood exceedance probability of every breach location, which showcases the contribution of each scenario and enables the behavior study of depth and velocity in regards to the levee breach mechanism and its location,
- the cumulated global flood exceedance probability taking into account every scenario.

Case study

Case study

Location of the case study

We apply the probabilistic approach presented in section to the protected area, located in Meadowland park in Brampton, Ontario, Canada, and protected by a levee on Etobicoke Creek River. For this protected area, city officials raised concerns about continuous flooding of the residential neighborhood even though a levee is in place. We applied the probabilistic flood assessment method developed to this protected area considering the characteristics of both river and levees.

Hydrology considerations

Meadowland park is located in the Etobicoke Creek watershed which drains $211 km^2$ with a mean river slope of 0.005. The watershed main land-uses are: 63% urban, 22% rural, and 15% natural land cover, while our local study area consists of mostly urban residential areas (Toronto Region Conservation Area, 2010). We base our unsteady flow propagation model on the overall type and shape of hydraulic events from the Water Office historical database, which provides water levels and flow values from the $02HC017$ hydraulic station located near our study area (Government of Canada, 2023).

Using flood frequency analysis, we determined peak flow values, hereby ranging from 85 to $530m^3.s^{-1}$ for a $12h$ event. We used simplified triangular hydrographs for a $48h$ duration to simulate flood events associated with return periods $100, 200, 350, 500, 750$, and $1,000 year$.

Geotechnical considerations

The levee is located approximately $80m$ away from the river stream steep vegetated banks, creating a mitigation floodplain. This case study is a 60 year old levee with a homogeneous silty embankment, $2m$ high throughout the $500m$ of length. The levee slopes are fairly consistent throughout the levee length and consist of $3:1$ (horizontal:vertical) for the water side and $2:1$ for the protected area side of the levee as shown on Figure 46. The asphalt trail on top of the levee crest follows the terrain's gentle slope, and welcomes both pedestrians and seldom utility vehicles. This levee is able to withstand a 100 year flood return period without overtopping.

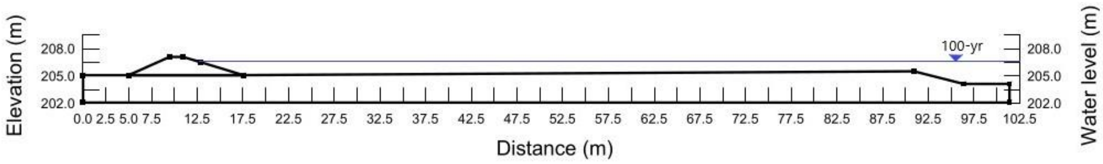

Figure 46: Schematics of the levee cross-section for segment 3

In our case study, the earth fill of the levee is homogeneous, therefore topography and geometry prevailed for the segmentation as shown in Figure 47.a. So we divided the levee into 5 homogeneous segments based mainly on topography and geometry considerations. The levee crest elevation follows the natural slope of the river, thus we considered an average crest elevation for each segment. The curvature of the levee, visible on Figure 47.b, was a decisive factor to the segmentation. We hypothesize that the failure probability is constant throughout a levee segment.

(a) (b)

Figure 47: (a) Levee segments; (b) Photography of the levee oriented toward downstream and located at the beginning of segment 3

At the request of York University, a geotechnical assessment was made by the company TerraProbe to assess geotechnical parameters of the case study area. The geotechnical assessment indicated a silty soil (gravel 10%, sand 41%, silt 31%, clay 18%) globally homogeneous, $0.3m^3.m^{-3}$ water content, $10^{-8}m.s^{-1}$ levee permeability, $10^{-6}m.s^{-1}$ foundation permeability, finished soil settlement, and estimated the earth fill cohesion to $0kPa$ and the angle of internal friction to 28^o. Those data were used in the GeoStudio software for the seepage analysis. As described in section , we estimated backward erosion failure probabilities by computing the critical hydraulic gradient to using Terzaghi's equation for expert judgment obtained values: porosity $n \in [0.3; 0.45]$, the solid particle density $\gamma_s \in [2,600; 2,800]\, kg.m^{-3}$ and $\gamma_w = 1,000 kg.m^{-3}$, and we assumed a critical gradient curve following a normal distribution $N(1.06; 0.27)$.

Hydraulic considerations

Toronto and Region Conservation Authority (TRCA) provided a steady flow hydraulic model of the Etobicoke Creek area made with HEC-RAS, which we adapted to run unsteady flow simulations with theoretical hydrographs, a 1D river, and a 2D area for the flood to propagate behind the levee. The levee was designed to withstand 100 year return period flood events but the city officials concerns and the age of the levee made assessing the performance of the levee anew important. The High Resolution Digital Elevation Model is derived from LiDAR data and satellite imagery provides a

DTM of $1m$ spatial resolution. The DTM used for the case study results from York2019 survey provided by National Resource Canada (NRCan) in open access. We assumed a breach final depth corresponding to the levee crest height. We decided to maintain a constant breach opening time for every simulation, enabling the comparison of depths or velocity between simulations.

Points of interest in the protected area for the probabilistic flood assessment

For the flood probability assessment, we consider five locations of interest from the protected area to analyse the flood results with. Figure 48 shows each point location:

- point 1 has been chosen in the residential neighborhood,
- points 2 and 3 stand behind the levee respectively at segment 3 and 4,
- point 4 is located on the parking lot, and the fifth point on the main road downstream of the levee.

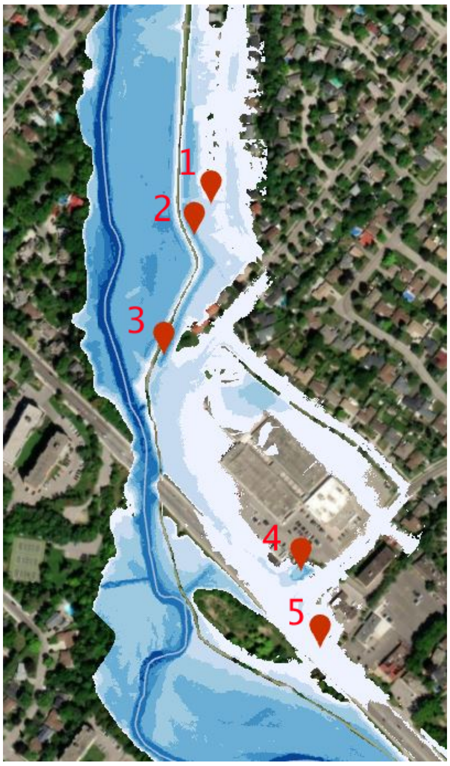

Figure 48: Points of interest location in the protected area

Results

Probabilistic assessment of flood in protected area related to segments and breaching mechanisms

Following the steps described in section 0.0.0.1 using a python script presented in Appendix 0.0.0.1, we compute the conditional failure probabilities of each simulation and the cumulative for each breach and failure mechanism. The result are the cumulated flood exceedance probabilities represented in Figure 49 and 50 for which each graph present 11 lines related potential 3 breaching mechanisms (O=Overtopping; P=Piping; NB=No Breach) and the cross-section of each $segment_i$ which failed (BXS_i). Each line is composed of 4-5 points each obtained for a different flood intensity (return periods from 100 year to 1,000 year).

To analyze the influence of the breach location and failure mechanisms on depth and velocity flood parameters for each segment considered individually, we present all point locations in Figure 49. To better showcase our results, we zoom in on points 1 and 5 (Figure 50), point 1 being close to the levee and point 5 being far from it. Points location are described in section 0.0.0.1.

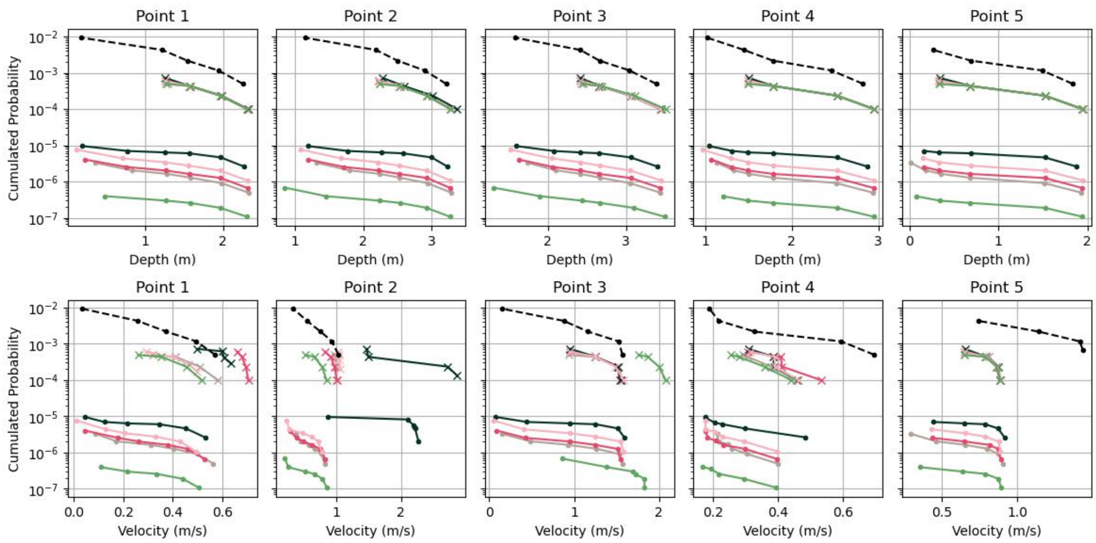

Figure 49: Cumulated flood exceedance probabilities for depth and velocity for every point

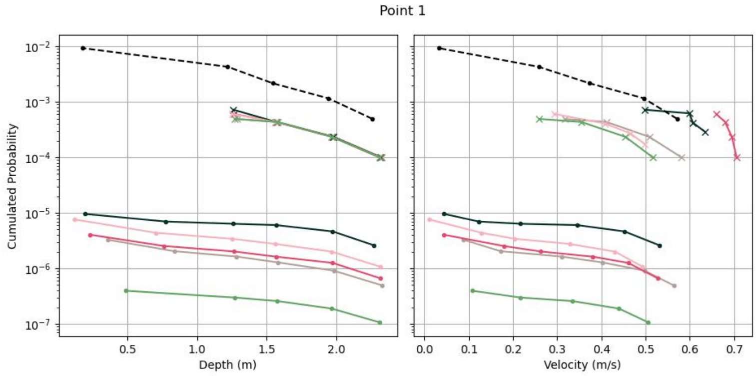

(a)

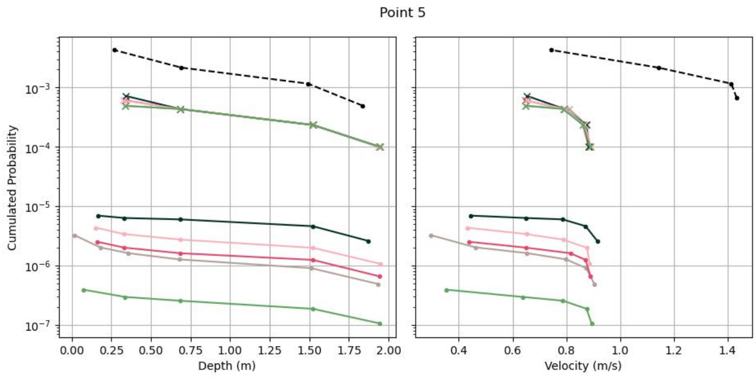

(b)

Figure 50: Cumulated flood exceedance probabilities for (a) water depth and velocity at point 1 (located in the residential area close to the levee), (b) water depth and velocity at point 5 (located on the main road away from the levee) for each simulation.

Global probabilistic assessment of flood in protected area

Following the steps described in section art2:cumulativeglobalprobability, we aggregate conditional failure probabilities of every simulation into a single cumulative curve as shown in Figure 51.

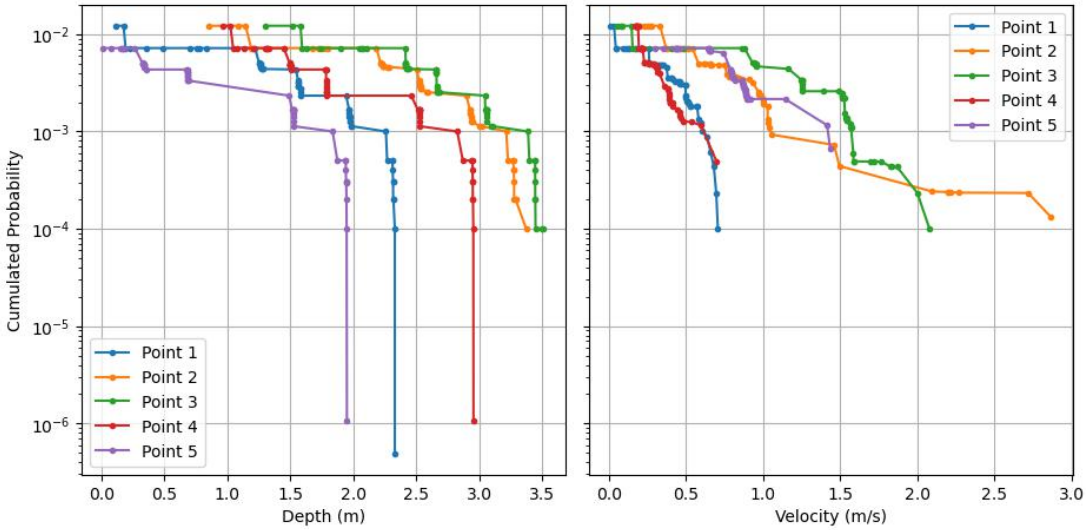

Figure 51: Aggregated cumulated flood exceedance probability of water depths and velocities of various locations within the flooded area. Point locations are given in section 0.0.0.1

Discussion

Influence of distance to the levee on depth and velocity probabilities

Depth in Figure 50 behaves uniformly throughout the protected area regardless of the closeness to the levee. Figure 51.a shows that depth intensity diminishes as the point location gets further from the levee. Points 2 and 3 are the closest to the levee, followed by points 1, 4, and 5. However, it seems for this case study that there is no correlation between depth and distance to the levee as point 1 shows lower depth values than point 4 even if it is closer to the levee compared to point 4. As a result, the residential area (point 1) does not stand out as being the most impacted by hydraulic events.

Figure 49 shows that for the furthest location from the levee (points 4 and 5), the "no breach" simulation velocity range is higher than for closer locations, suggesting that simulating levee breaching impacts flood propagation. Also, around the breach, flow velocity peaks and then dissipates the further we go from the breach location. Figure 51.b reinforce this observation by showing points 2 and 3 with higher velocity values than the other locations for the same probability. This is logically explained because they are located in front of the potential breach openings.

In Figure 51.b, point 5 (road location) shows similar probability evolution to point 2 and 3, for a lesser velocity range. Considering how far point 5 is located from the levee, this result raises questions. The reason could stem from the straight and flat terrain conditions offered by the asphalt road, presenting seldom obstacles to slow water propagation. The point 1 (residential area) and the point 4 (parking area) both show low velocity values (inferior to $0.75 m.s^{-1}$) even for high return periods hydraulic events.

According to this case study results, we can provide the following generalizations:

- Higher depth values are achieved close to the levee,
- In case of a breach, velocity peaks close to the breach location and dissipates quickly with distance to the levee which may reveal an absence of obstacles. Roads offer a favorable environment to flood propagation, though the impact of car clutter could hinder the flood propagation and adding floating debris, which are not accounted for in this study,
- Considering both depth and velocity is necessary as their behavior differs in range and probability, particularly velocity should be considered alongside levee breaches as it impacts the velocity range and location.

Contribution of breaching and non breaching scenarios to the aggregated probability

Depth contribution cannot be evaluated as the breach scenario contribution to the aggregated depth probability show but little variation as visible in Figure 49 and Figure 51.a, where the aggregated probabilities reflect this characteristic by behaving similarly.

The comparison between the velocity of points 2 and 3 show on the aggregated velocity probability of Figure 51.b that point 2 probability shows the highest range for lower probabilities than point 3. This is explained in Figure 49, where point 2 shows small velocity probability except for breach of segment 3, whereas point 3 shows high velocity probability for every scenario.

According to this case study results, we can provide the following generalizations:

- A no breach scenario slightly underestimates water depths in case of a breach but is a good approximation of the range of depth values reached, however velocity values tend to be overestimated for breach scenarios for locations downstream of the levee.
- The contribution to each scenario to the aggregated probabilities is identifiable for the velocity parameters, allowing to discretize between, no breach and breach scenario, including between breach scenario themselves.

Impact of levee failure mechanisms on depth and velocity probabilities

In Figure 49, the “no breach” scenario is distinguishable by higher cumulative probabilities than any other scenario. “Overflowing breach” scenarios, rank second, followed by “backward erosion” breach scenario, showcasing in the same occasion the reliability of the levee.

Backward erosion failures show consistant probabilities ranking for both depth and velocity. as shown in Figure 49. Whereas, overflowing failures result in almost identical range and probabilities for the depth parameter.

Breaching reduces velocity probabilities, this phenomenon is specially visible in Figure 50.d.

According to this case study results, we can provide the following generalizations:

- The “no breach” scenario has the highest probability, showing that the levee is more likely not to fail, confirming the reliability of this case study levee,
- Considering breaching scenarios has a small impact on depth probabilities but a significant one on velocity probabilities,
- The proposed method allows for a clear view of each failure mechanism contribution to flood exceedance probabilities and shows which critical failure mechanism to focus on.

Impact of breach location on flood hazard

Figure 49 shows that breach location has no influence on flood depth probabilities. Backward erosion exceedance probability decreases from levee segment 3, 4, 2, 1 to 5. Segments 3 and 4 are located at the levee curvature and are the most likely to fail, whereas the upstream segments 1 and 2 are the least strained and segment 5 is protected by the local topography.

However, the velocity probabilities are highly dependent on the location of the breach and the point of interest in the protected area (e.g. point 2 located in front of segment 3 shows high velocities when the breach is located at segment 3). Topography seems to play a decisive factor for velocity probabilities throughout the flooded area.

According to this case study results, we can provide the following generalizations:

- Breach location has no influence on flood depth probabilities.
- This method enables one to identify which segments are most critical, indicating which ones to focus on if one wants to improve levee reliability and safety of the protected area. In our study case, the most critical levee segments are segments 3 and 4.

Conclusion

In this study, we presented a probabilistic flood hazard assessment method of levee protected areas. Our method includes (i) river hydraulics, (ii) levee reliability for several flood events, (iii) flood propagation with levee failure scenarios, and (iv) aggregated probabilistic flood hazard mapping.

Our approach consists in levee reliability study for homogeneous levee segments, considering various levee failure mechanisms triggered by different flood intensities, propagating flood in the river and through the levee breach, statistically analyzing depth and velocity flood parameters located in the protected area. We propose a new approach to probabilistic flood hazard mapping for flood hazard assessments.

The Canadian case study showcases our new method advantages such as:

- the ability to identify the levee segment the most impactful on flood hazard as well as the most impacting failure mechanism on the reliability of a given levee segment,
- locate the most hazardous areas when considering depth and velocity probabilities,
- discriminate the most impactful failure mechanisms for flooding in the levee protected area.

In future works, we will explore the potential of dynamic flood mapping and capitalize on probabilistic flood hazard to propose a probabilistic flood risk map.

Chapter Six: Flood risk assessment

Summary

Preface

Flood risk assessments are continuously improving, driven by technology, data availability, and better understanding of the mechanisms involved in flooding events. Latest advancement in flood risk assessments include:

- integration of climate projections to project future flooding scenario, including changing rainfall patterns, sea-level rise, or extreme weather events,
- probabilistic flood modeling, which takes into account uncertainty and variability in rainfall, water discharge, sea levels, or geotechnical parameters. This approach provides a wide range of flood scenarios, helping decision-makers with providing various amplitude of flood hazard,
- sensor technology and communication systems enabled real-time flood monitoring and improved early warning systems, providing tools to guide evacuation and stakeholders response to the flood event,
- consideration of multiple hazards raising awareness to compound risks,
- machine learning algorithms are applied to flood risk assessment in analyzing large datasets to improve flood hazard predictions. This tool can be used to identify patterns and trends in historical data.

In this dissertation, probabilistic flood hazard modeling is the main element of interest. Main advantages of probabilistic flood modeling include the use of a quantitative scale and the ability to integrate different flood scenario. One drawback is its dependence on historical flood data and statistical analysis to estimate the probability of a flood event, which is associated with significant uncertainties.

A flood risk assessment requires the combination of flood hazard with a vulnerability assessment as described in section . First, we present a method to assess flood risk and focus on vulnerability. Then, the results of its application to Etobicoke Creek. Finally, we discuss the results and improvements to this flood risk assessment application.

Introduction

Flood risk assessment requires multiple scientific fields (e.g. hydrology, hydraulic, civil engineering, geography, human sciences). Flood risk assessment is a group work, cooperation from all fields is required to put together a coherent flood risk map. This coordination requires a well defined method so that each participant can focus on providing their contribution made with the right assumptions, simplifications, and precision scale so that each piece fit together. Core blocks of flood risk assessment include: data (e.g. hydraulic, topographic, social, economical assets), hydraulic model to propagate a flood, vulnerability assessment to combine it to the flood hazard obtained from the flood model.

At the core of every scientific field stand the technology to record data such as remote sensing technologies (e.g. satellite imagery, LiDAR) for terrain mapping and land-use, hydraulic stations provide historical data of river water discharge. The accuracy and reliability of those data is transmitted throughout every analysis. Hydrological models predicts river discharge based on hydrographs or rainfall patterns. The flood propagation model identify potential flood-prone areas. Modelling flood hazard was the main focus of this dissertation (section) and is essential to flood risk assessments. We can divide vulnerability assessment into 3 main type: social, economical, and environmental. Social vulnerability correspond to how population is able to evacuate or withstand the flood event. The social criteria is composed of sub-criteria including: demographics such as age or household composition, income level, population density, handicap, linguistic (language barrier), population awareness of floods, governance preparedness to floods (evacuation and emergency plans). Economical vulnerability correspond to the intrinsic resilience of the wealth creation industry of an area. Some sub-criteria are: the type of industry, the economic diversity, the infrastructure quality, the business resilience to flood, or the insurance coverage. Environmental vulnerability refers to the susceptibility of ecosystems to withstand flooding events. Several criteria can be considered: impact on habitat and ecosystems due to evolution of the river channel, a high biodiversity should be more adaptable to environmental changes, erosion control measures (because flooding lead to soil erosion and sedimentation), vegetation cover which minimizing soil erosion, water quality and potential polluting industries. Most environmental vulnerability criteria are vague and difficult to quantify due to scarcity of data and method (section). Therefore, most flood risk assessment do not take them into consideration or partially to fit their needs. For this same reason, this PhD dissertation does not dwell on environmental vulnerability.

First, a presentation of flood risk assessment methods, then the results of an application to Etobicoke Creek, potential improvements, and finally conclusion of the flood risk assessment application.

Materials and methods

A flood risk assessment is composed of flood hazard and flood vulnerability combined with a risk attribution method. There are many definition of flood risk (section), but in this dissertation, we consider flood risk as the combination of flood hazard, exposure, and vulnerability. This combination is done by overlaying flood hazard and vulnerability layers using a Geographic Information System (GIS). The advantage of such a method is the convenience of changing a component of flood risk, future projection of flood and vulnerability can be incorporated and additional weight can be attributed to a layer over the other.

Each criteria is not always quantifiable with a number or probability, hence the use of indicators or conversion into a common unit (e.g. monetary values). In general, the social risk has been less evaluated than the economic risk. Risk assessment methods are divided in qualitative and quantitative methods. Qualitative flood risk assessment mainly consist in risk matrices, attribute a qualitative estimate to an area risk by crossing flood hazard with potential consequences. Risk matrices also combine the probability of flooding with the potential consequences to calculate flood risk levels. Quantitative flood risk assessment is divided into which kind of damage (building or people) is assessed. This PhD dissertation focuses on quantitative flood risk assessment methods. We will present some of the most widely used methodologies, and develop which one we chose for our case study.

Quantitative risk assessment

Economical risk

Assessing damage to buildings can be done using one of the following approach:

- Flood Loss Estimation MOdels (FLEMO) such as HAZUS and CATDAT quantitatively assess direct and indirect economic losses due to flooding.
- Flood damage functions link flood parameters (e.g. depth, water extent) to economic losses. This method estimate monetary consequences of floods and can be integrated with probabilistic flood hazard models.
- Flood Risk Index (FRI) or Composite Flood Risk Index (CFRI), combine flood hazard and vulnerability into a single numerical value.

- GIS tools can analyze and visualize flood risk by overlaying flood hazard maps, vulnerability and exposure data. The method of GIS overlay considers mostly exposure but if hazard and vulnerability layers are added, this method is able to provide a comprehensive flood risk map.

Here are some example of application. The HAZUS model was developed by the Federal Emergency Management Agency (FEMA) of the United States of America (USA), has a standardized method to analyze natural risks such as floods, tsunamis, earthquakes, or hurricanes (Scawthorn et al., 2006). The model performs a hydrological analysis by calculating the flow discharge for each hydrologic region, using the Digital Elevation Model (DEM) and regional regression equations (Jennings et al., 1994). A 2D hydraulic analysis uses a rating curve to calculate flood depth as a function of the distance between the channel and the floodplain. Required input data are the DEM, flood frequency, flow rate, and cross sections. Direct and indirect economic losses are estimated using depth-damage curves for buildings, transportation, essential facilities, and utilities. The big advantage of the HAZUZ-MH software is that it contains input data from the United States Census and other national databases, which can be used directly.

The grid-based GIS approach for regional flood loss estimation, developed by Su et al., 2005 models a 1D flow for the channel, a 2D flow on the floodplain, and the urban drainage systems (Storm Water Management Model). The vulnerability analysis uses depth-damage curves for vehicles (e.g. motorcycles, cars), commerces and industries (e.g. manufacturing, wholesaler, service, retailer). Data to create those depth-damage curves were extracted from surveys, interviews, and damage claim information. An expected annual damage is computed as the integration of the flood exceedance probability curve, resulting in an expected annual damage for each grid cell.

Societal risk

Assessing damage to people can be done using the Life Safety approaches quantify the risk to human life such as the Local Individual Risk (LIR) and Societal Risk (SR) considered in the Netherlands. Some examples are provided below.
Jonkman et al., 2011 defines LIR as the annual probability of death of an average, unprotected person. This allows for a quantifiable indicator to limit construction permits while located within the 10^{-6} probability range as presented in Figure 52.a.

Jonkman, Maaskant, et al., 2009 defines mortality (a.k.a. fatalities) and evacuation rate parameters establish a fatality number as in Figure 52.b. Mortality functions are defined in 3 zones: around the breach, in the rapid raising water area, and other.

Jongejan et al., 2011 defines the evacuation rate rely on the forecast effectiveness, and the reliability of the defence system. Even with a timely warning, the population might be reluctant to leave, and the evacuation might fail due to congestion. Therefore, the evacuation rate is expressed as the reduction of exposed individuals in percentage following the event tree analysis proposed in Figure 52.c.

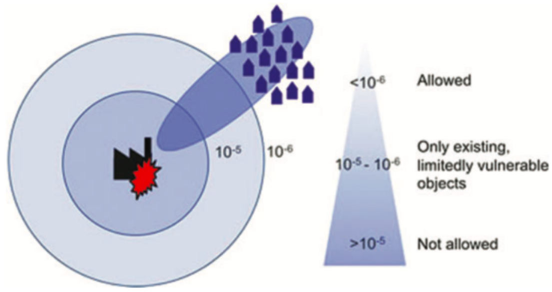

(a) Individual risk contours from Jonkman et al., 2011

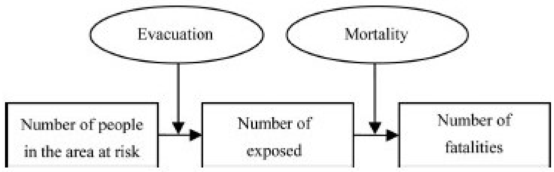

(b) Loss of life estimation schematics

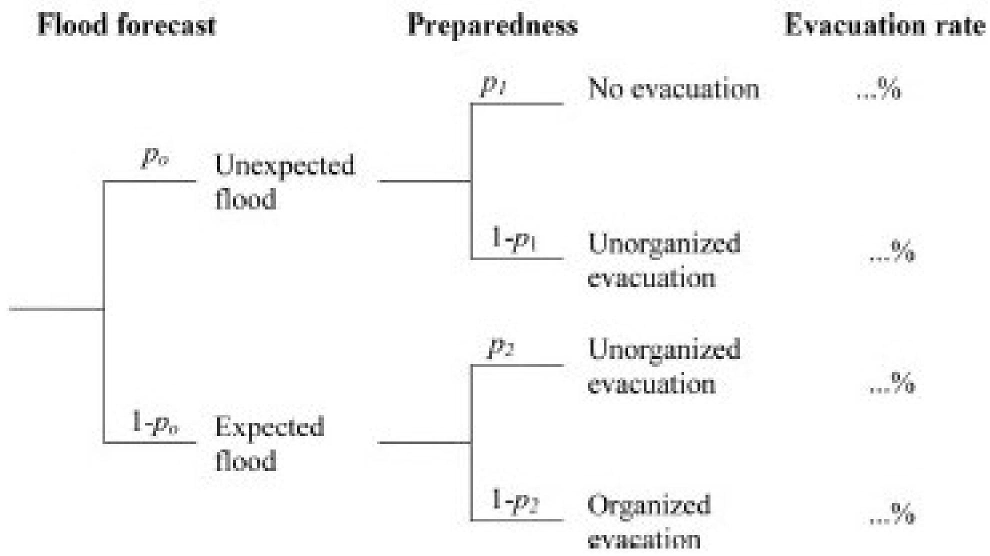

(c) Evacuation rate tree analysis

Figure 52: (a) Individual risk contours; (b) Loss of life; (c) Event tree analysis of evacuation rate from Jongejan et al., 2011

Maaskant et al., 2010 describes societal risk methods proposed in the Netherlands as the probability of an accident with many fatalities and represented by an FN-curve, which shows the probability of exceedance of a certain number of fatalities $P(N >= n)$. We refer to 3 methods: the frequentist approach, bayesian approach, and a simplified bayesian approach applied to a dike ring.

- the frequentist approach estimates of the number of fatalities in a flood to compute an FN-curve, along with upper and lower bounds which delimitate an uncertainty interval such as in Figure 53.a.
- the Bayesian approach has an FN-curve which correspond to the probability density function (PDF) as in Figure 53.b.
- the simplified Bayesian approach was introduced as an alternative when estimating the PDF requires too many flood scenarios. The simplification relies on

two assumptions: flood defences are low probability, high-impact events, and on the shape of FN-curves. Figure 53.c shows a comparison of the calculated FN-curve with the Bayesian approximation.

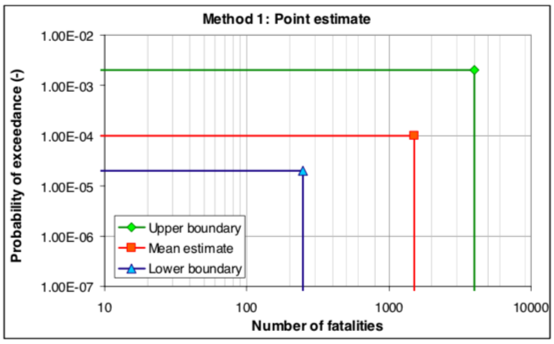

(a) Frequentist approach

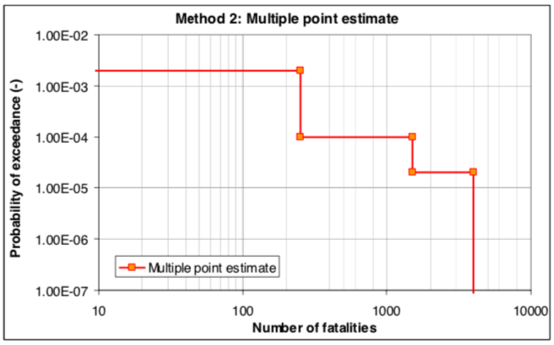

(b) Bayesian approach

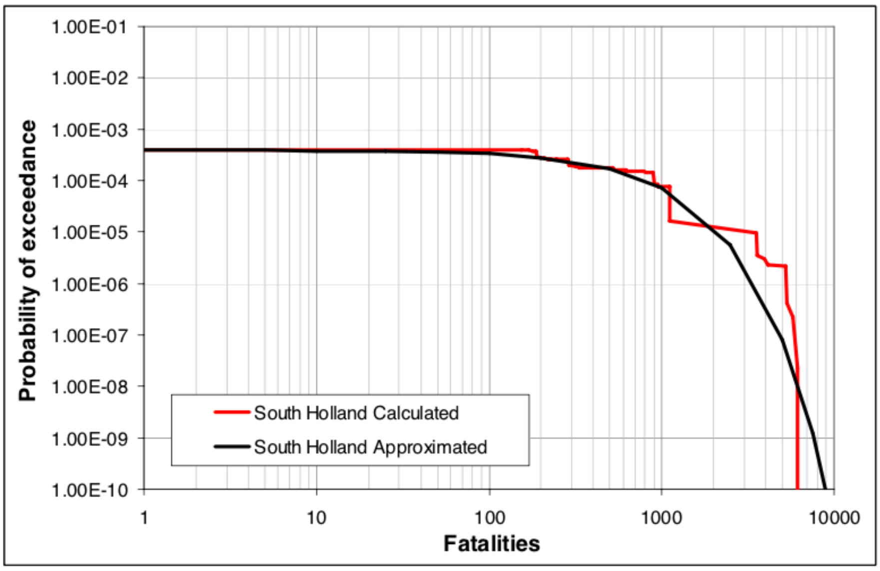

(c) Simplified bayesian approach

Figure 53: FN-curves resulting from societal risk estimation methods from Maaskant et al., 2010

Multi-Criteria Decision Analysis (MCDA) techniques allow stakeholders to weigh different factors and criteria (e.g. flood hazard, vulnerability, mitigation measures) to make informed decisions about flood risk reduction strategies (Romero, 2020). In this dissertation, we will use as a first approach GIS overlaying method and apply it to a case study in section 0.0.0.1.

Chosen flood risk assessment method

The choice of quantitative flood risk assessment method depends on the goals, availability of data, and scale. We chose to represent and analyze flood risk using GIS tools to overlay flood hazard maps with vulnerability data. This method is able to provide a comprehensive flood risk map and adaptable to future vulnerability scenario. The flood hazard part was presented in section , hazard intensity being expressed as water depth and velocity. Therefore this section will detail how to assess social and economic vulnerability.

First, we gather exposure parameters to take into account. Social exposure indicators are chosen from a list of indicators identified by Rincón et al., 2018: age, family structure, language proficiency, income, education, renters status, and population density. Economical exposure is represented by land-use data including (e.g. industry, the economic diversity, the infrastructure quality, the business resilience to flood, the insurance coverage, impervious and pervious areas, vegetation). Exposure datasets are gathered from household census database using the census tract reference maps provided by Statistics Canada, 2021. The census tract cover all metropolitan areas and agglomerations part of the census program. Exposure data is inventoried in a shapefile (e.g. location, geometry as points or polygons, number of inhabitants) and implemented in a GIS software.

Then, economic and social vulnerability layers are assessed using land-use data along with a building category (e.g. office buildings, schools, hospital, hotel, residential, houses, and light industry, parking, parks, forests). We consider parks and forests as not susceptible to floods. If available, data layer will contains main fields such as a building ID, layout of buildings, main construction material, number of floors, area (m^2), number of inhabitants. Then, flood damage function curves could be used to estimate economical vulnerability. However, when no such data is available, a qualitative level of risk can applied to each exposed element based on their risk level classification.

To overlay each layer, first, we import flood scenarios to a GIS software along with social and economic vulnerability shapefiles. Each layer is converted to a raster format and re-classified using the Reclassify Tool from ArcGIS to a common scale of 1 to 5 where 1 refers to a very low flood risk and 5 to a very high level of flood risk. Reclassifying a group raster consist in transforming the original scale to another scale suited for all raster. In this application, flood risk was expressed on a discrete scale from 1 to 5, 1 being the lowest level of risk and 5 the highest. For example, the hydraulic raster had a depth and velocity thresholds set based on thresholds causing instability and potentially life-threatening based from Jonkman and Penning-Rowsell, 2008 or national recommendation. The hydraulic raster scale was discretized in 5 sections each associated with a risk level. After re-classifying every map, the Weighted Overlay Tool of ArcGIS is used to spatially overlay each maps. The Weighted Overlay Tool approach is described in Figure 54.

Figure 54: Weighted Overlay Tool (ArcGIS) sample calculation from Rincón et al., 2018

We applied this method in a flood risk assessment (Mainguenaud, Usman T Khan, et al., 2023) for the Etobicoke Creek case study detailed in section . The flood risk assessment focused on estimating the propagation of the impacts of levee failure on flood risk.

Case study and results

Flood scenario and hazard map

The flood risk assessment considers a local area with earthen levees located in Etobicoke Creek, Greater Toronto Area (GTA). Levee failure by piping is considered for a 350 year return period flood event representative of the area considered. Two scenario are considered: a no-breach and a breaching scenario of the 3^{rd} levee segment. The flood model is set as showed in Figure 55.a and uses Diffuse Wave Equation (DWE) to generate maximum depth and velocity layers. The resulting flood hazard map consist in an overlay of depth and velocity (Figure 55.b). Depth and velocity values are ranged from the lowest to the highest value and assigned a new hazard level, preferentially with the same scale as the risk.

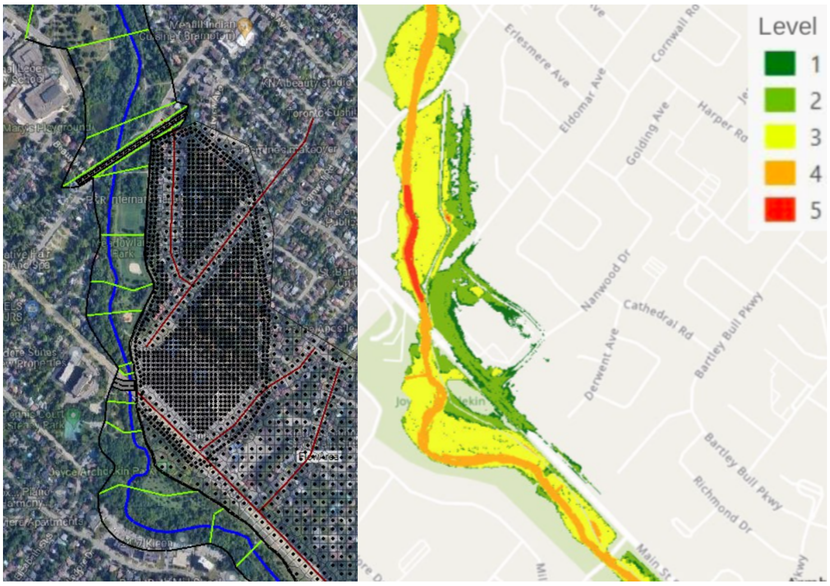

(a) (b)

Figure 55: (a) Flood propagation model geometry and (b) depth and velocity resulting overlay map for breach of the 3^{rd} levee segment

Exposure layer

Exposure data consist in social exposure (Table 10) and economical exposure. Social exposure were adapted from Rincón et al., 2018, while economical exposure is represented by land-use data including: industrial, commercial, institutional, pervious areas, and open recreational areas. Those datasets are gathered from household census database using the census tract reference maps provided by Statistics Canada, 2021. The datasets are reduced to the area of interest and exported into the ArcGIS software.

Social indicator	**Criterion**
Age	75 years and older 25 to 40 years
Language proficiency	No English nor French, French only
Income	Low income Measure after tax
Population	Population density per km^2

Table 10: Type of exposure data gathered for the flood risk assessment of the case study presented in section

Vulnerability layer

A qualitative table from Rincón et al., 2018 assessed vulnerability levels associated with social and economical exposure and is presented in Table 11.

Figure 56 represent the vulnerability levels resulting from the overlays of social and economical indicators.

Quantitative vulnerability level	Social exposure: percentage of population	Economical exposure: land-use type
5 - Very high	$> 80\%$	Industrial
4 - High	$61 - 80\%$	Commercial, residential buildings
3 - Medium	$41 - 60\%$	Government, institutional properties
2 - Low	$21 - 40\%$	Pervious build up areas
1 - Very low	$\leq 20\%$	Forest and recreational open areas

Table 11: Quantitative vulnerability levels associated with social and economical indicators

(a) (b)

Figure 56: Vulnerability rasters (a) social and (b) economical; in blue the river channel flowing from top to bottom

GIS overlay method

The overlay method is applied to obtain a flood risk map from the flood hazard, the social exposure, and the economical vulnerability resulting in Figure 57. Flood hazard and vulnerability rasters are reclassified in a new scale to estimate qualitative flood risk. Then, we overlayed the rasters to determine the spatial distribution of flood risk. We compared two scenarios: one with a levee breach and one without to better understand how levee failure impacts flood risks.

(a) (b)

Figure 57: No breach scenario (a) and breach scenario (b) flood risk maps

Discussion

Improvement of economical vulnerability layer

Economic vulnerability could be assessed using vulnerability functions to quantify the level of damage of a component for a given hazard intensity. Once the economic value for non-residential and residential buildings asked to the city or estimated from available databases. We could create vulnerability functions or depth-damage curves (percentage of damage vs flood depth) for each type building. The economic value of buildings could be directly added to the vulnerability shapefile. As presented by Romero, 2020, for a better resolution, the exposure shapefile would be converted from polygons to points. The economic value for each point would be calculated as the original value of the polygon divided by the number of points in the polygon.

Effect of social vulnerability layer on flood risk level

The social vulnerability map seem to have a smoothing effect on the final flood risk map. This effect originate from the lack of precision of the social exposure data compared to the scale of the study. The flat vulnerability level associated to the social layer dilute the levee failure impacts on the risk levels. In doing so, we can not study the effect of levee failure on flood risk, which is our main objective. To enable visualize the effect of levee failure on flood risk, we proceeded in applying only the economical layer to create an economical flood risk map as shown in Figure 58. The map shows their highest risk levels located in the river bed. This is due to high depth and velocity values in those area. However, our area of interest is the floodplain. We do notice a high risk located near the levee breach due to high velocities found in the breach vicinity. It is important to notice that downstream of the levee, the main road is impacted by the flood. This is a crucial element for flood risk management evacuation plans.

Figure 58: Economical flood risk map

Improvement to flood risk assessment

We can improve social vulnerability layer by applying a filter to better locate social vulnerability in buildings rather than as a flat criteria (Figure 59).

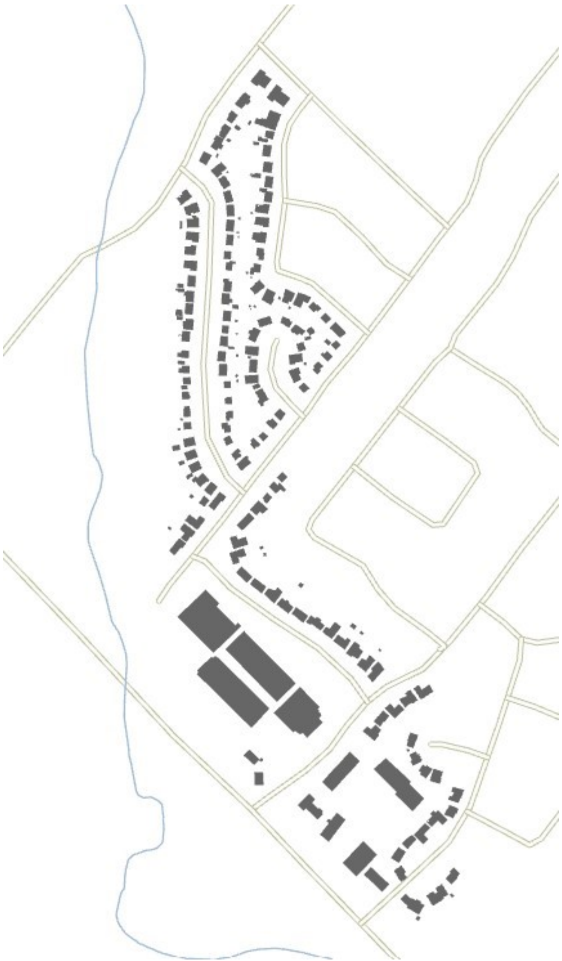

Figure 59: Building layer to improve the social data

Moreover, we can use the probabilistic flood hazard assessment from section 0.0.0.1 instead of considering a single flood scenario. A probabilistic flood risk map would provide a more comprehensive and dynamic approach for stakeholders to understand and mitigate the impacts of flooding. Adding probability distributions will enable decision-makers to develop a more informed risk management strategy.

Finally, we can add future scenario for both flood and vulnerability. We assess current vulnerability, but we could propose mitigation scenarios and apply it to our case study to estimate the efficiency of management strategies. Our flood hazard assessment consider levee failure, and there is already a floodplain to absorb seasonal flood events, a mitigation measure in such case could be the implementation of permeable surfaces in the residential area to helps absorb and slow down water in case of a levee breach. The water depth being quite low, this kind of mitigation method seem appropriate.

Conclusion

A flood risk assessment provides insight on which location to prioritize when implementing a flood management plan (e.g. a high exposure and low vulnerability means that the area is resilient to flood events). Flood Risk Management (FRM) main objective is to reduce exposure and vulnerability to mitigate the overall risk. To make informed decision, a flood risk assessment map must include every relevant flooding scenario, including levee failure scenarios. The systematic integration of levee failure studies is the next step toward improving flood risk assessments. To this end, we presented different existing methods to assess flood risk, one of which we applied to Etobicoke Creek. The main objective was to show the effect of levee failure on flood risk. Accounting for potential levee failure in a flood risk assessment results in changes to flood risk assessment, highlighting the importance of pursuing regular levee maintenance and include levee reliability into regular flood risk assessment routine. However, there are areas for improvement in vulnerability assessment methods as well. First, there is a need to standardize qualitative and quantitative approaches, ensuring quality datasets and ensure their applicability across diverse contexts. The combination of probabilistic flood hazard and vulnerability estimation methods provides a framework for understanding and improve mitigation of flood risk. Continuous research and development are essential to improve flood assessments so that in turn buildings and cities can adapt, improve their resilience facing social and climate changes.

Chapter Seven: Conclusion

Summary of research and main results

Natural disasters such as flooding impacts multiple countries around the globe, affecting the economy and social life. This phenomenon stems from various meteorological mechanisms and is exacerbated by climate change in some areas. Flooding takes various shapes, but this PhD dissertation focused on urban fluvial floods. In response to flood threats, structures were built over time to protect people and assets. However, defense structures may also fail, therefore flood hazard and risk assessments are a requirement in many countries, sometime conducted on a national scale. However, integrated flood assessment methods have room for improvement, leading to this research after identifying gaps in literature.

In this PhD dissertation, we developed a method to estimate quantitative flooding hazard taking into account levee breaches, using flood exceedance probabilities. This method will provide public authorities with flood hazard maps including the possibility of levee breaching. This information is essential to make an informed choice when attributing building permits or renovating in the floodplain area. As a preventive measure, appropriated mitigation solution can be anticipated for areas that area protected by a levee. The final purpose was the development of an integrated method for probabilistic flood hazard assessment. To this end, novel contributions of this PhD dissertation include:

- A method to assess levee failure probabilities integrating multiple failure mechanisms: internal erosion, overflow, and sliding. In addition to which an aggregation method of the failure probabilities was proposed
- A probabilistic flood hazard assessment method, taking into account uncertainties by simulating a large number of levee breach scenario
- Identification of possible improvement to the vulnerability layers, which in turn enables a more precise flood risk assessment

Assessment of levee failure probabilities

The failure probability of flood defence structures needs to maintain a satisfactory accuracy level as it is one of the first component of flood risk assessments and its uncertainties propagates throughout the flood risk assessment. The method developed in this PhD dissertation was applied to sliding, backward erosion, and overflowing failure mechanisms. The innovative element of this research is the development of a Monte-Carlo method to aggregate fragility curves, creating a single levee failure probability curve given a specific levee segment.

In an operational framework, establishing fragility curves require the consideration of 3 or more flood events, preferentially one before the levee is threatened by water levels, several around the expected failure, and one after the levee breaches. This representation of results is easy to read and understand. However, there is as many fragility curve as failure mechanisms. Aggregation of all relevant failure mechanism becomes a main concern as aggregated fragility curve guides stakeholder's understanding of levee failure and flood risk. This approach simplifies levee failure integration into a larger scale scheme of probabilistic flood hazard and flood risk analysis. This approach requires geotechnical (e.g. soil type, permeability, normal and shear strength, angle of friction) and hydraulic data (e.g. water levels, probability of occurrence). If data is scarce, the first option should be to request a geotechnical study of the area. Otherwise, technical literature can provide a range for geotechnical parameter values. The least option to go for is making an assumption. For hydraulic data, usually hydraulic stations are openly available. Otherwise, on-site survey backed up by historical reports about the river are the only last option before making an expert judgement based assumption.

The results showed that the order of magnitude of failure probabilities depends on the shape and material which defines the levee. In the case study, sliding was the failure mechanism with the lowest probability of occurrence.

We discussed the effect of using a transient (non-saturated soils) over a steady-state (saturated soils) model on backward erosion fragility curve. As shown in section , the steady-state model provides higher hydraulic gradient values than the transient model, however the levee saturation had little influence on gradient values. This conclusion cannot be generalized to other soil types than the one considered in the study case.

We discussed the effect of hydraulic gradients location in backward erosion probabilities estimation. Locations include the selected area of interest: (i) maximum gradient, (ii) mean gradient, (iii) mean gradient within the levee only, or (iv) the mean gradient within the foundation only. Mean gradients provided significantly lower backward erosion failure probabilities compared to the maximum hydraulic gradient. Therefore, a conservative approach is to consider maximum hydraulic gradients to estimate backward erosion fragility curves.

Limitations of this method include the necessary simplifications made to assess each failure mechanisms. Those simplifications were made for a scale of the structure or larger. Therefore, the applicability of this approach is limited to those scales.

Probabilistic flood hazard

We proposed a method for probabilistic flood hazard assessment considering levee reliability for several flood events, which resulted in a cumulative flood exceedance probability curve for each location of the flooded area. Using the levee performance method presented in this dissertation, we estimated the levee reliability for homogeneous segments. Then, we propagated the flood and analyzed depth and velocity parameters. This method result in a probabilistic flood hazard curve associated to each location of the levee protected area, providing a spatial representation of potential floods while considering levee failures.

The innovative aspect of this research is the development of a new approach to provide probabilistic flood hazard map for flood risk assessments while considering levee failure. This approach enables the identification of levee segments and failure mechanisms with the most impact on flooding.

In an operational framework, assessing probabilistic flood hazard with the presented method requires numerous flood propagation scenario including various flood events and systematic levee breaching. Once the hydraulic model is defined properly and run, the next flood propagation simulations will need a shorter running time due to locally saved terrain and other input data.

The post-processing required after raw data (depth, velocity) would be more efficient if it was integrated in a software but as a first approach, coding is sufficient. The cumulative flood exceedance probability curves can be computed for the whole flooded area.

This method has limitations, include the probabilistic flood hazard method relies on a previously established levee reliability assessment, applying this method to a large scale will increase the computational strain, and a dynamic graphic representation of the flood hazard would help visualize spatially the results. Moreover, without enough input data (geotechnic and hydraulic) applying this method is not possible.

Future work

Usage of Geographic Information System (GIS) tools to represent flood hazard

There is two way of visualizing flood hazard: probabilistic flood hazard map for a single flood parameter (either depth or velocity), and combining depth and velocity into a single flood map. So far, we proposed a proof of concept to assess probabilistic flood hazard as shown in section 0.0.0.1. Our next step is to generalize this approach to the flooded area. To this end, we want to expand regular flood mapping with a cumulated flood exceedance probability curve for every location by using GIS.

Another approach to flood mapping is to merge flood depth and velocity maps into a single flood hazard map. Depth and velocity parameters can be considered together using a GIS overlay tool to provide a flood hazard map. To overlay depth and velocity maps, first we decide on a common hazard level scale and both maps are re-classified to this scale. Then, both maps are assigned an equal weight. If a parameter is more valued than the other, different weight could be assigned and each cell value would be multiplied by it. Finally, overlayed cell values are added together, resulting in a flood hazard map.

Vulnerability

The vulnerability assessment as presented in section 0.0.0.1 showed limitations due to the precision of available data sets. When the social vulnerability is taken into account, the resulting flood risk map shows less information than when only economical vulnerability is taken into account. Therefore, only data sets of similar precision should be used, and we propose to improve the available data sets. The economical vulnerability data can be improved on by implementing damage curves based on the type of existing building in the flooded area.

The social vulnerability data can be improved on by refining the data grid rather than use the coarse grid available. This could be done by locating buildings in the flooded area and assigning a vulnerability level to each building. Moreover, as a new approach we want to include some variability to the population density data. Depending on the time of the day, population density should vary based on a building type expected occupancy.

Measuring change in risk under changing conditions

Climate change relies on multiple mechanisms. The resulting increase in temperature has a direct impact on flooding. Glaciers melting and and ocean thermal expansion lead to sea level rise (*Climate Change 2013: The Physical Science Basis. Contribution of Working Group I to the Fifth Assessment Report of the Intergovernmental Panel on Climate Change*, 2013). And the increase in air temperature leads to a decrease in the relative humidity, therefore warm air can hold more water than cold air (*Ecological Climatology: Concepts and Applications*, 2015), leading to an increase in precipitation intensity. This dissertation's case study was chosen based on creating a new method to integrate levee failure into flood risk assessments. Therefore, nor the scale, nor the location of the case study was suitable to showcase the impact of climate change. Regardless, we anticipated a way of including climate change scenarios with our method. To this end, we propose to consider new hydraulic events and changes in vulnerability.

First, we propose 2 approaches to integrate an increase in precipitation: either create new hydraulic events or increase existing flood event probabilities. The new hydraulic events can be guided by climate projection for the area, the peak flow and shape of the hydrograph can be modified to fit the type of scenario (e.g. increase of peak flow, successive raining events, heavy rainfall after a draught which affects soil permeability). The other option is to downscale climate data to drive the hydrological model to obtain the hydraulic loadings on the levee. Flood events that use to occur rarely would have a frequency increase. In our model, that would mean keeping the flood propagation and levee failure probabilities but increasing flood event probabilities.

Second, to simulate the changes in vulnerability triggered by urban policies, we can define different population density and land-use scenarios. For example, projections about aging population, increase of city center density, city development which decreases water absorption. Several scenario can be estimated based on current policies, and exploring new ones. In our model, that would mean changing vulnerability maps.

Bibliography

Abdulazim, Y., Minna, K., & Harald, K. (2009). Effect of anisotropy and destructuration on behavior of haarajoki test embankment. *International Journal of Geomechanics*, *9*(4), 153–168. https://doi.org/10.1061/(ASCE)1532-3641(2009)9:4(153) (cit. on p. 30)
doi: 10.1061/(ASCE)1532-3641(2009)9:4(153)

Abid, S. K., Sulaiman, N., Wei, C. S., & Nazir, U. (2021). Flood vulnerability and resilience: Exploring the factors that influence flooding in sarawak. *IOP Conference Series: Earth and Environmental Science*, *802*(1), 012059. https://doi.org/10.1088/1755-1315/802/1/012059 (cit. on p. 34)

Aguilar-Lopez, J. P., Warmink, J. J., Bomers, A., Schielen, R. M. J., & Hulscher, S. J. M. H. (2018). Failure of grass covered flood defences with roads on top due to wave overtopping: A probabilistic assessment method. *Journal of Marine Science and Engineering*, *6*(3), 74. https://doi.org/10.3390/jmse6030074 (cit. on pp. 65, 85)

Aksha, S. K., Juran, L., & Resler, L. M. (2018). Spatial and temporal analysis of natural hazard mortality in nepal. *Environmental Hazards*, *17*(2), 163–179. https://doi.org/10.1080/17477891.2017.1398630 (cit. on p. 34)
doi: 10.1080/17477891.2017.1398630

Alberta Environment and Parks. (2023). https://landusekn.ca/resource/bow-river-basin-state-watershed. (Cit. on p. 52)

Alhasan, Z., Duchan, D., & Říha, J. (2016). The probabilistic solution of dike breaching due to overtopping. In S. Erpicum, B. Dewals, P. Archambeau, & M. Pirotton (Eds.), *Sustainable hydraulics in the era of global change* (pp. 505–512). CRC Press. https://www.researchgate.net/profile/Zakaraya-Alhasan-2/publication/305872742_The_probabilistic_solution_of_dike_breaching_due_to_overtopping_Proceedings_of_the_4th_IAHR_Europe_Congress_Liege_Belgium_27-29_July_2016/links/5a8a9c5ea6fdcc6b1a42966c/The-probabilistic-solution-of-dike-breaching-due-to-overtopping-Proceedings-of-the-4th-IAHR-Europe-Congress-Liege-Belgium-27-29-July-2016.pdf. (Cit. on p. 20)
posted on researchgate only but referenced in WebOfScience Quid of the credibility of this paper ?

Alhasan, Z., Duchan, D., & Říha, J. (2019). Influence of surface lining type on the probability of dike breaching due to overtopping. *Journal of Flood Risk Management*, *12*(S2), e12534. https://doi.org/10.1111/jfr3.12534 (cit. on p. 65)

Allard, D., Comunian, A., & Renard, P. (2012). Probability aggregation methods in geoscience. *Mathematical Geosciences*, *44*(5), 545–581. https://doi.org/10.1007/s11004-012-9396-3 (cit. on p. 14)

Allsop, W., Kortenhaus, A., & Morris, M. (2007). *Failure mechanisms for flood defence structures* (tech. rep. T04-06-01). FLOODsite. http://www.floodsite.net/html/partner_area/project_docs/T04_06_01_failure_%20mechanisms_D4_1_v1_1_p01.pdf. (Cit. on p. 2)

Altarejos-García, L., Escuder-Bueno, I., Serrano-Lombillo, A., & de Membrillera-Ortuño, M. G. (2012). Methodology for estimating the probability of failure by sliding in concrete gravity dams in the context of risk analysis. *Structural Safety*, *36-37*, 1–13. https://doi.org/10.1016/j.strusafe.2012.01.001 (cit. on p. 12)

ASCE. (2007). *The new orleans hurricane protection system: What went wrong and why.* (Cit. on p. 1).

Aubertin, M., Mbonimpa, M., Bussière, B., & Chapuis, R. P. (2003). A model to predict the water retention curve from basic geotechnical properties. *Canadian Geotechnical Journal*, *40*(6), 1104–1122. https://doi.org/10.1139/t03-054 (cit. on p. 71)

Baldassarre, G. D., Viglione, A., Carr, G., Kuil, L., Salinas, J., & Blöschl, G. (2013). Sociohydrology: Conceptualising human flood interactions. *Hydrology and Earth System Sciences*, *17*. https://doi.org/10.5194/hess-17-3295-2013 (cit. on p. 83)

Baldassarre, G. D., Schumann, G., Bates, P. D., Freer, J. E., & Beven, K. J. (2010). Floodplain mapping: A critical discussion of deterministic and probabilistic approaches. *Hydrological Sciences Journal*, *55*(3), 364–376. https://doi.org/10.1080/02626661003683389 (cit. on p. 84)

Balica, S., & Wright, N. G. (2010). Reducing the complexity of the flood vulnerability index. *Environmental Hazards*, *9*(4), 321–339. https://doi.org/10.3763/ehaz.2010.0043 (cit. on p. 33)
doi: 10.3763/ehaz.2010.0043

Bedient, P. B., Huber, W. C., & Vieux, B. E. (2013). *Hydrology and floodplain analysis* (M. J. Horton, Ed.; International 5^{th} edition). Pearson Education Limited. https://ds.amu.edu.et/xmlui/bitstream/handle/123456789/17409/Hydrology%20and%20Floodplain%20Analysis%2C%205th%20ed%20%28%20PDFDrive%20%29%20%281%29.pdf?sequence=1&isAllowed=y. (Cit. on p. 2)

Beffa, C. (2000). A statistical approach for spatial analysis of flood prone areas. *International symposium on flood defence, Kassel, Germany*, *8* (cit. on p. 63).

Beilicci, E., & Beilicci, R. (2012). A comparative analysis of two flood wave propagation models. In Surveying Geology & Mining Ecology Management (Ed.), *International multidisciplinary scientific geoconference : Sgem; sofia* (pp. 523–530). (Cit. on p. 84).

Bellos, V., & Tsakiris, G. (2015). Flash flood simulation in small catchments based on combined hydrodynamic and hydrologic approach. *9th world congress of EWRA, Istanbul, 10-13 June 2015* (cit. on p. 13).

Blaikie, P., Cannon, T., Davis, I., & Wisner, B. (2004). *At risk: Natural hazards, people's vulnerability and disasters* (2nd). Routledge. https://doi.org/10.4324/9780203714775. (Cit. on p. 33)

Bligh, W. (1927). *The practical design of irrigation works*. an Nostrand Co. (Cit. on p. 23).

Bomers, A., Schielen, R. M. J., & Hulscher, S. J. M. H. (2019). Consequences of dike breaches and dike overflow in a bifurcating river system. *Natural Hazard*, *97*, 309–334. https://doi.org/10.1007/s11069-019-03643-y (cit. on pp. 7, 14)

Bonelli, S. (2012). *Erosion on geomaterials*. John Wiley & Sons. (Cit. on pp. 21, 22).

Bowles, D. S., Chauhan, S. S., Anderson, L. R., & Grove, R. C. (2012). Baseline risk assessment for herbert hoover dike. *ANCOLD Proceedings of Technical Groups, Dams and Water for the Future*. https://www.researchgate.net/profile/David-Bowles-3/publication/316282375_Baseline_Risk_Assessment_for_Herbert_Hoover_Dike/links/58f95c0aaca2723d79d26f00/Baseline-Risk-Assessment-for-Herbert-Hoover-Dike.pdf (cit. on p. 15)

Brandt, S. (2000). Classification of geomorphological effects downstream of dams. *CATENA*, *40*(4), 375–401. https://doi.org/10.1016/S0341-8162(00)00093-X (cit. on p. 10)

Brody, S. D., & Highfield, W. E. (2013). Open space protection and flood mitigation: A national study. *Land Use Policy*, *32*, 89–95. https://doi.org/10.1016/j.landusepol.2012.10.017 (cit. on p. 9)

Brown, C. A., & Graham, W. J. (1988). Assessing the threat to life from dam failure. *Journal of the American Water Resources Association*, *24*(6), 1303–1309. https://doi.org/10.1111/j.1752-1688.1988.tb03051.x (cit. on p. 10)

Cardona, O., Van Aalst, M., Birkmann, J., Fordham, M., Mc Gregor, G., Rosa, P., Pulwarty, R., Schipper, E., Sinh, B., Décamps, H., Keim, M., Davis, I., Ebi, K., Lavell, A., Mechler, R., Murray, V., Pelling, M., Pohl, J., Smith, A., & Thomalla, F. (2012). Determinants of risk: Exposure and vulnerability. *Managing the Risks of Extreme Events and Disasters to Advance Climate Change Adaptation*, *9781107025066*, 65–108. https://doi.org/10.1017/CBO9781139177245.005 (cit. on p. 32)

Ceccato, F., Malvestio, S., & Simonini, P. (2022). Effect of animal burrows on the vulnerability of levees to concentrated erosion. *Water*, *14*, 2777. https://doi.org/10.3390/w14182777 (cit. on p. 85)

Chan, S., Abid, S., Sulaiman, N., Nazir, U., & Azam, K. (2022). A systematic review of the flood vulnerability using geographic information system. *HELIYON*, *8*(3), e09075. https://doi.org/10.1016/j.heliyon.2022.e09075 (cit. on p. 32)

Cho, S. E. (2007). Effects of spatial variability of soil properties on slope stability. *Engineering Geology*, *92*(3-4), 97–109. https://doi.org/10.1016/j.enggeo.2007.03.006 (cit. on pp. 64, 71)

CIRIA, Ministry of Ecology, & USACE. (2013). *The international levee handbook*. CIRIA. https://www.ciria.org/ItemDetail?iProductCode=C731F&Category=FREEPUBS. (Cit. on pp. 1, 2, 14, 18, 19, 21, 22, 24, 25, 27, 28, 63, 64, 66, 67, 85)

City of Calgary. (2013). *Historical flood of 2013 in calgary* (tech. rep.). *url : https : //www.calgary.ca/uep/water/flood−info/flooding−history−calgary.html.* (Cit. on pp. 51, 63, 72).

City of Calgary. (2020). *Historical flow rates for the bow and elbow rivers* (tech. rep.). url: https://data.calgary.ca/Environment/River-Level-and-Flow-Monitoring-Stations/wifh-4ta2. (Cit. on pp. 53, 73).

Climate change 2013: The physical science basis. contribution of working group i to the fifth assessment report of the intergovernmental panel on climate change. (2013). Cambridge England: Cambridge University Press. https://doi.org/10.1017/CBO9781107415324. (Cit. on p. 117)

Cocaign, G. (2018). *Development of a flood risk assessment method by considering dike failure mechanism* (Master's thesis). Polytech Clermont Ferrand - Département Génie Civil. 2 Av. Blaise Pascal, TSA 60206, CS 60026, F 63178 Aubière Cedex (France). (Cit. on p. 69).

Cocaign, G., Picton, T., Khan, U. T., Beullac, B., Sharma, J., Mainguenaud, F., & Peyras, L. (2020). Flood risk assessment of the city of calgary considering flood control barrier performance. *4th European Conference on Flood Risk Management*. https://api.semanticscholar.org/CorpusID:238032164 (cit. on p. 54)

Conitz, F., Zingraff-Hamed, A., Lupp, G., & Pauleit, S. (2021). Non-structural flood management in european rural mountain areas - are scientists supporting implementation? *Hydrology*, *8*(4), 167. https://doi.org/10.3390/hydrology8040167 (cit. on p. 64)

Costabile, P., Costanzo, C., & Macchione, F. (2017). Performances and limitations of the diffusive approximation of the 2-dnshallow water equations for flood simulation in urban and rural areas. *Applied Numerical Mathematics*, *116*(SI), 141–156. https://doi.org/10.1016/j.apnum.2016.07.003 (cit. on p. 85)

Damien, S., Laurent, P., Rémy, T., & Youssef, D. (2008). Levee performance assessment methods integrated in a gis to support planning maintenance actions. *Journal of Infrastructure Systems*, *14*(3), 201–213. https://doi.org/10.1061/(ASCE)1076-0342(2008)14:3(201) (cit. on p. 15)
doi: 10.1061/(ASCE)1076-0342(2008)14:3(201)

Dawson, R. J., Hall, J., Sayers, P., Bates, P., & Rosu, C. (2005). Sampling-based flood risk analysis for fluvial dike systems. *Stochastic Environment Research and Risk Assessment*, *19*(6), 388–402. https://doi.org/10.1007/s00477-005-0010-9 (cit. on p. 65)

Dawson, R., Speight, L., Hall, J., Djordjevic, S., Savic, S., & Leandro, J. (2008). Attribution of flood risk in urban areas. *Journal of hydroinformatics*, *10.4*, 275–288 (cit. on p. 35).

Diaconu, D. C., Costache, R., & Popa, M. C. (2021). An overview of flood risk analysis methods. *Water*, *13*(474). https://doi.org/10.3390/w13040474 (cit. on p. 45)

D'Oria, M., Maranzoni, A., & Mazzoleni, M. (2019). Probabilistic assessment of flood hazard due to levee breaches using fragility functions. *Water Ressources Research*, *55*(11), 8740–8764. https://doi.org/10.1029/2019WR025369 (cit. on p. 84)

Dottori, F., Salamon, P., Bianchi, A., Alfieri, L., Hirpa, F. A., & Feyen, L. (2016). Development and evaluation of a framework for global flood hazard mapping. *Advances in Water Resources*, *94*, 87–102. https://doi.org/10.1016/j.advwatres.2016.05.002 (cit. on p. 85)

Douvinet, J., Van De Wiel, M. J., Delahaye, D., & Cossart, E. (2015). A flash flood hazard assessment in dry valleys (northern france) by cellular automata modelling. *Natural Hazards*, *75*(3), 2905–2929. https://doi.org/10.1007/s11069-014-1470-3 (cit. on p. 9)

Dráb, A., & Říha, J. (2010). An approach to the implementation of european directive 2007/60/ec on flood risk management in the czech republic. *Natural Hazard and Earth System Sciences*, *10*(9), 1977–1987. https://doi.org/10.5194/nhess-10-1977-2010 (cit. on p. 63)

Durand, E., Maurin, J., Bridoux, B., & Boulay, A. (2016). Cardigues: An integrated tool for levee system diagnosis and assessment. *SCOUR AND EROSION*, 603–610 (cit. on p. 15).

Dysli, M. (2000). Swiss standard sn 670 010b, characteristic coefficients of soils. *Association of Swiss Road and Traffic Engineers: Strasse und Verkehr*, *86*(2000), 93–94 (cit. on p. 67).

Ebert, A., Kerle, N., & Stein, A. (2009). Urban social vulnerability assessment with physical proxies and spatial metrics derived from air- and spaceborne imagery and gis data. *Natural Hazards*, *48*(2), 275–294. https://doi.org/10.1007/s11069-008-9264-0 (cit. on p. 34)

Ecological climatology: Concepts and applications. (2015). Cambridge, England: Cambridge University Press. https://doi.org/10.1017/CBO9781107339200. (Cit. on p. 117)

El Bilali, A., Talebc, I., Nafiia, A., & Talebb, A. (2022). A practical probabilistic approach for simulating life loss in an urban area associated with a dam-break flood. *International Journal of Disaster Risk Reduction*, *76*(1), 10301 (cit. on p. 32).

Elenas, A., Saadi, M., & Athanasopoulos-Zekkos, A. (2013). A gis-enabled approach for assessing damage potential of levee systems based on underlying geology and river morphology. *Mathematical Problems in Engineering*, *2013*, 936468. https://doi.org/10.1155/2013/936468 (cit. on p. 30)

Emblemsvøag, J., & Endre Kjølstad, L. (2006). Qualitative risk analysis: Some problems and remedies. *Management Decision*, *44*(3), 395–408. https://doi.org/10.1108/00251740610656278 (cit. on p. 45)

ERINOH. (2017). *Érosion interne dans les ouvrages hydrauliques : Méthodologie de caractérisation expérimentale* (Vol. volume 1). Presse des Ponts. (Cit. on pp. 18, 21, 22, 24, 46)

Auteur : IREX : Institut pour la recherche appliquée et l'expérimentation en génie civil.

Escuder-Bueno, I., Castillo-Rodriguez, J. T., Zechner, S., Jobstl, C., Perales-Momparler, S., & Petaccia, G. (2012). A quantitative flood risk analysis methodology for urban areas with integration of social research data. *Natural Hazard and Earth*

System Sciences, *9*(2843-2863). https://doi.org/10.5194/nhess-12-2843-2012 (cit. on p. 45)

Esculier, F., Le Noë, J., Barles, S., Billen, G., Créno, B., Garnier, J., Lesavre, J., Petit, L., & Tabuchi, J.-P. (2019). The biogeochemical imprint of human metabolism in paris megacity: A regionalized analysis of a water-agro-food system. *Journal of Hydrology*, *573*, 1028–1045. https://doi.org/10.1016/j.jhydrol.2018.02.043 (cit. on p. 9)

European Environment Agency. (2007). *Directive 2007/60/ec of the european parliament and of the council on the assessment and management of flood risks* (tech. rep.). http://eur-lex.europa.eu/legal-content/EN/TXT/?uri=CELEX:32007L0060. (Cit. on pp. 1, 63, 85).

Farshid, V., H., J. F., T., T. F., Masood, A., Aneseh, A., & Amir, A. (2020). Levee fragility behavior under projected future flooding in a warming climate. *Journal of Geotechnical and Geoenvironmental Engineering*, *146*(12), 04020139. https://doi.org/10.1061/(ASCE)GT.1943-5606.0002399 (cit. on p. 30)
doi: 10.1061/(ASCE)GT.1943-5606.0002399

Fauchard, C., & Mériaux, P. (2007). *Geophysical and geotechnical methods for diagnosing flood protection dikes. guide for implementation and interpretation*. Éditions Quae. (Cit. on p. 15).

Ferdous, M. R., Wesselink, A., Brandimarte, L., Baldassarre, G. D., & Rahman, M. M. (2019). The levee effect along the jamuna river in bangladesh. *Water International*, *44*(15), 496–519. https://doi.org/10.1080/02508060.2019.1619048 (cit. on p. 83)

Ferrari, A., Dazzi, S., Vacondio, R., & Mignosa, P. (2020). Enhancing the resilience to flooding induced by levee breaches in lowland areas: A methodology based on numerical modelling. *Natural Hazard and Earth System Sciences*, *20*(1), 59–72. https://doi.org/10.5194/nhess-20-59-2020 (cit. on p. 84)

Field, C.B., Barros, V., Dokken, D., Mach, K., Mastrandrea, M., Bilir, T., Chatterjee, M., Ebi, K., Estrada, Y., Genova, R., Girma, B., Kissel, E., Levy, A., MacCracken, S., Mastrandrea, P., & White, L. (2014). Climate change 2014: Impacts, adaptation, and vulnerability. Cambridge University Press. (Cit. on pp. 1, 63).

Figueiredo, R., Romão, X., & Paupério, E. (2021). Component-based flood vulnerability modelling for cultural heritage buildings. *International Journal of Disaster Risk Reduction*, *61*, 102323. https://doi.org/10.1016/j.ijdrr.2021.102323 (cit. on p. 34)

Finkl, C. W. (Ed.). (2013). *Coastal hazards* (Vol. 6). Springer. (Cit. on p. 8).

Fischer, S., & Schumann, A. (2021). Multivariate flood frequency analysis in large river basins considering tributary impacts and flood types. *Water Ressources Research*, *57*(8), e2020WR029029. https://doi.org/10.1029/2020WR029029 (cit. on p. 7)

Flikweert, J., Sayers, P., & Stevens, R. (2015). *Modelling decision support framework (mdsf2) for flood risk management strategies : Oversight report* (tech. rep. SC120062/R1). Environment Agency. (Cit. on pp. 3, 35).

Flood Review Task Force. (2013). *Manitoba 2011 flood review task force report: Report for the minister of infrastructure and transportation.* (tech. rep.). Manitoba Infrastructure and Transportation. Winnipeg, Manitoba. https://vdocuments.net/manitobas-2011-flood-review-report.html?page=1. (Cit. on p. 8)

Formentin, S. M., & Zanuttigha, B. (2018). A new method to estimate the overtopping and overflow discharge at over-washed and breached dikes. *Coastal Engineering*, *140*, 240–256. https://doi.org/10.1016/j.coastaleng.2018.08.002 (cit. on pp. 19, 65)

Fredlund, D., & Xing, A. (1994). Equations for the soil-water characteristic curve. *Canadian Geotechnical Journal*, *31*(4), 521–532. https://doi.org/10.1139/t94-061 (cit. on p. 71)

Froehlich, D. C. (1995). Embankment dam breach parameters revisited. *ASCE Conference on Water Resources Engineering, New York*, 887–891 (cit. on p. 89).

Fry, J. (2016). Lessons on internal erosion in embankment dams from failures and physical models. In W.
bibinitperiod M. Harris (Ed.), *Scour and erosion* (pp. 41–58). Taylor & Francis Group, London. (Cit. on p. 65).

Fujisawa, K., Kobayashi, A., Yamamoto, K., & Aoyama, S. (2007). Failure mechanism of an embankment due to overflow. *17th International Offshore and Polar Engineering Conference* (cit. on p. 21).

Geerse, C., Slomp, R., & de Waal, J. (2011). *Hydra-zoet for the fresh water systems in the netherlands - probabilistic model for the assessment of dike heights.* (tech. rep. PR2168). HKV Consultants. Document%20available%20at:%20http://resolver.tudelft.nl/uuid:df52bac6-e390-4a5d-a8de-a0566649af92. (Cit. on pp. 39, 40)

GeoStudio. (2021a). *Stability modeling with geostudio* (tech. rep.). GEO-SLOPE International Ldt. (Cit. on p. 27).

GeoStudio. (2021b). *Stability modeling with geostudio.* (tech. rep.). GEO-SLOPE International Ltd. https://www.geoslope.com/learning/support-resources#dnn_BooksHeaderPane. (Cit. on p. 66)

Gouldby, B., sayers, P., Mulet-Marti, J., Hassan, M., & Benwell, D. (2008). A methodology for regional-scale flood risk assessment. In T. T. Ltd (Ed.), *Proceedings of the institution of civil engineers - water management* (pp. 169–182). https://doi.org/10.1680/wama.2008.161.3.169. (Cit. on pp. 3, 35, 64)

Government of Alberta. (2022). *Agricultural region of alberta soil inventory database* (tech. rep.). url: https://soil.agric.gov.ab.ca/agrasidviewer/. (Cit. on pp. 67, 73).

Government of Canada. (2013). *Historical hydrometric data for calgary, station 05bh004* (tech. rep.). $https://wateroffice.ec.gc.ca/$. (Cit. on p. 53).

Government of Canada. (2022). *Real-time hydrometric data graph for bow river at calgary, station 05bh004.* (tech. rep.). $https://wateroffice.ec.gc.ca/report/real_time_e.html?st$
$05BH004$. (Cit. on pp. 53, 73).

Government of Canada. (2023). *Real-time hydrometric data graph for etobicoke creek at brampton, station 02hc017* (tech. rep.). $https://eau.ec.gc.ca/report/real_time_f.html?stn =$
$02HC017$. (Cit. on pp. 57, 90).

Griffiths, D. V., & Lane, P. A. (1999). Slope stability analysis by finite elements. *Géotechnique*, *49*(3), 387–403. https://doi.org/10.1680/geot.1999.49.3.387 (cit. on p. 27)

Hager, W. H. (1987). Lateral outflow over side weirs. *Journal of Hydraulic Engineering*, *113*(4), 491–504. https://doi.org/10.1061/(ASCE)0733-9429(1987)113:4(491) (cit. on pp. 21, 68)
doi: 10.1061/(ASCE)0733-9429(1987)113:4(491)

Hall, J. W., Tarantola, S., Bates, P. D., & Horritt, M. S. (2005). Distributed sensitivity analysis of flood inundation model calibration. *Journal of Hydraulic Engineering*, *131*(2), 117–126. https://doi.org/10.1061/(ASCE)0733-9429(2005)131:2(117) (cit. on p. 84)

Hall, J. W., Dawson, R. J., Sayers, P. B., Rosu, C., Chatterton, J. B., & Deakin, R. (2003). A methodology for national-scale flood risk assessment. In T. T. Ltd (Ed.), *Proceedings of the institution of civil engineers - water and maritime engineering* (pp. 235–247). https://doi.org/10.1680/wame.2003.156.3.235. (Cit. on pp. 35, 64, 65)

Hathout, M., Vuillet, M., Carvajal, C., Peyras, L., & Diab, Y. (2019). Expert judgment calibration and combination for assessment of river levee failure probability. *Reliability Engineering and System Safety*, *188*, 377–392. https://doi.org/10.1016/j.ress.2019.03.019 (cit. on p. 77)

Hathout, M., Peyras, L., Carvajal, C., Diab, Y., & Vuillet, M. (2020). Development of an approach to evaluate the failure probabilities of river levees based on expert judgement : Application to a case study. *Journal of Flood Risk Management*, *13*(2), e12603. https://doi.org/10.1111/jfr3.12603 (cit. on pp. 65, 85)

He, B., Huang, X., Ma, M., Chang, Q., Tu, Y., Li, Q., Zhang, K., & Hong, Y. (2018). Analysis of flash flood disaster characteristics in china from 2011 to 2015. *Natural Hazards*, *90*(1), 407–420. https://doi.org/10.1007/s11069-017-3052-7 (cit. on p. 9)

Hedges, T., Reis, M., & Owen, M. (1998). Random wave overtopping of simple sea walls: A new regression model. *Proceedings of the Institution of Civil Engineers - Water and Maritime Engineering*, *130*(1), 1–10. https://doi.org/10.1680/iwtme.1998.30223 (cit. on p. 65)

Hoffmans, G. J. C. M. (2022). Influence of hydraulic flow regime on backward erosion piping. *Journal of Hydraulic Research*, *60*(4), 667–674. https://doi.org/10.1080/00221686.2021.2022027 (cit. on p. 24)
doi: 10.1080/00221686.2021.2022027

Hough, B. (1969). *Basic soil engineering*. Ronald Press Company. (Cit. on p. 55).

Hydraulics Research Station. (1980). *Design of seawalls allowing for wave overtopping* (tech. rep. EX924). Hydraulics Research Station. England. https://eprints.hrwallingford.com/35/. (Cit. on pp. 20, 65)

Hydrologic Engineering Center. (2023). *Hec-ras technical reference manual. version 1.5.* (tech. rep.). *https://www.hec.usace.army.mil/confluence/rasdocs/ras1dtechref/lates a−dam−break−study−with−hec−ras/estimating−dam−breach−parameters/estimating−breach−parameters*. (Cit. on p. 88).

ICOLD. (2020). *World Register of Dams* (tech. rep.). International Commission On Large Dams. https://www.icold-cigb.org/GB/world_register/general_synthesis.asp. (Cit. on p. 10)

International Commission on Large Dams. (2017). *Internal erosion of existing dams, levees and dikes, and their fondations* (Bulletin No. 164). ICOLD and CIGB. https://www.google.com/url?sa=t&rct=j&q=&esrc=s&source=web&cd=&ved=2ahUKEwi1yPWXwcT8AhX_VKQEHYlyAV8QFnoECAgQAQ&url=http%3A%2F%2Fwww.ussdams.org%2Fwp-content%2Fuploads%2F2016%2F04%2FB164.pdf&usg=AOvVaw1rwK7zBAGErOWvxOIbKpV9. (Cit. on p. 64)

Jakob, M., Holm, K., Weatherly, H., Liu, S., & Ripley, N. (2013). Debris flood risk assessment for mosquito creek, british columbia, canada. *Natural Hazards*, *65*(3), 1653–1681. https://doi.org/10.1007/s11069-012-0436-6 (cit. on p. 10)

Janbu, N., Hirschfeld, R. C., & Poulos, S. J. (1973). *Slope stability computations*. John Wiley & Sons. (Cit. on p. 26).

Jennings, M. E., Thomas, W. O., & Riggs, H. (1994). *Nationwide summary of us geological survey regional regression equations for estimating magnitude and frequency of floods for ungaged sites, 1993* (Vol. 94). US Geological Survey. (Cit. on p. 103).

Ji, J., & Chan, C. (2014). Long embankment failure accounting for longitudinal spatial variation - a probabilistic study. *Computers and Geotechnics*, *61*, 50–56. https://doi.org/10.1016/j.compgeo.2014.05.001 (cit. on p. 30)

Jongejan, R. B., & Maaskant, B. (2015). Quantifying flood risks in the netherlands. *Risk Analysis*, *35*(2), 252–264. https://doi.org/10.1111/risa.12285 (cit. on pp. 40, 41, 47)

Jongejan, R., Stefess, H., Roode, N., ter Horst, W., & Maaskant, B. (2011). The vnk2 project : A detailed, large-scale quantitative flood risk analysis for the netherlands. *5th International Conference on Flood risk Management (ICFM5)* (cit. on pp. 103, 104).

Jongman, B., Winsemius, H. C., Aerts, J. C., Coughlan de Perez, E., Van Aalst, M. K., Kron, W., & Ward, P. J. (2015). Declining vulnerability to river floods and the global benefits of adaptation. *Proceedings of the National Academy of Sciences*, *112*(18), e2271–e2280 (cit. on p. 33).

Jonkman, S. N., & Penning-Rowsell, E. (2008). Human instability in flood flows. *Journal of the American Water Resources Association*, *44*(5), 1208–1218. https://doi.org/10.1111/j.1752-1688.2008.00217.x (cit. on p. 106)

Jonkman, S. N., Lentz, A., & Vrijling, J. K. (2010). A general approach for the estimation of loss of life due to natural and technological disasters. *Reliability Engineering & System Safety*, *95*(11), 1123–1133. https://doi.org/10.1016/j.ress.2010.06.019 (cit. on p. 34)

Jonkman, S. N., Kok, M., & Vrijling, J. K. (2008). Flood risk assessment in the netherlands: A case study for dike ring south holland. *Risk Analysis*, *28*(5), 1357–1374. https://doi.org/10.1111/j.1539-6924.2008.01103.x (cit. on pp. 2, 34, 40, 42)

Jonkman, S. N., Maaskant, B., Boyd, E., & Levitan, M. L. (2009). Loss of life caused by the flooding of new orleans after hurricane katrina: Analysis of the relationship between flood characteristics and mortality. *Risk Analysis*, *29*(5), 676–698. https://doi.org/10.1111/j.1539-6924.2008.01190.x (cit. on p. 103)

Jonkman, S. N., Stive, M. J. F., & Vrijling, J. K. (2009). New orleans is a lesson to the dutch. *Journal of Coastal Research*, *21*(6), xi–xii. https://doi.org/10.2112/1551-5036(2005)21[xi:NOIALT]2.0.CO;2 (cit. on p. 39)

Jonkman, S. N., Jongejan, R., & Maaskant, B. (2011). The use of individual and societal risk criteria within the dutch flood safety policy-nationwide estimates of societal risk and policy applications. *Risk Analysis*, *31*(2), 282–300. https://doi.org/10.1111/j.1539-6924.2010.01502.x (cit. on pp. 34, 103, 104)

Jozsef, D., & M., Z. L. (2015). Dike failure mechanisms and breaching parameters. *Journal of Geotechnical and Geoenvironmental Engineering*, *141*(9), 04015039. https://doi.org/10.1061/(ASCE)GT.1943-5606.0001335 (cit. on p. 12) doi: 10.1061/(ASCE)GT.1943-5606.0001335

Julínek, T., Duchan, D., & Říha, J. (2020). Mapping of uplift hazard due to rising groundwater level during floods. *Journal of Flood Risk Management*, *13*(4), e12601. https://doi.org/10.1111/jfr3.12601 (cit. on p. 65)

Keef, C., Svensson, C., & Tawn, J. A. (2009). Spatial dependence in extreme river flows and precipitation for great britain. *Journal of Hydrology*, *378*(3-4), 240–252. https://doi.org/10.1016/j.jhydrol.2009.09.026 (cit. on p. 8)

Khan, U. T., He, J., & Valeo, C. (2018). River flood prediction using fuzzy neural networks: An investigation on automated network architecture. *Water Science and Technology*, *2017*(1), 238–247. https://doi.org/10.2166/wst.2018.107 (cit. on pp. 8, 51, 63, 72)

Klijn, F., Samuels, P., & Van Os, A. (2008). Towards flood risk management in the eu: State of affairs with examples from various european countries. *International Journal of River Basin Management*, *6*(4), 307–321. https://doi.org/10.1080/15715124.2008.9635358 (cit. on p. 63)

Klijn, F., Kreibich, H., de Moel, H., & Penning-Rowsell, E. (2015). Adaptive flood risk management planning based on a comprehensive flood risk conceptualisation. *Mitigation and Adaptation Strategies for Global Change*, *20*(6), 845–864. https://doi.org/10.1007/s11027-015-9638-z (cit. on p. 34)

Knight, D. W., Hazlewood, C., Lamb, R., Samuels, P. G., & Shiono, K. (2018). *Practical channel hydraulics: Roughness, conveyance and afflux* (2^{nd} edition). CRC Press. https://doi.org/10.1201/9781315157771. (Cit. on p. 2)

Koks, E. E., Bočkarjova, M., de Moel, H., & Aerts, J. C. J. H. (2015). Integrated direct and indirect flood risk modeling: Development and sensitivity analysis. *Risk Analysis*, *35*(5), 882–900. https://doi.org/10.1111/risa.12300 (cit. on p. 34)

Kolen, B., Slomp, R., & Jonkman, S. N. (2013). The impacts of storm xynthia february 27-28, 2010 in france: Lessons for flood risk management. *Journal of Flood Risk Management*, *6*(3), 261–278. https://doi.org/10.1111/jfr3.12011 (cit. on p. 1)

Kotek, L., & Tabas, M. (2012). Hazop study with qualitative risk analysis for prioritization of corrective and preventive actions. *Procedia Engineering*, *42*, 808–815. https://doi.org/10.1016/j.proeng.2012.07.473 (cit. on p. 43)

Kubal, C., Haase, D., Meyer, V., & Scheuer, S. (2009). Integrated urban flood risk assessment - adapting a multicriteria approach to a city. *Natural Hazard and Earth System Sciences*, *9*(6), 1881–1895. https://doi.org/10.5194/nhess-9-1881-2009 (cit. on p. 64)

Lane, E. W. (1935). Security from under-seepage-masonry dams on earth foundations. *Transactions of the American Society of Civil Engineers*, *100*(1), 1235–1272. https://doi.org/10.1061/TACEAT.0004655 (cit. on p. 24)

Lane, E. (1954). *The importance of fluvial morphology in hydraulic engineering* (tech. rep. No. 372). American Society of Civil Engineers. Denver, CO, United States Department of the Interior. https://semspub.epa.gov/work/01/554355.pdf. (Cit. on p. 10)

Lasage, R., Veldkamp, T. I. E., de Moel, H., Van, T. C., Phi, H. L., Vellinga, P., & Aerts, J. C. J. H. (2014). Assessment of the effectiveness of flood adaptation strategies for hcmc. *Natural Hazards and Earth System Sciences*, *14*(16), 1441–1457. https://doi.org/10.5194/nhess-14-1441-2014 (cit. on p. 34)

Lavoie, B., & Mahdi, T.-F. (2017). Comparison of two-dimensional flood propagation models: Srh-2d and hydro_as-2d. *Natural Hazard*, *86*(3), 1207–1222. https://doi.org/10.1007/s11069-016-2737-7 (cit. on p. 85)

Lee, K. T., & Ho, J.-Y. (2009). Prediction of landslide occurence based on slope-instability analysis and hydrological model simulation. *Journal of hydrology*, *375*(3), 489–497. https://doi.org/10.1016/j.jhydrol.2009.06.053 (cit. on p. 18)

Lee, S., & Lee, S. (2017). Reliability approach on internal erosion risk assessment of earth dam and levee. *Geo-Risk*, *285*, 188–197. https://doi.org/10.1061/9780784480724.018 (cit. on p. 65)

Leitão, J. P., Almeida, M. d. C., Simöes, N. E., & Martins, A. (2013). Methodology for qualitative urban flooding risk assessment. *Water Science and Technology*, *68*(4), 829–838. https://doi.org/10.2166/wst.2013.310 (cit. on p. 44)

Lemaire, M., Chateauneuf, A., & Mitteau, J.-C. (2005). *Fiabilité des structures. couplage mécano-fiabiliste statique*. Hermes-Science, Lavoisier. (Cit. on p. 46).

Lendering, Kasper. (2016). Failure probability of regional flood defences. In E. Sciences (Ed.), *3rd european conference on flood risk management (floodrisk 2016)* (pp. 1–12). EDP Sciences. https://doi.org/10.1051/e3sconf/20160701002. (Cit. on p. 64)

Li, T., Bai, Z., Peng, X., & He, T. (2013). Finite proximate method for simulating flood propagation in complicated river channel and flood detention area. *Mechatronics and applied Mechanics II*, *300*, 814–820. https://doi.org/10.4028/www.scientific.net/AMM.300-301.814 (cit. on p. 84)

Maaskant, B., Jonkman, S., & Jongejan, R. (2010). The use of individual and societal risk criteria within the dutch flood safety policy (part 2): Estimation of the individual and societal risk for the dike rings in the netherlands. *European Safety and Reliability Conference (ESREL 2009): Reliability, Risk, and Safety: Theory and Applications, Prague, Czech Republic*, 2099–2104 (cit. on pp. 104, 105).

Mainguenaud, F., Peyras, L., Khan, U. T., Carvajal, C., Sharma, J., & Beullac, B. (2023). A probabilistic approach to levee reliability based on sliding, backward erosion and overflowing mechanisms: Application to an inspired canadian case study. *Journal of Flood Risk Management*, e12921. https://doi.org/10.1111/jfr3.12921 (cit. on pp. 5, 50, 62, 85–87)

Mainguenaud, F., Usman T Khan, L. P., Carvajal, C., Beullac, B., & Sharma, J. (2023). Mapping the impact of levee failure on flood risks: A toronto case study. *EGU General Assembly 2023, Vienna, Austria, 24–28 Apr 2023*, (EGU23-3616). https://doi.org/10.5194/egusphere-egu23-3616 (cit. on pp. 5, 50, 107)

Mainguenaud, F., Khan, U. T., Peyras, L., Carvajal, C., Beullac, B., & Sharma, J. (2024). Probabilistic assessment of flood hazard of a levee protected area considering different breaching scenarios. application to a levee on etobicoke creek river. *Journal of Flood Risk Management* (cit. on pp. 5, 50, 82).

Maranzoni, A., D'Oria, M., & Mazzoleni, M. (2022). Probabilistic flood hazard mapping considering multiple levee breaches. *Water Ressources Research*, *58*(4), e2021WR030874. https://doi.org/10.1029/2021WR030874 (cit. on pp. 30, 84, 86)

Maranzoni, A., D'Oria, M., & Rizzo, C. (2023). Quantitative flood hazard assessment methods: A review. *Journal of Flood Risk Management*, *16*(1), e12855. https://doi.org/10.1111/jfr3.12855 (cit. on pp. 30, 84)

Marchand, M. (2009). *Modelling coastal vulnerability: Design and evaluation of a vulnerability model for tropical storms and floods* (Vol. 5). IOS Press. (Cit. on p. 34).

Martin, D. E., Thompson, S., Ballard, M., & Linton, J. (2017). Two-eyed seeing in research and its absence in policy: Little saskatchewan first nation elders' experiences of the 2011 flood and forced displacement. *The International Indigenous Policy Journal*, *8*(4). https://doi.org/10.18584/iipj.2017.8.4.6 (cit. on p. 8)

Masseroni, D., Cislaghi, A., Camici, S., Massari, C., & Brocca, L. (2017). A reliable rainfall–runoff model for flood forecasting: Review and application to a semi-urbanized watershed at high flood risk in italy. *Hydrology Research*, *48*(3), 726–740. https://doi.org/10.2166/nh.2016.037 (cit. on p. 8)

Mazzoleni, M., Bacchi, B., Barontini, S., Baldassarre, G. D., Pilotti, M., & Ranzi, R. (2014). Flooding hazard mapping in floodplain areas affected by piping breaches in the po river, italy. *Journal of Hydraulic Engineering*, *19*(4), 717–731. https://doi.org/10.1061/(ASCE)HE.1943-5584.0000840 (cit. on p. 85)

Mazzorana, B., Comiti, F., Volcan, C., & Scherer, C. (2011). Determining flood hazard patterns through a combined stochastic–deterministic approach. *Natural Hazards*, *59*(1), 301–316. https://doi.org/10.1007/s11069-011-9755-2 (cit. on p. 84)

Meire, D., De Doncker, L., Declercq, F., Buis, K., Troch, P., & Verhoeven, R. (2010). Modelling river-floodplain interaction during flood propagation. *Natural Hazard*, *55*(1), 111–121. https://doi.org/10.1007/s11069-010-9554-1 (cit. on p. 84)

Menoni, S., & Pergalani, F. (1996). An attempt to link risk assessment with land use planning: A recent experience in italy. *Disaster Prevention and Management: An International Journal*, *5*(1), 6–21. https://doi.org/10.1108/09653569610109523 (cit. on p. 33)

Merz, B., Thieken, A. H., & Gocht, M. (2007). Flood risk management in europe: Innovation in policy and practice. advances in natural and technological hazards research. In S. Begum, M. J. F. Stive, & J. W. Hall (Eds.). Springer Netherlands. https://doi.org/https://doi.org/10.1007/978-1-4020-4200-3_13. (Cit. on p. 84)

Messner, F., & Meyer, V. (2006). Flood damage, vulnerability, and risk perception. challenges for flood damage research. In J. Schanze, E. Zeman, & J. Marsalek (Eds.), *Flood risk management: Hazards, vulnerability and mitigation measures* (pp. 149–167). Springer, Dordrecht Netherlands. (Cit. on p. 2).

Meyer, V., Scheuer, S., & Haase, D. (2009). A multicriteria approach for flood risk mapping exemplified at the mulde river, germany. *Natural Hazards*, *48*(1), 17–39. https://doi.org/10.1007/s11069-008-9244-4 (cit. on pp. 2, 31)

Modarres, M., Kaminskiy, M. P., & Krivtsov, V. (2016). *Reliability engineering and risk analysis: A practical guide, third edition*. CRC Press. (Cit. on p. 46).

Moges, S. A., & Taye, M. T. (2019). Regional flood frequency curves for remote rural areas of the nile river basin: The case of baro-akobo drainage basin, ethiopia. In A. M. Melesse, W. Abtew, & G. Senay (Eds.), *Extreme hydrology and climate variability* (pp. 385–393). Elsevier. https://doi.org/10.1016/B978-0-12-815998-9.00030-0. (Cit. on p. 13)

Mohamed, M. A., Samuels, P., Morris, M., & Ghataora, G. (2002). Improving the accuracy of prediction of breach formation through embankment dams and flood embankments. *River Flow* (cit. on p. 85).

Mohammed, M. H., Zwain, H. M., & Hassan, W. H. (2021). Modeling the impacts of climate change and flooding on sanitary sewage system using swmm simulation: A case study. *Results in Engineering*, *12*, 100307. https://doi.org/10.1016/j.rineng.2021.100307 (cit. on pp. 2, 9)

Morales-Hernandez, M., García-Navarro, P., Burguete, J., & Brufau, P. (2013). A conservative strategy to couple 1d and 2d models for shallow water flow simulation. *Computer and Fluids*, *81*, 26–44. https://doi.org/10.1016/j.compfluid.2013.04.001 (cit. on p. 85)

Morgenstern, N. R., & Price, V. (1965). The analysis of the stability of general slip surfaces. *Geotechnique*, *15*(1), 79–93. https://doi.org/https://doi.org/10.1680/geot.1965.15.1.79 (cit. on p. 66)

Mouyeaux, A., Carvajal, C., Bressolette, P., Peyras, L., Breul, P., & Bacconnet, C. (2018). Probabilistic stability analysis of an earth dam by stochastic finite element method based on field data. *Computer and Geotechnics*, *101*, 34–47. https://doi.org/10.1016/j.compgeo.2018.04.017 (cit. on p. 64)

Naess, L. O., Norland, I. T., Lafferty, W. M., & Aall, C. (2006). Data and processes linking vulnerability assessment to adaptation decision-making on climate change in norway. *Global Environmental Change*, *16*(2), 221–233. https://doi.org/10.1016/j.gloenvcha.2006.01.007 (cit. on p. 33)

Naseri, K., & Hummel, M. A. (2022). A bayesian copula-based nonstationary framework for compound flood risk assessment along us coastlines. *Journal of Hydrology*, *610*, 128005. https://doi.org/10.1016/j.jhydrol.2022.128005 (cit. on p. 9)

Nasiri, H., Mohd Yusof, M. J., & Mohammad Ali, T. A. (2016). An overview to flood vulnerability assessment methods. *Sustainable Water Resources Management*, *2*(3), 331–336. https://doi.org/10.1007/s40899-016-0051-x (cit. on pp. 32, 34)

National Audit Office. (2011). *Flood risk management in england* (tech. rep.). Retrieved 13 09 2023 from http://www.nao.org.uk/wp-content/uploads/2011/10/10121521.pdf. (Cit. on p. 38).

Neal, J., Keef, C., Beven, K., & Leedal, D. (2013). Probabilistic flood risk mapping including spatial dependence. *Hydrological Process*, *27*, 1349–1363. https://doi.org/10.1002/hyp.9572 (cit. on p. 7)

OECD. (2014). *Water governance in the netherlands. fit for the future?* https://doi.org/10.1787/9789264102637-en. (Cit. on p. 39)

Oliver, J., Qin, X. S., Larsen, O., Meadows, M., & Fielding, M. (2018). Probabilistic flood risk analysis considering morphological dynamics and dike failure. *Natural Hazard*, *91*(1), 287–307. https://doi.org/10.1007/s11069-017-3126-6 (cit. on p. 83)

Özer, I. E., van Damme, M., & Jonkman, S. N. (2020). Towards an international levee performance database (ilpd) and its use for macro-scale analysis of levee breaches and failures. *Water*, *12*(1). https://doi.org/10.3390/w12010119 (cit. on p. 24)

Paquier, A., & Goutal, N. (2016). Dam and levee failures: An overview of flood wave propagation modeling. *La Houille Blanche*, *102*(1), 5–12. https://doi.org/10.1051/lhb/2016001 (cit. on p. 89)

Parker, D. J., Green, C. H., & Thompson, P. M. (1987). *Urban flood protection benefits*. Avebury Technical. (Cit. on p. 2).

Parliament of the United Kingdom. (2010). *Flood management act* (tech. rep.). url: https://www.legislation.gov.uk/ukpga/2010/29/contents. (Cit. on p. 35).

Peck, R., Hanson, W., & Thornburn, T. (1991). *Foundation engineering, 2nd edition*. Wiley. (Cit. on p. 67).

Penning-Rowsell, E. C. (2015). A realistic assessment of fluvial and coastal flood risk in england and wales. *Transactions of the Institute of British Geographers*, *40*, 44–61. https://doi.org/10.1111/tran.12053 (cit. on pp. 35, 37)

Peyras, L., Boissier, D., Carvajal, C., Bacconnet, C., Royet, P., Bécue, J., Gaillard, T., & Talon, A. (2010). *Analyse de risques et fiabilité des barrages. application aux barrages-poids en béton*. Editions Universitaires Européennes. (Cit. on p. 70).

Peyras, L., Carvajal, C., Felix, H., Bacconnet, C., Royet, P., Becue, J.-P., & Boissier, D. (2012). Probability-based assessment of dam safety using combined risk analysis and reliability methods – application to hazards studies. *European Journal of Environmental and Civil Engineering*, *16*(7), 795–817. https://doi.org/10.1080/19648189.2012.672200 (cit. on pp. 45, 64)

Peyras, L., Tourment, R., Vuillet, M., Beullac, B., Delaunay, C., & Bambara, G. (2015). Development of an expert-led gis-based approach for assessing the performance of river levees : The digsure method and tool. *Journal of Flood Risk Management*. https://doi.org/10.1111/jfr3.12178 (cit. on p. 3)

Pheulpin, L., Bacchi, V., & Bertrand, N. (2019). Ensitivity analysis of levee breach parameters: Application to the garonne river [in french]. *Digues Maritimes et Fluviales de Protection contre les Inondations*. https://doi.org/10.5281/ZENODO.2530017 (cit. on p. 3)

Pickert, G., Weitbrecht, V., & Bieberstein, A. (2011). Breaching of overtopped river embankments controlled by apparent cohesion. *Journal of Hydraulic Research*, *49*(2), 143–156. https://doi.org/10.1080/00221686.2011.552468 (cit. on p. 65)

Picton, T. (2019). *Probabilistic flood risk assessment concerning calgary's dike system performance* (Master's thesis). Polytech Clermont Ferrand - Département Génie Civil. 2 Av. Blaise Pascal, TSA 60206, CS 60026, F 63178 Aubière Cedex (France). (Cit. on pp. 16, 54, 55, 66, 67, 73).

Piton, G., Carladous, S., Recking, A., Tacnet, J. M., Liébault, F., Kuss, D., Queffélean, Y., & Marco, O. (2016). Why do we build check dams in alpine streams? an historical perspective from the french experience. *Earth Surface Processes and Landforms*, *42*(1), 91–108. https://doi.org/10.1002/esp.3967 (cit. on p. 10)

Pohl, C., & Vavrina, L. (2008). Stability evaluation of dikes along the north-sea at wave overtopping. *Proceedings of the Chinese-German Joint Symposium on Hydraulic and Ocean Engineering, Darmstadt, Germany, August 24-30*, 76–80. at%20request:%20https://www.researchgate.net/publication/237437765_Stability_Evaluation_of_Dikes_along_the_North-Sea_at_Wave_Overtopping (cit. on p. 65)

Pomeroy, J. W., Stewart, R. E., & Whitfield, P. H. (2016). The 2013 flood event in the south saskatchewan and elk river basins: Causes, assessment and damages. *Canadian Water Resources Journal/Revue Canadienne des Ressources Hydriquesydriques*, *41*(1-2), 105–117. https://doi.org/10.1080/07011784.2015.1089190 (cit. on pp. 1, 7, 53, 63, 72)

Prinsen, G., Sperna Weiland, F., & Ruijgh, E. (2015). The delta model for fresh water policy analysis in the netherlands. *Water Resources Management*, *29*(2), 645–661. https://doi.org/10.1007/s11269-014-0880-z (cit. on p. 40)

Purvis, M. J., Bates, P. D., & Hayes, C. M. (2008). A probabilistic methodology to estimate future coastal flood risk due to sea level rise. *Coastal Engineering*, *55*(12), 1062–1073. https://doi.org/10.1016/j.coastaleng.2008.04.008 (cit. on p. 8)

Richards, K. S., & Reddy, K. R. (2007). Critical appraisal of piping phenomena in earth dams. *Bulletin of Engineering Geology and the Environment*, *66*(4), 381–402. https://doi.org/10.1007/s10064-007-0095-0 (cit. on p. 22)

Richards, L. A. (1931). Capillary conduction of liquids through porous mediums. *Physics*, *1*(5), 318–333. https://doi.org/10.1063/1.1745010 (cit. on pp. 29, 70)

Rifai, I., El Kadi Abderrezzak, K., Erpicum, S., Archambeau, P., Violeau, D., Pirotton, M., & Dewals, B. (2018). Floodplain backwater effect on overtopping induced fluvial dike failure. *Water Ressources Research*, *54*(11), 9060–9073. https://doi.org/10.1029/2017WR022492 (cit. on p. 85)

Říha, J., Petrula, L., & Hala, M. (2020). Statistical analysis of experimentally determined critical hydraulic gradients for heave. *Géotechnique Letters*, *10*(2), 377–384. https://doi.org/10.1680/jgele.19.00054 (cit. on p. 65)

Rincón, D., Khan, U. T., & Armenakis, C. (2018). Flood risk mapping using gis and multi-criteria analysis : A greater toronto area case study. *Geosciences*, *8*(275). https://doi.org/10.3390/geosciences8080275 (cit. on pp. 106–109)

Rogger, M., Agnoletti, M., Alaoui, A., Bathurst, J. C., Bodner, G., Borga, M., Chaplot, V., Gallart, F., Glatzel, G., Hall, J., Holden, J., Holko, L., Horn, R., Kiss, A., Kohnová, S., Leitinger, G., Lennartz, B., Parajka, J., Perdigão, R., … Blöschl, G. (2017). Land use change impacts on floods at the catchment scale: Challenges and opportunities for future research. *Water Resources Research*, *53*(7), 5209–5219. https://doi.org/10.1002/2017WR020723 (cit. on p. 9)

Romero, D. R. (2020). *Probabilistic flood risk assessment under climate change scenarios in the humber river watershed* (Master's thesis). York university. (Cit. on pp. 2, 105, 110).

Rongen, G., Morales-Nàpoles, O., & Kok, M. (2022). Expert judgment-based reliability analysis of the dutch flood defense system. *Reliability Engineering & System Safety*, *24*, 108535. https://doi.org/10.1016/j.ress.2022.108535 (cit. on pp. 65, 85)

Roscoe, K., Hanea, A., Jongejan, R., & Vrouwenvelder, T. (2020). Levee system reliability modeling: The length effect and bayesian updating. *Safety*, *6*(7). https://doi.org/10.3390/safety6010007 (cit. on p. 15)

Rosqvist, T., Molarius, R., Virta, H., & Perrels, A. (2013). Event tree analysis for flood protection. an exploratory study in finland. *Reliability Engineering & System Safety*, *112*, 1–7. https://doi.org/10.1016/j.ress.2012.11.013 (cit. on p. 63)

Royet, P., Palma-Lopes, S., Fauchard, C., Mériaux, P., & Auriau, L. (2012). *Rapid and cost-effective dike condition assessment methods: Geophysics and remote sensing* (tech. rep. WP3-01-12-20). FloodProBE. (Cit. on p. 14).

Rudd, A. C., Bell, V. A., & Kay, A. L. (2017). National-scale analysis of simulated hydrological droughts (1891-2015). *Journal of Hydrology*, *550*, 368–385. https://doi.org/10.1016/j.jhydrol.2017.05.018 (cit. on p. 36)

Russell, A., & Sayers, P. (2022). Assessing future flood risk and developing integrated flood risk management strategies: A case study from the uk climate change risk assessment. *Sustainability*, *14*, 13945. https://doi.org/10.3390/su142113945 (cit. on pp. 2, 36)

Samuels, P., Gouldby, B., Klijn, F., Messner, F., van Os, A., Sayers, P., Schanze, J., & Udale-Clarke, H. (2009). *Language of risk - project definitions* (2^{nd} edition, tech. rep. T32-04-01). FLOODsite. http://www.floodsite.net/. (Cit. on pp. 3, 32) I called it 2009-Gouldby-L previously

Samuels, P., Morris, M., Sayers, P., Creutin, J.-D., Kortenhaus, A., Klijn, F., Mosselman, E., Os, A. V., & Schanze, J. (2009). Flood risk management: Research and practice. In S. et al (Ed.). Taylor & Francis Group. (Cit. on p. 1).

Sandink, D. (2013). Lot-side risk reduction through voluntary retrofit programs, code interpretation and by-laws. *Urban flooding in Canada*, *52* (cit. on p. 9).

Santos, P. P., Reis, E., Pereira, S., & Santos, M. (2019). A flood susceptibility model at the national scale based on multicriteria analysis. *Science of the Total Environment, 667*(2019), 325–337. https://doi.org/10.1016/j.scitotenv.2019.02.328 (cit. on p. 45)

Sayers, P., Horritt, M., Penning-Rowsell, E., McKenzie, A., & Thompson, D. (2016). The analysis of future flood risk in the uk using the future flood explorer. *3rd European Conference on Flood Risk Management (FLOODrisk 2016), 7*(21005). https://doi.org/10.1051/e3sconf/20160721005 (cit. on p. 35)

Sayers, P., Horritt, M., Carr, S., Kay, A., Mauz, J., Lamb, R., & Penning-Rowsell, E. (2020). *Third uk climate change risk assessment (ccra3): Future flood risk - main report* (tech. rep. P1128). Sayers and Partners for the committee on Climate Change. (Cit. on pp. 2, 35, 36, 38).

Scawthorn, C., Flores, P., Blais, N., Seligson, H., Tate, E., Chang, S., Mifflin, E., Thomas, W., Murphy, J., Jones, C., & Lawrence, M. (2006). Hazus-mh flood loss estimation methodology. ii. damage and loss assessment. *Natural Hazards Review, 7*(2), 72–81. https://doi.org/10.1061/(ASCE)1527-6988(2006)7:2(72) (cit. on p. 103)
doi: 10.1061/(ASCE)1527-6988(2006)7:2(72)

Schmertmann, J. H. (2000). The no-filter factor of safety against piping through sands. *Judgement and Innovation*, 65–132. https://doi.org/10.1061/9780784405376.006 (cit. on p. 24)

Scorzini, A. R., & Leopardi, M. (2017). River basin planning: From qualitative to quantitative flood risk assessment: The case of abruzzo region (central italy). *Natural Hazards, 88*(1), 71–93. https://doi.org/10.1007/s11069-017-2857-8 (cit. on pp. 44, 45)

Scussolini, P., Tran, T. V. T., Koks, E., Diaz-Loaiza, A., Ho, P. L., & Lasage, R. (2017). Adaptation to sea level rise: A multidisciplinary analysis for ho chi minh city, vietnam. *Water Resources Research, 53*(12), 10841–10857. https://doi.org/10.1002/2017WR021344 (cit. on p. 34)

Sellmeijer, H., De la Cruz, J. L., Van Beek, V. M., & Knoeff, H. (2011). Fine-tuning of the backward erosion piping model through small-scale, medium-scale and ijkdijk experiments. *European Journal of Environmental and Civil Engineering, 15*(8), 1139–1154. https://doi.org/10.1080/19648189.2011.9714845 (cit. on pp. 65, 67, 85)

Sellmeijer, J. B., & Koenders, M. A. (1991). A mathematical model for piping. *Applied Mathematical Modelling, 15*(11), 646–651. https://doi.org/https://doi.org/10.1016/S0307-904X(09)81011-1 (cit. on p. 24)

Sharafati, A., Yaseen, Z. M., & Pezeshki, E. (2020). Strategic assessment of dam overtopping reliability using a stochastic process approach. *Journal of Hydrologic Engineering, 25*(7), 04020029. https://doi.org/10.1061/(ASCE)HE.1943-5584.0001938 (cit. on p. 65)

Sibley, H., Vroman, N., & Shewbridge, S. (2017). Quantitative risk-informed design of levees. In J. Huang, G. Fenton, L. Zhang, & D. Griffiths (Eds.), *Geo-risk 2017:*

Impact of spatial variability, probabilistic site characterization, and geohazards (pp. 76–90). (Cit. on p. 30).

Simm, J., Wallis, M., Smith, P., Tourment, R., Veylon, G., Deniaud, Y., Durand, E., McVicker, J., & Hersh-Burdick, R. (2012). The significance of failure modes in the design and management of levees. a perspective from the international levee handbook team. *Proceedings of the 2nd European Conference on Flood Risk Management* (cit. on pp. 1, 2).

Skempton, A. W., & Brogan, J. M. (1994). Experiments on piping in sandy gravels. *Geotechnique*, *44*(3), 449–460. https://doi.org/10.1680/geot.1994.44.3.449 (cit. on p. 22)

Slomp, R., de Waal, J., Ruijgh, E., Kroon, T., Snippen, E., & van Alphen, J. (2014). The dutch delta model for policy analysis on flood risk management in the netherlands. *6th International Conference on Flood risk Management (ICFM6)* (cit. on p. 40).

Smith, K., & Ward, R. (1998). *Floods: Physical processes and human impacts*. Wiley. (Cit. on p. 2).

Smith, M. B., Koren, V. I., Zhang, Z., Reed, S. M., Pan, J.-J., & Moreda, F. (2004). Runoff response to spatial variability in precipitation: An analysis of observed data. *Journal of Hydrology*, *298*(1), 267–286. https://doi.org/10.1016/j.jhydrol.2004.03.039 (cit. on p. 8)

Snieder, E., Shakir, R., & Khan, U. T. (2020). A comprehensive comparison of four input variable selection methods for artificial neural network flow forecasting models. *Journal of Hydrology*, *583*, 124299. https://doi.org/10.1016/j.jhydrol.2019.124299 (cit. on p. 63)

Soldati, A., Chiozzi, A., Nikolic, Z., Vaccaro, C., & Benvenuti, E. (2022). A promethee multiple-criteria approach to combined seismic and flood risk assessment at the regional scale. *Applied Sciences-Basel*, *12*(3). https://doi.org/10.3390/app12031527 (cit. on p. 31)

Solin, L., & Skubincan, P. (2013). Flood risk assessment and management: Review of concepts, definitions and methods. *Geographical Journal*, *65*, 23–44 (cit. on pp. 2, 31, 32).

Sonnen, M. B. (2002). Discussion of "comparison of anns and empirical approaches for predicting watershed runoff"by jagadeesh anmala, bin zhang, and rao s. govindaraju. *Journal of Water Resources Planning and Management*, *128*(5), 377–379. https://doi.org/10.1061/(ASCE)0733-9496(2002)128:5(377) (cit. on p. 8)
doi: 10.1061/(ASCE)0733-9496(2002)128:5(377)

Statistics Canada. (2021). *Census tract toronto metropolitan area* (tech. rep.). §. (Cit. on pp. 106, 108).

Stephenson, V., & D'Ayala, D. (2014). A new approach to flood vulnerability assessment for historic buildings in england. *Natural Hazards and Earth System Sciences*, *14*(5), 1035–1048. https://doi.org/10.5194/nhess-14-1035-2014 (cit. on p. 34)

Su, M.-D., Kang, J.-L., Chang, L.-F., & Chen, A. S. (2005). A grid-based gis approach to regional flood damage assessment. *Journal of Marine Science and Technology*, *13*(3). https://doi.org/10.51400/2709-6998.2125 (cit. on p. 103)

Takahara, T., Sugimoto, T., & Sanada, H. (2016). A study on the seismic segmentation method of levee using the natural frequency of multiple layers. In J. G. S. S. Publication (Ed.), *The 15th asian regional conference on soil mechanics and geotechnical engineering* (pp. 1679–1683). https://doi.org/10.3208/jgssp.JPN-064. (Cit. on pp. 15, 16)

Tanner, A., & Arvai, J. (2018). Perceptions of risk and vulnerability following exposure to a major natural disaster: The calgary flood of 2013. *Risk Analysis*, *38*(3), 548–561. https://doi.org/10.1111/risa.12851 (cit. on p. 63)

Tanoue, M., Hirabayashi, Y., & Ikeuchi, H. (2016). Global-scale river flood vulnerability in the last 50 years. *Scientific Reports*, *6*(1), 36021. https://doi.org/10.1038/srep36021 (cit. on pp. 32, 33)

Tapsell, S. M., Priest, S. J., Parker, D. J., Penning-Rowsell, E. C., Viavattene, C., Wilson, T., Handmer, J. W., Wijdeveld, A., Haasnoot, M., Penailillo, R., van den Ende, F., van Noort, P., Messner, F., Meyer, V., Haase, D., Scheuer, S., Schildt, A., Lutoff, C., & Ruin, I. (2008). *Socio-economic and ecological evaluation and modelling methodologies* (tech. rep. T10-07-13). European Commission, FLOODsite project. http://www.floodsite.net/. (Cit. on p. 2)

Tasseff, B., Bent, R., & Van Hentenryck, P. (2019). Optimization of structural flood mitigation strategies. *Water Ressources Research*, *55*(2), 1490–1509. https://doi.org/10.1029/2018WR024362 (cit. on p. 64)

Teng, J., Jakeman, A., Vaze, J., Croke, B., Dutta, D., & Kim, S. (2017). Flood inundation modelling: A review of methods, recent advances and uncertainty analysis. *Environmental Modelling and Software*, *90*, 201–216. https://doi.org/10.1016/j.envsoft.2017.01.006 (cit. on pp. 30, 83)

ten Veldhuis, J. A., Clemens, F. H., & van Gelder, P. H. (2011). Quantitative fault tree analysis for urban water infrastructure flooding. *Structure and Infrastructure Engineering*, *7*(11), 809–821. https://doi.org/10.1080/15732470902985876 (cit. on p. 45)

Terraprobe Inc. (2023). *Geotechnical assessment etobicoke dike* (tech. rep. No. 1-22-0506). Toronto and Region Conservation Authority (TRCA). City of Brampton, Ontario. (Cit. on pp. 60, 61).

Terzaghi, K. (1943). *Theoretical soil mechanics*. John Wiley & Sons. (Cit. on pp. 65, 68, 85, 86).

Thywissen, K. (2006). *Components of risk, a comparative glossary*. United Nations University, Institute for Environment; Human Security. (Cit. on p. 31).

Toronto Region Conservation Area. (2010). *Etobicoke and mimico creeks watersheds technical update report* (tech. rep.). TRCA. https://trcaca.s3.ca-central-1.amazonaws.com/app/uploads/2016/03/10130030/2.0-StudyArea-PhysicalSetting.pdf. (Cit. on pp. 55, 56, 60, 61, 90)

Toronto Region Conservation Area. (2023). *Etobicoke creek watershed plan 2024-2034* (tech. rep.). Toronto city, Peel region, Mississauga, Brampton city, Pearson, TRCA, Caledon, and Mississauga of the credit first nation. (Cit. on pp. 55, 56).

Tourment, R., Wallis, M., Beullac, B., Kortenhaus, A., Schaaf, D., & Schelfhout, H. (2014). The risk analysis of levee systems. *3rd IAHR Europe Congress, Book of Proceedings 2014*, 1–13. https://hal.science/hal-01059061/file/ax2014-pub00041163.pdf (cit. on p. 1)

Tourment, R., Beullac, B., de Leeuw, A., Diermanse, F., Gouldby, B., & Wallis, M. (2016). The risk analysis of levee systems: A comparison of international best practices. In E. Sciences (Ed.), *3rd european conference on flood risk management*. https://doi.org/10.1051/e3sconf/20160703009. (Cit. on pp. 42, 43)

Tourment, R., Beullac, B., & Poulain, D. (2017). Management and safety of flood defense systems. In F. Vinet (Ed.), *Floods* (pp. 31–44). ISTE Press, Elsevier. https://doi.org/10.1016/B978-1-78548-269-4.50003-2. (Cit. on p. 1)

TRCA Information Technology and Recordq Management. (2021). https://trca.ca/conservation/watershed-management/etobicoke-creek-watershed-plan/. (Cit. on p. 55)

Tufano, R., Guerriero, L., Corona, M. A., Cianflone, G., Di Martire, D., Letto, F., Novellino, A., Rispoli, C., Zito, C., & Calcaterra, D. (2023). Multiscenario flood hazard assessment using probabilistic runoff hydrograph estimation and 2d hydrodynamic modelling. *Natural Hazard*, *116*(1), 1029–1051. https://doi.org/10.1007/s11069-022-05710-3 (cit. on p. 85)

United Nations. (1984). Proceedings of the seminars on flood vulnerability analysis and on the principles of floodplain management for flood loss prevention. *Water Resources Series*, *58*. https://hdl.handle.net/20.500.12870/3623 (cit. on p. 33)

US Bureau of Reclamation. (2011). *Dam safety risk analysis: Best practices and risk methodology training manual* (tech. rep.). Available%20at:%20https://www.usbr.gov/damsafety/risk/methodology.html. (Cit. on p. 16)

Van, M., Rosenbrand, E., Tourment, R., Smith, P., & Zwanenburg, C. (2022). *Failure paths for levees* (tech. rep.). In International Society of Soil mechanics, Geotechnical Engineering (ISSMGE) Technical Committee TC201 'Geotechnical aspects of dikes, and levees'. https://doi.org/10.53243/R0006. (Cit. on p. 63)

Van Alphen, J. (2015). The delta programme and updated flood risk management policies in the netherlands. *6th International Conference on Flood risk Management (ICFM6)*. https://doi.org/10.1111/jfr3.12183 (cit. on pp. 3, 39, 40)

Van Beek, V., Bezuijen, A., Sellmeijer, J., & Barends, F. (2014). Initiation of backward erosion piping in uniform sands. *Géotechnique*, *64*(12), 927–941. https://doi.org/10.1680/geot.13.P.210 (cit. on p. 22)

van der Meij, R., van den Ham, G., Morris, M., Lhomme, J., Tourment, R., & Maurel, P. (2012). Combining different data sources for assessment of urban flood defences. In F. Klijn & T. Schweckendiek (Eds.), *Comprehensive flood risk management research for policy and practice* (1st edition). (Cit. on p. 2).

van Gelder, P., Buijs, F., ter Horst, W., Kanning, W., Van, C. M., Rajabalinejad, M., de Boer, E., Gupta, S., Shams, R., van Erp, N., Gouldby, B., Kingston, G., Sayers, P., Wills, M., Kortenhaus, A., & Lambrecht, H.-J. (2008). Reliability analysis of flood defence structures and systems in europe. *Flood Risk Management: Research and Practice* (cit. on pp. 3, 46)
Previously refered by 2009-Gelder-L in bibtex.

Van Genuchten, M. T. (1980). A closed-form equation for predicting the hydraulic conductivity of unsaturated soils. *Soil Science Society of America Journal*, *44*(5), 892–898. https://doi.org/10.2136/sssaj1980.03615995004400050002x (cit. on p. 71)

van Herk, S., Rijke, J., Zevenbergen, C., & Ashley, R. (2015). Understanding the transition to integrated flood risk management in the netherlands. *Environmental Innovation and Societal Transitions*, *15*, 84–100. https://doi.org/10.1016/j.eist.2013.11.001 (cit. on p. 39)

van Noortwijk, J., Vrouwenvelder, A., Calle, E., & Slijkhuis, K. (1999). Probability of dike failure due to uplifting and piping. *Safety and Reliability. Proceedings of the ESREL '99, 10th European Conference on Safety and Reliability, Munich-Garching, Germany, 13-17 September / G.I. Schuëller, P. Kafka (editors), 1165-1170*, 1165–1170 (cit. on p. 65).

Visser, P. J. (1998). *Breach growth in sand-dikes* (Doctoral dissertation). Civil Engineering and Geosciences. http://resolver.tudelft.nl/uuid:3721e23b-d34c-45a9-8b36-e5930462d8e2. (Cit. on p. 19)

Visser, P. J., Kraak, A. W., Bakker, W. T., Smit, M. J., Snip, D. W., Steetzel, H. J., & van de Graaff, J. (1995). A large-scale experiment on breaching in sand-dikes. *Coastal dynamics'95 Proceedings of the International Conference on Coastal Research in Terms of Large Scale Experiments*, 583–594 (cit. on pp. 68, 87).

Vojinovic, Z., Hammond, M., Golub, D., Hirunsalee, S., Weesakul, S., Meesuk, V., Medina, N., Sanchez, A., Kumara, S., & Abbott, M. (2016). Holistic approach to flood risk assessment in areas with cultural heritage: A practical application in ayutthaya, thailand. *Natural Hazards*, *81*(1), 589–616. https://doi.org/10.1007/s11069-015-2098-7 (cit. on p. 43)

Vorogushyn, S., Merz, B., & Apel, H. (2009). Development of dike fragility curves for piping and micro-instability breach mechanisms. *Natural Hazard and Earth System Sciences*, *9*, 1383–1401. https://doi.org/10.5194/nhess-9-1383-2009 (cit. on p. 66)

Vorogushyn, S., Merz, B., Lindenschmidt, K. .-., & Apel, H. (2010). A new methodology for flood hazard assessment considering dike breaches. *Water Ressources Research*, *46*(8), W08541. https://doi.org/10.1029/2009WR008475 (cit. on p. 84)

Vrijling, J. (2001). Probabilistic design of water defense systems in the netherlands. *Reliability Engineering & System Safety*, *74*(3), 337–344. https://doi.org/10.1016/S0951-8320(01)00082-5 (cit. on p. 64)

Vuik, V., Van Balen, W., & Van Vuren, S. (2017). Fully probabilistic assessment of safety against flooding along the dutch coast. *Journal of Flood Risk Management*, *10*(3), 349–360. https://doi.org/10.1111/jfr3.12153 (cit. on pp. 64, 65, 85)

Vuillet, M., Peyras, L., Serre, D., & Diab, Y. (2012). Decision-making method for assessing performance of large levee alignment. *Journal of Decision Systems*, *21*(2), 137–160. https://doi.org/10.1080/12460125.2012.680354 (cit. on pp. 16, 17)

Vuillet, M., Peyras, L., Carvajal, C., & Diab, Y. (2016). Developing a probabilistic multi-criteria method for river levee performance evaluation in support of diagnostic analysis. *Journal Infrastructure System*, *22*(3). https://doi.org/10.1061/(ASCE)IS.1943-555X.0000283 (cit. on p. 3)

Waal, J. P. D., & der Meer, J. W. V. (1992). Wave runup and overtopping on coastal structures. In B. L. Edge (Ed.), *Coastal engineering 1992* (pp. 1758–1771). ASCE. https://doi.org/10.1061/9780872629332.133. (Cit. on p. 65)

Ward, P. J., de Moel, H., & Aerts, J. C. J. H. (2011). How are flood risk estimates affected by the choice of return-periods? *Natural Hazard and Earth System Sciences*, *11*(12), 3181–3195. https://doi.org/10.5194/nhess-11-3181-2011 (cit. on pp. 14, 40)

Ward, P. J., van Pelt, S. C., de Keizer, O., Aerts, J. J., J. C. J. H.and Beersma, van den Hurk, B. J. J. M., & te Linde, A. H. (2014). Including climate change projections in probabilistic flood risk assessment. *Journal of Flood Risk Management*, *7*(2), 141–151. https://doi.org/10.1111/jfr3.12029 (cit. on p. 2)

Watson, R., Zinyowera, M. C., Moss, R. H., & Dokker, D. J. (1996). *Climate change 1995: Impacts, adaptations and mitigation of climate change: Scientific-technical analyses. contribution of working group ii to the second assessment report of the intergovernmental panel on climate change*. Cambridge University Press. (Cit. on p. 33).

Weerasinghe, K. M., Gehrels, H., Arambepola, N., Vajja, H. P., Herath, J., & Atapattu, K. (2018). Qualitative flood risk assessment for the western province of sri lanka. *Procedia Engineering*, *212*, 503–510. https://doi.org/10.1016/j.proeng.2018.01.065 (cit. on p. 44)

Winchell, M., Gupta, H. V., & Sorooshian, S. (1998). On the simulation of infiltration and saturation excess runoff using radar-based rainfall estimates: Effects of algorithm uncertainty and pixel aggregation. *Water Resources Research*, *34*(10), 2655–2670. https://doi.org/10.1029/98WR02009 (cit. on p. 8)

Wojciechowska, K., Pleijter, G., Zethof, M., Havinga, F., Haaren, D. V., & Ter Horst, W. (2015). Application of fragility curves in operational flood risk assessment. *5th International Symposium on Geotechnical Safety and Risk*, 528–534. https://doi.org/10.3233/978-1-61499-580-7-528 (cit. on pp. 66, 72)

Wu, W. (2016). *Inputs and outputs of dlbreach - a simplified physically-based dam/levee breach model (version 2016.4)* (tech. rep.). Department of Civil and Environmental Engineering, Clarkson University, New York, USA. Downloadable%20at:%20https://webspace.clarkson.edu/~wwu/Reports/DLBreach_FileFormat_Apr-2016.pdf. (Cit. on p. 89)

Yilmaz, K., Darama, Y., Oruc, Y., & Melek, A. B. (2017). Assessment of flood hazards due to overtopping and piping in dalaman akkopru dam, employing both shallow water flow and diffusive wave equations. *Natural Hazard*, *117*, 979–1003. https://doi.org/10.1007/s11069-023-05891-5 (cit. on p. 85)

Zhan, W., Zhang, L., & Wang, L. (2023). Probabilistic assessment of earthen levees considering soil spatial variability. In S. Najjar, Z. Medina-Cetina, & J. Ching (Eds.), *Geo-risk 2023: Advances in modeling uncertaintyand variability* (pp. 124–131). (Cit. on p. 30).

Zhang, B., & Govindaraju, R. S. (2000). Prediction of watershed runoff using bayesian concepts and modular neural networks. *Water Resources Research*, *26*(3), 753–762. https://doi.org/10.1029/1999WR900264 (cit. on p. 8)

Zuzana Boukalová, V. B. (2008). Flood risk management: Research and practice. CRC Press. (Cit. on p. 14).

Appendices

Appendix A: Global flood exceedance probability conditional on the 350 year return period

We are faced with 3 possible breaching outcomes for each levee segment (Figure 1). As every "no breach" flood event results in the same depth and velocity outcome, we considered 11 scenarios instead.

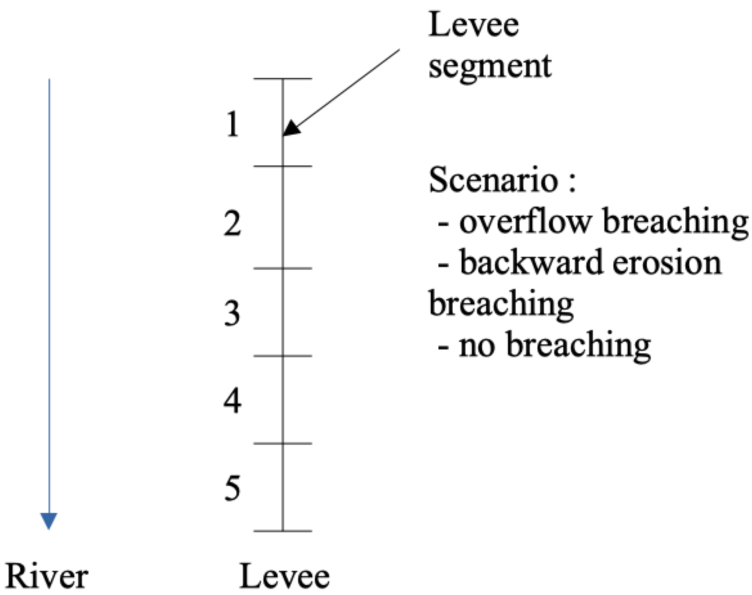

Figure 1: Schematics of the levee system

Throughout the flood return period 350 year, we consider 2 failure mechanisms (backward erosion and overflow) for each levee segment (labelled as breach location in Figure 2. The non-failure probability associated to the no breach event is the sum of every breach simulation complementary probability, hence artificially superior to 1.

Breach Location	Failure Mode	Return Period (yrs)	Flood Probability (1/T), T the return period	Number of failure mechanism considered	Failure / non failure probability	Global flood exceedance probability conditional on return period	Verification sum global flood exceedance probability conditional on return period	Global flood exceedance probability
NB	none	350	2,86E-3	2,00	7,39E+0	7,39E-1	1,00E+0	2,11E-3
BXS1	backward erosion	350	2,86E-3	2,00	1,23E-3	1,23E-4		3,51E-7
BXS1	overflow	350	2,86E-3	2,00	2,00E-1	2,00E-2		5,71E-5
BXS2	backward erosion	350	2,86E-3	2,00	1,37E-3	1,37E-4		3,91E-7
BXS2	overflow	350	2,86E-3	2,00	6,00E-1	6,00E-2		1,71E-4
BXS3	backward erosion	350	2,86E-3	2,00	1,18E-3	1,18E-4		3,38E-7
BXS3	overflow	350	2,86E-3	2,00	1,00E+0	1,00E-1		2,86E-4
BXS4	backward erosion	350	2,86E-3	2,00	2,29E-3	2,29E-4		6,55E-7
BXS4	overflow	350	2,86E-3	2,00	6,00E-1	6,00E-2		1,71E-4
BXS5	backward erosion	350	2,86E-3	2,00	1,41E-4	1,41E-5		4,02E-8
BXS5	overflow	350	2,86E-3	2,00	2,00E-1	2,00E-2		5,71E-5

Figure 2: Global flood exceedance probabilities for the 350 year flood event

Appendix B: Python script

main

August 31, 2023

[ ]:
```
import pandas as pd
import numpy as np
import sys
import matplotlib.pyplot as plt

sys.path.append(r"G:\My␣
↪Drive\02_phd\00_projects_major\20_lsh\src\experiments\clustering\florence")
```

[ ]:
```
# read the sumlation data file
filename = "dat/DataArcGIS-MM.csv"
df=pd.read_csv(filename)

# set some constants
n_levees = 5
n_failure_mechs = {0:0, 100:1, 200:2, 350:2, 500:2, 750:2, 1000:2}

df["FloodProbability"] = 1/df["ReturnPeriod"]
df["BreachLocation_FailureMode"] = ["{}_{}".format(row["BreachLocation"],␣
↪row["FailureMode"]) for _,row in df.iterrows()]

# for each return period, we calculate the failure probability as sum of 1- the␣
↪failure probability at all other locations
return_periods = np.unique(df["ReturnPeriod"])
for rp in return_periods:
    idx_not_nb = (df["BreachLocation"] != "NB").values & (df["ReturnPeriod"] ==␣
↪rp).values
    idx_nb = (df["BreachLocation"] == "NB").values & (df["ReturnPeriod"] == rp).
↪values
    df.loc[idx_nb, "FailureProbability"] = np.sum(1 - df.loc[idx_not_nb,␣
↪"FailureProbability"])

# calculate some other probabilities
df["NumFailureMechs"] = [n_failure_mechs[x] for x in df["ReturnPeriod"]]
df["GlobalFloodExceedProbConditional"] = df["FailureProbability"] * (1/
↪df["NumFailureMechs"]) * (1/n_levees)
df["GlobalFloodExceedProb"] = df["FloodProbability"] *␣
↪df["GlobalFloodExceedProbConditional"]
```

```
print(df.head(5))
```

```
  SimulationID  FailureProbability BreachLocation  ReturnPeriod FailureMode  \
0        NB100            4.995565             NB           100        NONE
1        NB200            4.997409             NB           200        NONE
2        NB350            7.393791             NB           350        NONE
3        NB500            4.985267             NB           500        NONE
4        NB750            4.969865             NB           750        NONE

       DP-1      VP-1     DP-2      VP-2     DP-3      VP-3     DP-4  \
0  0.000000  0.000000  0.00000  0.000000  0.00000  0.000000  0.00000
1  0.175781  0.031979  1.14439  0.329716  1.57953  0.145693  1.02338
2  1.219410  0.257845  2.18317  0.541653  2.41255  0.878128  1.44754
3  1.543370  0.373160  2.50119  0.753000  2.65971  1.164720  1.78238
4  1.941330  0.495274  2.89677  0.929549  3.04398  1.525750  2.45863

       VP-4      DP-5     VP-5  FloodProbability BreachLocation_FailureMode  \
0  0.000000  0.000000  0.00000          0.010000                    NB_NONE
1  0.187670  0.000000  0.00000          0.005000                    NB_NONE
2  0.217994  0.266174  0.74344          0.002857                    NB_NONE
3  0.328253  0.692139  1.14301          0.002000                    NB_NONE
4  0.595075  1.491520  1.43479          0.001333                    NB_NONE

   NumFailureMechs  GlobalFloodExceedProbConditional  GlobalFloodExceedProb
0                1                          0.999113               0.009991
1                2                          0.499741               0.002499
2                2                          0.739379               0.002113
3                2                          0.498527               0.000997
4                2                          0.496987               0.000663
```

[ ]:
```
# here we verify the probability sums (not sure why one is 0.5 but it's the␣
↪same in the excel doc)
verrification_sum = {x:df.loc[df["ReturnPeriod"] ==␣
↪x,"GlobalFloodExceedProbConditional"].sum() for x in return_periods}
print(pd.Series(verrification_sum, name="ReturnPeriod"))
```

```
100     1.0
200     0.5
350     1.0
500     1.0
750     1.0
1000    1.0
Name: ReturnPeriod, dtype: float64
```

[ ]:
```
def get_probability_curve(df:pd.DataFrame, column:str, probability_column:
↪str="GlobalFloodExceedProb", ascending=True) -> pd.DataFrame:
```

```
    # this function will copy a slice of a dataframe, sort it, and return the␣
 ↪associated cumulative probabilities

    if column not in df.columns: raise ValueError('{} not found in dataframe'.
 ↪format(column))
    if probability_column not in df.columns: raise ValueError('{} not found in␣
 ↪dataframe'.format(probability_column))

    # copy a sorted subset of the main dataframe and calculate cumulative␣
 ↪probability
    df_sorted = df.sort_values(column,␣
 ↪ascending=ascending)[[probability_column,column]].copy()
    df_sorted["CumSum"] = df_sorted[probability_column].cumsum(axis=0)
    return df_sorted

def cm2inch(x):
    # simple function to convert cm to inch for matplotlib units
    if type(x) is tuple: return (x[0]/2.54, x[1]/2.54)
    else: return x/2.54
```

[ ]:
```
# colours to distinguish DP and VP
colours={"DP":'darkblue',"VP":'darkorange'}

# set iterables
profiles = ["DP","VP"]
sites = range(1,6,1)
fig, axs = plt.subplots(figsize=(cm2inch((24,12))), nrows=2, ncols=5,␣
 ↪sharey=True)

for ii, profile in enumerate(profiles):
    for iii, site in enumerate(sites):
        col = "{}-{}".format(profile,site)

        df_sorted = get_probability_curve(df=df, column=col)
        # plot the cumulative probability against either the depth or velocity
        axs[ii,iii].plot(df_sorted[col],df_sorted["CumSum"],'.-',␣
 ↪color=colours[profile])
        axs[ii,iii].set_title(col)
        axs[ii,iii].grid('minor')
        if iii == 0: axs[ii,iii].set_ylabel('CumProb')
        #axs[ii,iii].set_xlabel(profile)

fig.tight_layout()
```

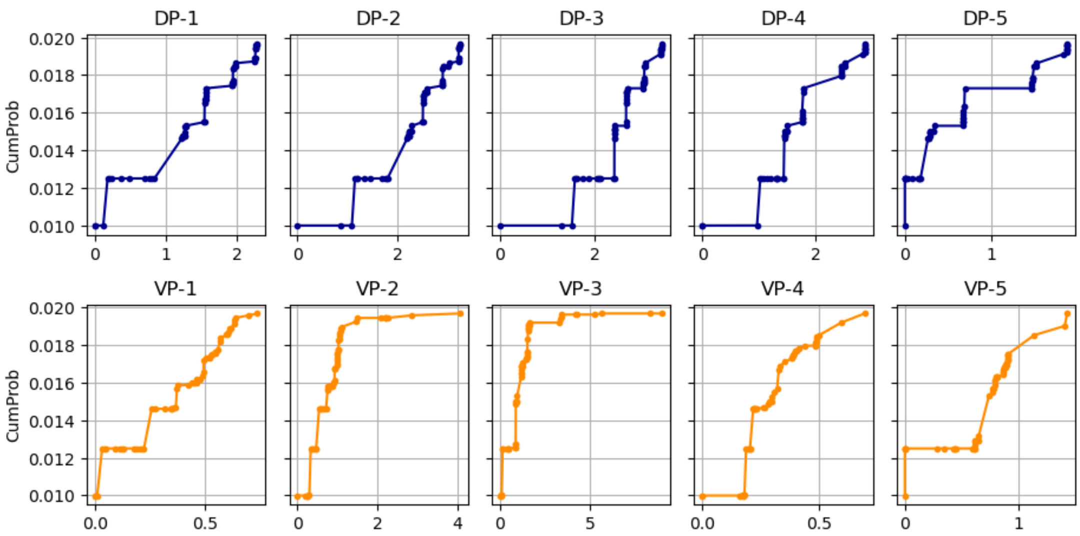

[ ]:
```
# create plots that show all depth and velocity data
# assign fig2 since we will simply plot these using the data from thr previous␣
↪fig, rather than iterating over the dataset again or saving it on the fly

fig2, axs2 = plt.subplots(figsize=(cm2inch((24,12))), nrows=1, ncols=2,␣
↪sharey=True)

markers = ['o','x','.','+','v']

for ii, profile in enumerate(profiles):
    for iii, ax in enumerate(axs[ii,:]):
        axs2[ii].plot(ax.lines[0].get_xdata(),ax.lines[0].get_ydata(),␣
↪marker=markers[iii], label=ax.title.get_text())
    axs2[ii].legend()
    axs2[ii].grid()
    axs2[ii].set_title(profile)

fig2.tight_layout()
```

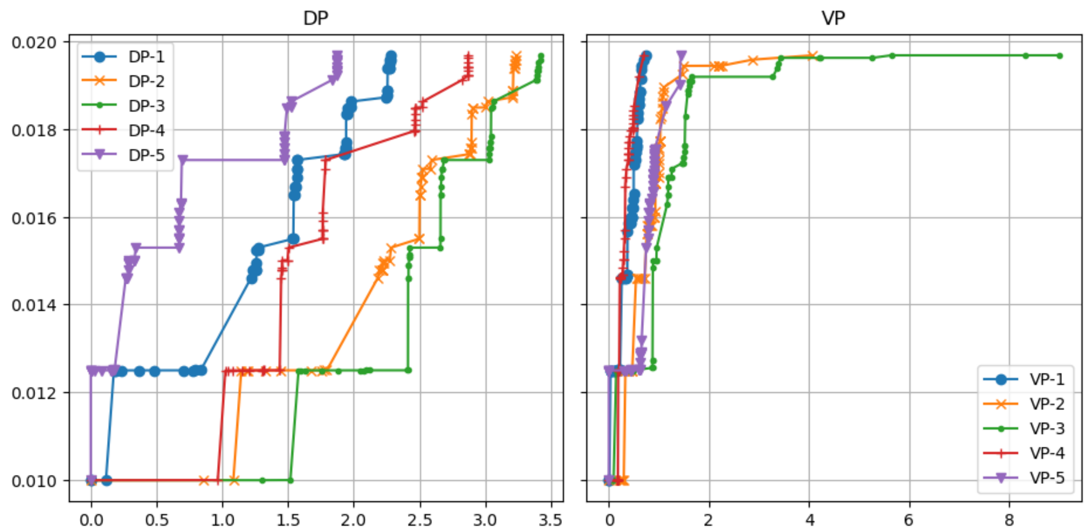

[ ]:

```python
# next we want to plot curves for specific location / failure type combinations;
 ↪ each curve will have n points associated with n RPs
# for each one, we again want to sort by depth, then get the cumulative␣
 ↪probability

scenarios = np.unique(df["BreachLocation_FailureMode"])
fig3, axs3 = plt.subplots(figsize=(cm2inch((24,12))), nrows=2, ncols=5,␣
 ↪sharey=True)

for ii, profile in enumerate(profiles):
    for iii, site in enumerate(sites):
        col = "{}-{}".format(profile,site)
        for loc_fail in scenarios:
            df_sorted =␣
 ↪get_probability_curve(df=df[df["BreachLocation_FailureMode"] == loc_fail],␣
 ↪column=col)

            # plot the cumulative probability against either the depth or␣
 ↪velocity
            axs3[ii,iii].plot(df_sorted[col],df_sorted["CumSum"],'.-',␣
 ↪label=loc_fail)
            axs3[ii,iii].set_title(col)
            axs3[ii,iii].grid()
            axs3[ii,iii].set_yscale("log")

            if iii == 0: axs3[ii,iii].set_ylabel('CumProb')

fig3.tight_layout()
```

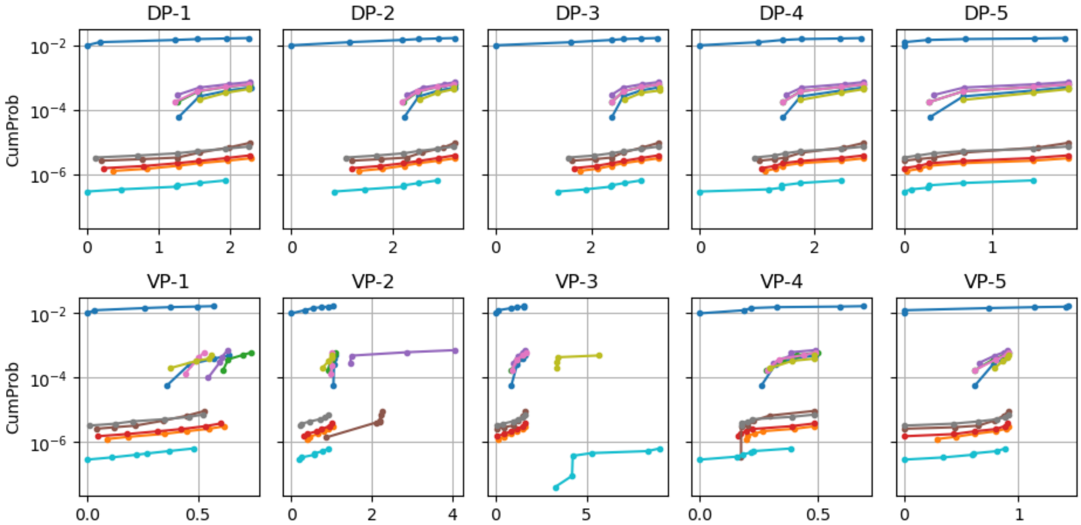
DP-1
DP-2
DP-3
DP-4
DP-5
VP-1
VP-2
VP-3
VP-4
VP-5
CumProb
CumProb
10^{-2}
10^{-4}
10^{-6}

[ ]:

[ ]:

[ ]: